CHARACTERIZATION OF MIDGUT EPITHELIAL REPAIR IN ADULT AND LARVAL DROSOPHILA IN RESPONSE TO ENTERIC INFECTION

A Dissertation

Presented to the Faculty of the Graduate School

of Cornell University

In Partial Fulfillment of the Requirements for the Degree of

Doctor of Philosophy

by

Philip Lewis Houtz

December 2018

CHARACTERIZATION OF MIDGUT EPITHELIAL REPAIR IN ADULT AND LARVAL DROSOPHILA IN RESPONSE TO ENTERIC INFECTION

Philip Lewis Houtz, Ph. D.

Cornell University 2018

The epithelium of the gastrointestinal (GI) tract serves vital roles as both digestive tissue and a barrier against pathogens and other harmful material from the environment. In order to maintain homeostasis, intestinal epithelia must undergo continuous tissue turnover by the activity of dedicated intestinal stem cells (ISCs), which divide to self-renew and differentiate into new epithelial cells. Regulating constant tissue renewal in spite of physical and microbial challenges requires careful coordination by cellular signaling to link the detection of damage or stress with adequate repair.

In this thesis, I investigated the regulatory networks controlling intestinal epithelial cell behavior to promote repair of infectious damage in the midgut of *Drosophila melanogaster*. In both healthy and diseased conditions, pro-regenerative cytokines function as central coordinators of gut renewal, linking inflammation to stem cell activity. In *Drosophila*, the primary reparative cytokine, Unpaired 3 (Upd3), serves to stimulate the JAK/STAT pathway in epithelial cells in response to pathogenic damage. In the beginning of my PhD, I familiarized myself with the tools and techniques associated with the study of *Drosophila* midgut repair. The details of these procedures were compiled and published as a chapter in *Methods in Molecular Biology*, *Animal Models for Stem Cell Therapy*. I then began an investigation of the regulation of cytokine activity in the *Drosophila* midgut. I found that the transcriptional activation of *upd3* in midgut enterocytes is regulated by the Hippo, Src-MAPK, and TGF-B pathways, which are known to be

similarly active in ISCs following enteric damage, and required for subsequent repair responses. This work was published in *PLOS Genetics* in 2017. Following my findings of the regulatory pathways that initiate epithelial repair in the adult midgut, I investigated how the larval *Drosophila* midgut, which lacks dedicated ISCs and basal tissue turnover, is able to cope with bacteria-induced damage. Larval *Drosophila* were found to be more susceptible to infection, and survivors experienced a developmental delay in the onset of pupation. Infected larvae that survive to reach pupation experienced no further delay in their development rate to adult eclosion, and experience no lasting negative impact on their lifespan. I discovered that the larval midgut epithelium was able to undergo limited repair following enteric infection-induced cell loss, by temporary recruitment of adult midgut progenitor (AMP) cells to be differentiated into new enterocytes. Fascinatingly, I found that AMP differentiation in response to epithelial damage is also regulated by Upd3 and the JAK/STAT pathway. In addition to the aforementioned publications, I collaborated with DJ Dutta of Bruce Edgars lab as a middle author in her 2015 *Cell Reports* paper.

Altogether, my work has identified key regulatory networks that act to control epithelial renewal in the GI tract. I have found that JAK/STAT, Notch, EGFR and TGF-B/Dpp signaling pathways are activated in multiple epithelial cell types following pathogenic damage to gut tissue. Interestingly, the activation of these pathways directs both conventional, ISC-mediated tissue repair, as well as alternative methods of regeneration during development, in the absence of dedicated ISCs. This suggests that these pathways serve a conserved function to initiate healing in response to enteric infections, but are nonetheless dynamic in the means by which this is accomplished under different sets of constraints.

BIOGRAPHICAL SKETCH

Philip Houtz is a sixth year PhD student in the Entomology Department of Cornell University. He previously graduated from the University of Kentucky with a BS major in Agricultural Biotechnology, as well as minors in Entomology and Chemistry. After graduating from the University of Kentucky, Philip Houtz came to Cornell University and entered an Entomology PhD program. He arrived to the program with funding from the Presidential Life Sciences Fellowship and, after a year of rotating between labs, joined the laboratory of Dr. Nicolas Buchon. He has since performed research that has led to two first-author publications, as well as a collaborative paper in which he was a middle author, and a third first-author publication ready for submission to *Dev Cell* in the next several weeks.

ACKNOWLEDGEMENTS

I would first like to thank my PhD advisor, Nicolas Buchon, without whom my research and thesis would not have been possible, for all of the support and education that he has provided to me. The motivation, knowledge, and advice that he has imparted to me have been incredibly important to my maturation as a researcher and I hope to continue to develop these traits. In addition, I want to acknowledge the members of the Buchon lab, who have been instrumental in assisting my PhD education and research. The members of my PhD committee, Dr. Brian Lazzaro, Dr. Cynthia Leifer and Dr. Natasza Kurpios must also be acknowledged for their longstanding support of my PhD work and education. My rotation in Dr. Cynthia Leifer's lab was a great experience, and her advice and guidance during committee meetings and for the completion of my dissertation have been indispensable. Dr. Brian Lazzaro and Dr. Natasza Kurpios likewise were of great support in my growth as a scientist. I would also like to thank our research collaborators, including Dr. Yu-Chen Tsai, Dr. Bruce Edgar, DJ Dutta, and Dr. Won-Jae Lee.

TABLE OF CONTENTS

CHAPTER I

INTRODUCTION

1. Scientific questions and dissertation contents.

What are the genetic mechanisms that link bacterially-induced intestinal epithelial damage with subsequent tissue repair? Epithelial turnover of the gastrointestinal (GI) tract is a vital process for maintaining gut homeostasis in spite of physical and microbial challenges. Disruption of gut epithelial barrier integrity or the continual process of intestinal turnover inevitably results in disease and death in the whole organism. When I began my PhD projects, I first familiarized myself with the tools and techniques used in studying intestinal repair in adult *Drosophila melanogaster.* The methods that I learned for monitoring and manipulating epithelial renewal following bacterial damage in the Drosophila midgut were compiled into a chapter in *Methods in Molecular Biology*, *Animal Models for Stem Cell Therapy*, which comprises Chapter II of this dissertation. After establishing the basic tools and techniques that I would use, I proceeded to explore my scientific questions.

I first wanted to address the question: what is the genetic network that controls the transcription of *upd3,* the principle JAK/STAT cytokine that boosts midgut epithelial renewal in *Drosophila* adults, following enteric damage? To approach this question, I began by determining the transcriptional enhancer sequence that is utilized to regulate *upd3* following intestinal tissue loss following oral infection by the plant and insect pathogen, *Ecc15*. I then determined the transcription factors that are able to bind to and activate this sequence via a functional, enterocyte-specific RNAi screen of Drosophila transcription factors, paired with a Yeast One-Hybrid screen and a database search of annotated transcription factor binding sites. My findings of the transcription factors that directly control *upd3* transcription in enterocytes following *Ecc15*-induced midgut damage was ultimately published in *PLOS Genetics* in 2017. This paper is presented in this dissertation as Chapter III.

Given that the larval *Drosophila* midgut lacks dedicated intestinal stem cells for tissue renewal, I later undertook an additional project to address the question: how does the larval *Drosophila* midgut handle bacterially-induced damage? I discovered that the larval midgut actually does undergo a limited degree of tissue repair following the cell loss induced by oral *Ecc15* infection, and that this is accomplished by differentiation of a portion of the imaginal adult midgut progenitor cells (AMPs). This naturally led me to my next question: what is the genetic network that promotes AMP differentiation following infectious damage? I used an RNAseq analysis of unchallenged and *Ecc15*-infected to determine candidate pathways that are activated in the larva midgut by infection and, upon testing them, determined that AMP differentiation for tissue repair is under the control of the JAK/STAT pathway. I have written up the results of this study for publication in the journal, *Cell Host & Microbe*, and this paper comprises Chapter IV of this dissertation.

Lastly, in Chapter V, I discuss the implications of my research as a whole and the future directions that can be taken from my published and unpublished findings. Furthermore, one can find unpublished data from my research, referred to in the future directions section of the dissertation, in Chapter VI, the Appendix.

2. Composition of the Drosophila midgut epithelium.

Drosophila melanogaster has developed into an exceptional model for studying intestinal physiology and repair processes in the face of pathogenic challenges (Apidianakis and Rahme, 2011; Broderick et al., 2014; Buchon et al., 2013a; Lee and Lee, 2014). It owes this partially to its annotated genome and the wealth of readily available genetic tools, and partially to its comparable physiology to mammalian systems. Indeed, similar to the mammalian gut, the midgut of

Drosophila melanogaster is comprised of several genetically and physiologically distinct regions and sub-regions (there are 5 major regions, and up to 14 sub-regions in the adult *Drosophila* midgut) (Buchon and Osman, 2015; Buchon et al., 2013b; Dutta et al., 2015; Marianes and Spradling, 2013). The epithelium of adult *Drosophila melanogaster* flies is a monolayer consisting of absorptive enterocytes (ECs), secretory enteroendocrine cells (EEs), and intestinal stem cells (ISCs) that divide and differentiate to replace lost ECs or EEs through a non-dividing intermediate cell type, the enteroblast (EB) (Micchelli and Perrimon, 2006; Ohlstein and Spradling, 2006). Recent studies have suggested that EBs differentiate only into ECs, and EEs are derived from ISC differentiation through a distinct post-mitotic progenitor, known as the pre-EE (Zeng and Hou, 2015). The midgut epithelium is ensheathed in visceral muscle (VM), which provides peristalsis to promote passage of the food bolus through the lumen, and also serves as a niche by regulating ISC division and differentiation (Biteau and Jasper, 2011; Buchon et al., 2010; Guo et al., 2013).

3. Bacterial damage and subsequent epithelial renewal.

The midgut performs a necessary role as a barrier to infection, and ingestion of pathogenic bacteria initiates a cascade of immune and tissue turnover responses that ultimately cause the loss of ECs from the epithelial layer via cell extrusion or delamination. This tissue loss subsequently triggers ISC proliferation and differentiation to replace lost cells, thus ensuring a return to homeostatic conditions once the infection has passed. Thus, enteric pathogenic infections can be used as a tool to perturb gut homeostasis and observe the response of the gut epithelium in a physiological context of natural infection. In the case of my experiments, I utilize the gram-negative bacteria, *Erwinia carotovora carotovora 15* (*Ecc15*), which triggers an Imd-dependent immune response as well as boosted production of reactive oxygen species (ROS) upon ingestion

in adult Drosophila. This aggravates a massive loss of midgut epithelial cells, that is, however, non-lethal to adult flies, as the midgut regenerates itself within 48hr (Buchon et al., 2009). Initiation of midgut regeneration is triggered by the transcription of the JAK/STAT cytokine, Upd3, in ECs following tissue loss. Upd3 is the principle cytokine for regulating midgut regeneration in *Drosophila*, and binds the receptor, Domeless, in the VM and EBs where JAK/STAT activation causes induction of epithelial growth factors and promote ISC differentiation (Buchon et al., 2009, Buchon et al., 2010, Jiang et al., 2009). Activation of EGFR promotes the proliferation and differentiation of ISCs, but additional pathways, such as the DPP/TGF-B pathway and Hippo, are also activated in ISCs and EBs, and necessary for proper regulation of midgut regeneration (Zhou et al., 2015 and Jin et al., 2013). Coordination of these pathways downstream of JAK/STAT activation by injury-induced Upd3 transcription and secretion is crucial for proper replacement of lost epithelial tissue (Fig. 1.1).

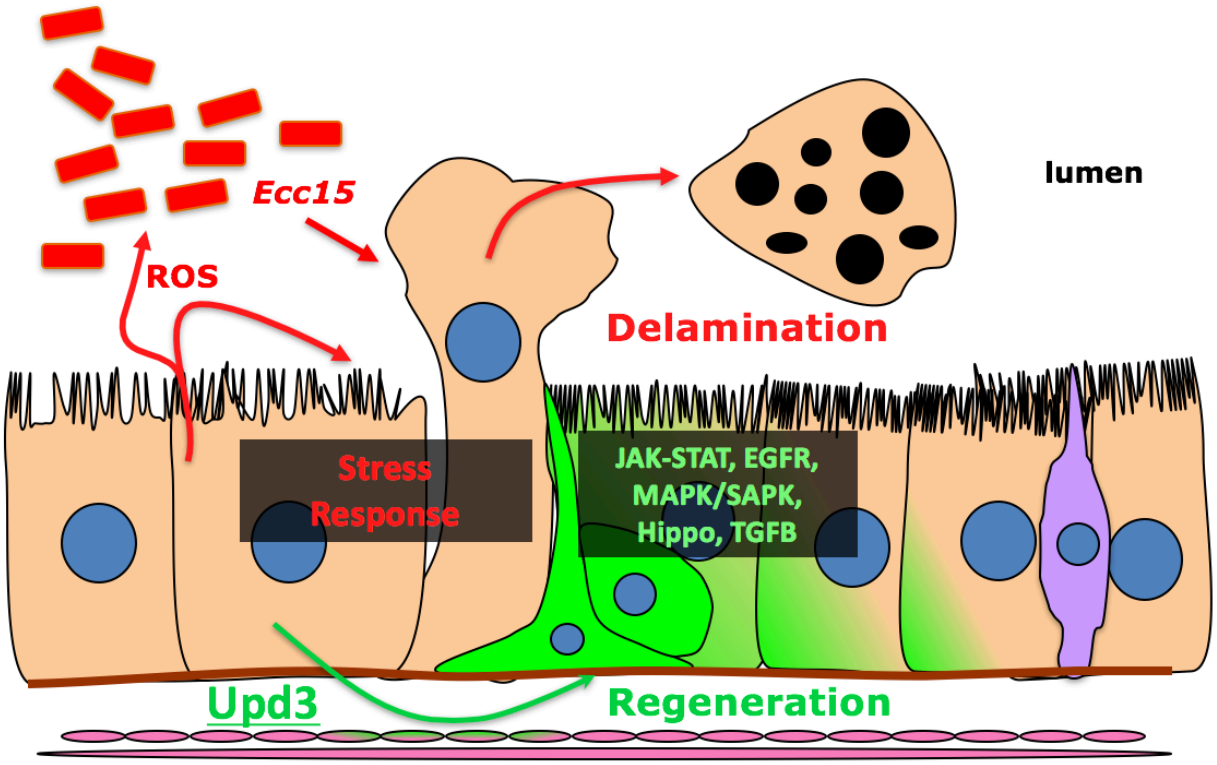

Figure 1.1. Model of midgut epithelium regeneration following *Ecc15* infection. Ecc15 infection in the adult Drosophila midgut triggers the production of ROS, which further aggravates epithelial stress and triggers removal of ECs via delamination into the gut lumen. In response to cell loss, remaining ECs activate transcription of Upd3, which is then secreted and activates JAK/STAT in the VM and progenitor cells. This in turn triggers the cascade of additional pathway activation in ISCs and EBs to promote proliferation and differentiation, including the EGFR, MAPK, Hippo, and TGF-B pathways.

References

1. Apidianakis, Y., Rahme, L.G., 2011. Drosophila melanogaster as a model for human intestinal infection and pathology. Dis. Model. Mech. 4, 21e30. http:// dx.doi.org/10.1242/dmm.003970.

2. Biteau, B., Jasper, H., 2011. EGF signaling regulates the proliferation of intestinal stem cells in Drosophila. Development 138, 1045e1055. http://dx.doi.org/ 10.1242/dev.056671.

3. Broderick, N.A., Buchon, N., Lemaitre, B., 2014. Microbiota-induced changes in Drosophila melanogaster host gene expression and gut morphology. MBio 5. http://dx.doi.org/10.1128/mBio.01117-14 e01117e14.

4. Buchon, N., Broderick, N. A., Poidevin, M., Pradervand, S. & Lemaitre, B. Drosophila intestinal response to bacterial infection: activation of host defense and stem cell proliferation. Cell Host Microbe 5, 200–211 (2009).

5. Buchon, N., Broderick, N. A., Kuraishi, T. & Lemaitre, B. Drosophila EGFR pathway coordinates stem cell proliferation and gut remodeling following infection. BMC Biol. 8, 152 (2010).

6. Buchon, N., Broderick, N.A., Lemaitre, B., 2013a. Gut homeostasis in a microbial world: insights from Drosophila melanogaster. Nat. Rev. Microbiol. 11, 615e626. http://dx.doi.org/10.1038/nrmicro3074.

7. Buchon, N., Osman, D., David, F.P.A., Yu Fang, H., Boquete, J.-P.P., Deplancke, B., Lemaitre, B., Fang, H.Y., Boquete, J.-P.P., Deplancke, B., Lemaitre, B., 2013b. Morphological and molecular characterization of adult midgut compartmentalization in Drosophila. Cell Rep. 3, 1725e1738. http://dx.doi.org/10.1016/ j.celrep.2013.04.001.

8. Buchon, N., Osman, D., 2015. All for one and one for all: regionalization of the Drosophila intestine. Insect Biochem. Mol. Biol. 1e7. http://dx.doi.org/10.1016/ j.ibmb.2015.05.015.

9. Dutta, D., Dobson, A.J.J., Houtz, P.L.L., Patel, P.H., Edgar, B.A.A., Buchon, N., Revah, J., Korzelius, J., Gl€aßer, C., Revah, J., Korzelius, J., Patel, P.H., Edgar, B.A.A., Buchon, N., 2015. Regional cell-specific transcriptome mapping reveals regulatory complexity in the adult Drosophila midgut. Cell Rep. 12, 346e358. http:// dx.doi.org/10.1016/j.celrep.2015.06.009.

10. Guo, Z., Driver, I., Ohlstein, B., 2013. Injury-induced BMP signaling negatively regulates Drosophila midgut homeostasis. J. Cell Biol. 201, 945e961. http:// dx.doi.org/10.1083/jcb.201302049.

11. Jiang, H., Edgar, B.A., 2009. EGFR signaling regulates the proliferation of Drosophila adult midgut progenitors. Development 136, 483e493. http://dx.doi.org/ 10.1242/dev.026955.

12. Lee, K.-A., Lee, W.-J., 2014. Drosophila as a model for intestinal dysbiosis and chronic inflammatory diseases. Dev. Comp. Immunol. 42, 102e110. http:// dx.doi.org/10.1016/j.dci.2013.05.005.

13. Marianes, A., Spradling, A.C., 2013. Physiological and stem cell compartmentalization within the Drosophila midgut. Elife 2, e00886. http://dx.doi.org/10.7554/ eLife.00886.

14. Micchelli, C.A., Perrimon, N., 2006. Evidence that stem cells reside in the adult Drosophila midgut epithelium. Nature 439, 475e479. http://dx.doi.org/10.1038/ nature04371.

15. Ohlstein, B., Spradling, A., 2006. The adult Drosophila posterior midgut is maintained by pluripotent stem cells. Nature 439, 470e474. http://dx.doi.org/ 10.1038/nature04333.

16. Zeng, X., Hou, S.X., 2015. Enteroendocrine cells are generated from stem cells through a distinct progenitor in the adult Drosophila posterior midgut. Development 142, 644e653. http://dx.doi.org/10.1242/dev.113357.

CHAPTER 2

METHODS TO ASSESS INTESTINAL STEM CELL ACTIVITY IN RESPONSE TO MICROBES IN *DROSOPHILA MELANOGASTER*

This chapter represents a published book chapter in Methods in Molecular Biology: Animal Models for Stem Cell Therapy, Humana Press, entitled "Methods to Assess Intestinal Stem Cell Activity in Response to Microbes in Drosophila melanogaster" (2014) by Philip Lewis Houtz and Nicolas Buchon.

Summary

Drosophila melanogaster presents itself as a powerful model for studying the somatic stem cells of the gut and how bacteria affect intestinal homeostasis. The *Gal4/UAS/Gal80^{ts}* system allows for temporally controlled expression of fluorescent proteins, RNAi knock-down, and other genetic constructs targeted to specific cell populations in the midgut. Similarly, FLP/FRT mediated somatic recombinations in intestinal stem cells (ISCs) are utilized to visualize and analyze the clonal lineages of individual or populations of stem cells. Live imaging microscopy as well as immunofluorescence allows both qualitative and quantitative characterization of stem cell shape, proliferation and differentiation. Here, we detail the use of these tools and techniques for studying gut performance during and following a bacterial infection in the adult fruit fly.

1. Introduction

The gut of *Drosophila melanogaster* is composed of a monolayer of epithelial cells, surrounded by two layers of visceral muscles and arranged into a tube with three distinct compartments: the foregut, the midgut, and the hindgut (**Fig. 2.1**) ***(1, 2)***. The foregut and hindgut are derived from the ectoderm and their epithelium is covered by chitin, while the midgut is derived from the endoderm, covered by a chitinous matrix (the peritrophic matrix), and serves as the primary site of nutrient processing and absorption ***(1)***. Three types of cells compose the epithelia of the midgut: large, nutrient absorbing enterocytes (ECs), small, secretory enteroendocrine (EE) cells, and pluripotent intestinal stem cells (ISCs).

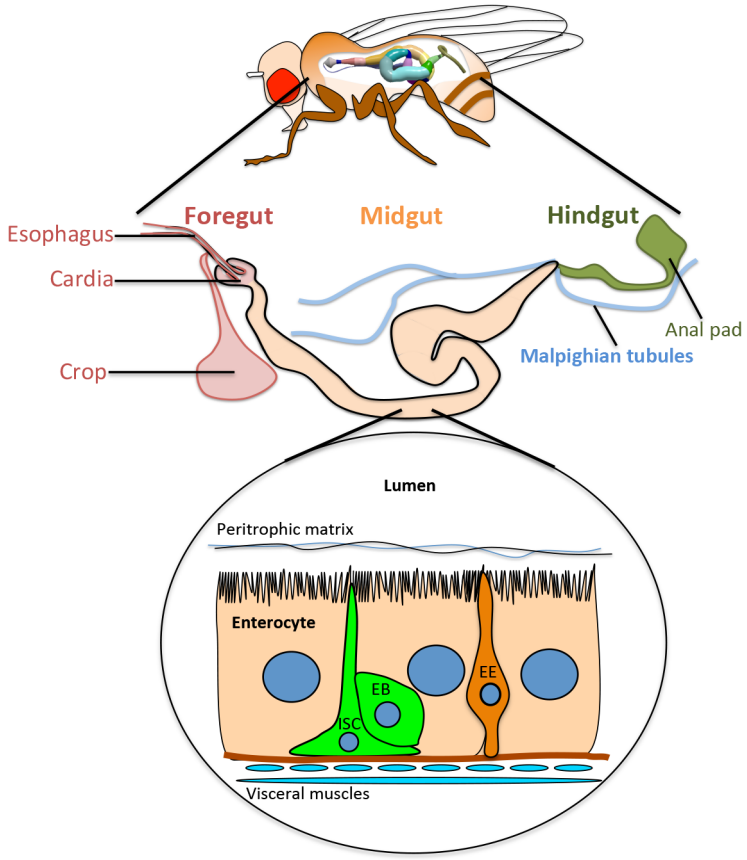

Figure 2.1. The *Drosophila* gut. The gut of an adult fruit fly is organized into three distinctive regions: the foregut, the midgut and the hindgut. The foregut comprises the esophagus and the crop, which acts as a storage organ and initiates nutrient processing. Food is then passed on to the midgut where the majority of nutrient digestion and absorption occurs. Finally, the hindgut functions to reabsorb water from waste material before its removal. The midgut epithelium is

surrounded by visceral muscles and is composed of four primary cell types: Enterocytes (ECs), Enteroendocrine (EE) cells, Intestinal Stem Cells (ISCs), and Enteroblasts (EBs). ECs and EEs are differentiated and carry out absorptive and neurosecretory functions, respectively. ISCs replenish old or destroyed cells through self-renewing division, yielding a new ISC and an EB, which is dedicated to differentiate into either an EC or an EE cell.

ISCs in *Drosophila*, like those in mammals, maintain the gut by self-renewing division, yielding one new ISC and one non-dividing progenitor cell called an enteroblast (EB) ***(3, 4)***. EB cells undergo further fate decision and ultimately differentiate to become new ECs or EE cells, replacing the old intestinal cell population ***(5)***. Complete turnover of the midgut is accomplished by this process in 10-15 days under basal conditions, but is greatly accelerated in response to intestinal damage and microbial pathogens ***(2, 6, 7)***. The discovery of ISCs in the midgut of *Drosophila*, as well as the wealth of genetic tools established in the fruit fly, make it an ideal and exciting model for studying the behavior of ISCs during infection.

In this chapter, we describe techniques for performing oral infections in *Drosophila* and monitoring ISC proliferation and subsequent lineage. The *Gal4/UAS/Gal80^{ts}* system allows for fluorescence and lacZ labeling of particular intestinal cell types by making expression of a reporter gene dependent upon the expression of cell-specific enhancers. In addition, immunostaining allows cell types to be labeled according to cell-specific, targetable antigens. Furthermore, visualization of progenitor lineages, stem cell division rates, and global tissue renewal can be accomplished with diverse genetic systems such as: *esg-Gal4^{ts}*, *tub-FRT-lacZ clones*, *esg$^{F/O}$*, *MARCM* and *Twin-spot MARCM* (described below).

2. Materials

2.1 Fly Rearing and Husbandry

1. *Drosophila* diet: 50g baker's yeast, 40g sucrose, 60g cornmeal, 7g agar, 16mL Moldex (10%), 8mL acid mix (*see* **Notes 1 and 2**), 1000mL deionized water.
2. Standard fly vials (~22mm in diameter) with *Drosophila* diet.
3. Facilities to maintain flies at 18°C and 29°C.

2.2 Bacterial Cultures

1. Sterile Luria Bertani Broth (LB).
2. LB agar plates: 1.5% agar in LB, poured into sterile culture plates.
3. Sterile, disposable inoculation loops.
4. Autoclaved Erlenmeyer flasks.
5. Pathogenic bacteria stocks: *Erwinia carotovora* subsp. *carotovora* 15 (*Ecc15*), *Pseudomonas entomophila*, *Serratia marcescens* str. Db11, or *Pseudomonas aeruginosa* (*see* **Note 3**).
6. Shaking incubator thermostated at 29°C.

2.3 Fly Genetics

1. *Gal4/UAS/Gal80^{ts}* system (**Fig. 2.2A**): Allows labeling of specific cells in the gut (*see* **Note 4**). We can induce the *Gal4/UAS* system to visualize different cell populations in the gut by expressing fluorescent proteins in specific cell types. For instance, the *esg-Gal4^{ts}* system (*esg-Gal4, Gal80^{ts} UAS-GFP* flies) allows for visualization of progenitors to monitor ISC shape, number, and proliferation ***(4, 6)***.

2. *tub-FRT-lacZ* clones: Randomly labels individual stem cells and their progeny in a heat shock-inducible manner (*see* **Note 5**) ***(8)***. Used to study ISC proliferation and ISC lineage.
3. $esg^{F/O}$ system: Systematically labels all ISCs and their progeny with GFP in an inducible manner (**Fig. 2.2B**) ***(7)***. Used to study proliferation of progenitors, ISC lineage, and tissue renewal over time (*see* **Note 6**).
4. MARCM (Mosaic Analysis with a Repressible Cell Marker) clones: Randomly labels individual stem cells and the progeny of one of the two daughter cells ***(9, 10)***. For its application to ISC lineage, see Singh *et al.* ***(11)***.
5. Twin-spot MARCM system: Randomly labels dividing ISCs and progeny in a heat shock-inducible manner ***(12, 13)***. After mitosis of the parent cell, the two daughter cells are tagged with a different fluorescent reporter. This allows observing the fate of the two daughter cells of an ISC division, monitoring both proliferation and the proportion of symmetric versus asymmetric division (*see* **Note 7**) (**Fig. 2.2C**).
6. Additional molecular markers to study ISC in the gut of *Drosophila* can be found in Singh *et al.* ***(11)***.
7. 37°C water bath.

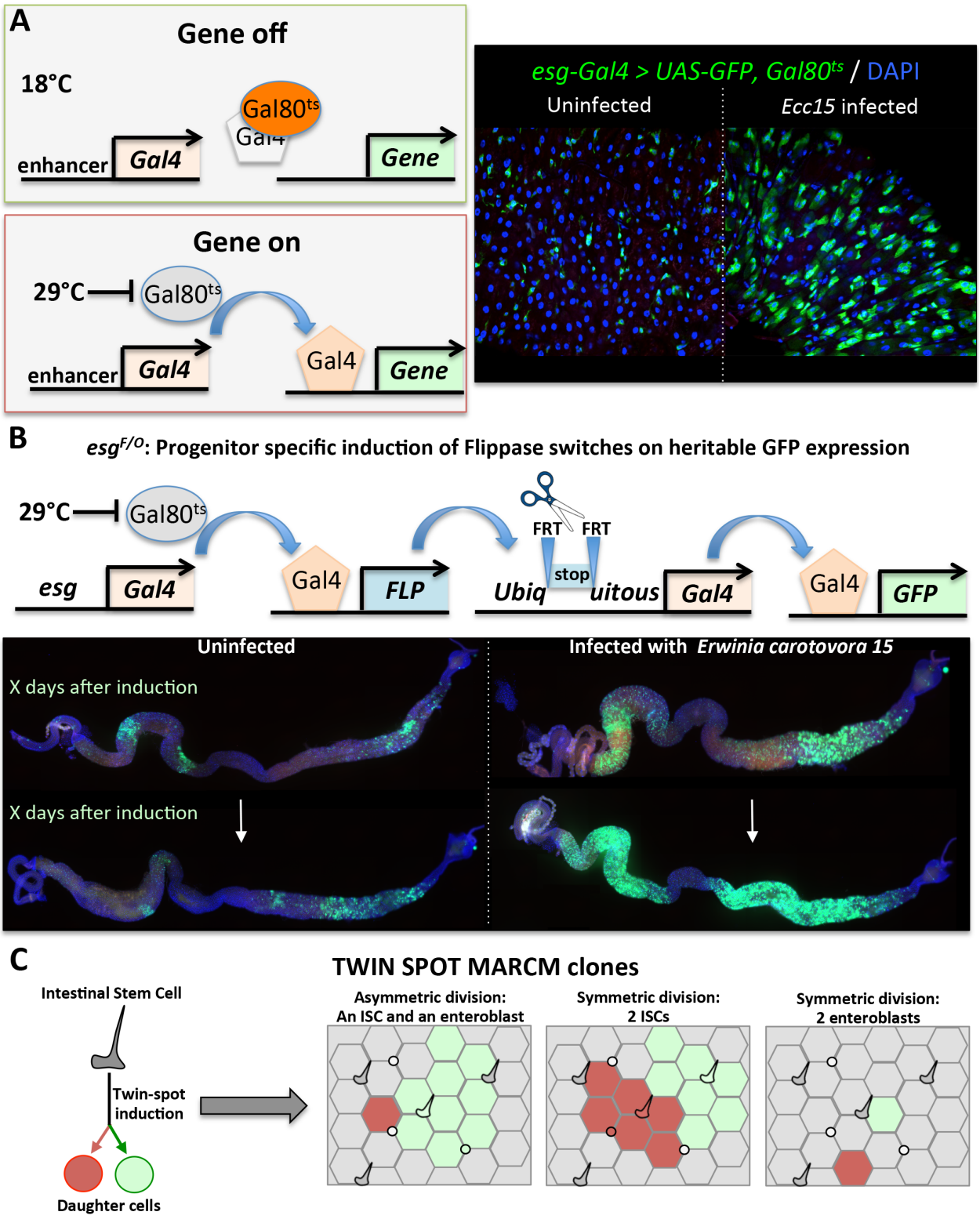

Figure 2.2. Fly genetic tools for studying Intestinal Stem Cell activity. (**A**) *Left*: The *Gal4/UAS/Gal80^{ts}* system allows the expression of *UAS-GFP*, and other *UAS*-regulated transgenes, to be induced by Gal4 in a temperature dependent manner in only the cells where the promoter of the *Gal4* transgene is active. Gal80^{ts} inhibits Gal4 at 18°C, preventing GFP expression

controlled by *UAS*, but becomes inactivated at 29°C. *Right*: Choosing a promoter expressed in progenitors (*esg*) allows us to visualize the activation of progenitor cells during infection, as illustrated by the diffuse GFP signal in infected guts (right panel). (**B**) The $esg^{F/O}$ system drives the temperature dependent expression of FLP recombinase in progenitors (when moved to 29°C). This triggers the FLP out of the CD2 cassette and the activation of the *act-Gal4* ubiquitous driver in subsequent ISC progeny that therefore expresses GFP. The proportion of GFP positive cells in the midgut reflects turnover rates. Infection with *Ecc15* induces an acceleration of epithelium renewal (see microscopy examples in lower panel). (**C**) The *Twin-spot MARCM* system induces the expression of different heritable markers (GFP and RFP) in the two daughter cells of an ISC. This allows establishment of the symmetrical or asymmetrical behavior of ISC divisions, discernible through the analysis of the subsequent lineage of the two daughter cells.

2.4 Oral Infection

1. Absorbent pads (e.g. Whatman filter paper), cut to the diameter of the fly vials (usually 22mm).
2. Empty fly vials.
3. Fly vials with *Drosophila* diet.
4. Concentrated sucrose solution in sterilized water (*see* **Note 8**).
5. Bacterial pellet: The infectious dose varies for different bacteria species (*i.e. Ecc15* pellet should have an $OD_{600} = 200$).

2.5 Gut Dissection

1. Multi-well glass dish.
2. Source of CO_2 for anaesthetization (**Fig. 2.3A**).
3. Forceps (x2).
4. 70% EtOH.
5. Sterile 1X PBS (Phosphate Buffer Saline).

2.6 Live Imaging

1. Sterile, 1.5mL or 2mL centrifuge tubes.

2. PBT solution (0.05% Tween20): Add 25µL of Tween20 to 50mL 1X PBS and mix.
3. DAPI staining solution: Add 1µL of 20mg/mL DAPI dilactate in sterile water to 50mL PBT. Store at 4°C.
4. PBS/glycerol (1:1) or Antifadent mounting medium (Citifluor AF1 or Vectashield).
5. Glass microscope slides.
6. Glass coverslips.
7. Nail polish (to seal coverslips on slides).

2.7 Immunostaining

1. Sterile, 1.5mL or 2mL centrifuge tubes.
2. PBT solution (0.1% Tween20): Add 50µL of tween 20 to 50mL 1X PBS and mix.
3. 4% paraformaldehyde (PFA) fixative in PBT (0.1% tween 20). Store solution at -20°C or at 4°C not more than 2 days.
4. PBTA: PBT solution (0.1% Tween20) with 1% BSA.
5. Primary antibody stocks: mouse anti-GFP (Roche), mouse anti-RFP (Clontech), rabbit anti-PH3 (Millipore) for cells undergoing mitosis, mouse anti-Prospero (Developmental Studies Hybridoma Bank) for EE cells, anti-PDM1 for ECs ***(14)***. Additional primary antibodies used to study ISC in the gut of *Drosophila* can be found in Singh *et al*. ***(11)***.
6. Secondary antibody stocks: Alexa-488 anti-mouse (Invitrogen), Alexa-594 anti-rabbit (Invitrogen).
7. PBS/glycerol (1:1) or Antifadent mounting medium (Citifluor AF1 or Vectashield).
8. Glass microscope slides.
9. Glass coverslips.

10. Nail polish (to seal coverslips on slides).

3. Methods

3.1 Fly Rearing and Husbandry

1. *Drosophila* stocks: Maintain flies by transferring adults to new vials every 2-3 days at room temperature or in a 25°C incubator, or every 7 days in an 18°C incubator (stocks with a Gal80^{ts} system). Maintain ~12 hrs light/dark cycle.

3.2 Bacterial Cultures

1. Pour 500mL of sterile LB media into a sterile, autoclaved Erlenmeyer flask with foil cover (*see* **Note 9**).
2. Locate a single colony on an LB bacterial stock plate and gently scrape it onto a sterile, disposable inoculation loop.
3. Transfer the colony to the Erlenmeyer flask with LB media and seal the flask with a sterile cover (for aerobic bacteria, it should not be air-tight).
4. Secure the Erlenmeyer flask in a shaking incubator at 29°C or 37°C, depending on the growth requirements of the bacteria, and incubate for 16 hrs while shaking at 200 rpm (*see* **Note 10**) to reach stationary growth phase.
5. Pour the liquid culture into a sterile centrifuge flask and centrifuge at 4°C and 4000rpm for 15 min.
6. Empty most of the LB media from the centrifuge flask.
7. Use a pipette and sterile tips to re-suspend the bacterial pellet in the remaining LB media. Transfer the liquid, concentrated bacterial pellet into a sterile 15mL tube.

8. Make a 1:1000 dilution of the pellet in sterile water in a separate test tube. Measure the OD_{600} absorbance of the dilution and subsequently calculate the concentration of the bacterial pellet. Adjust the bacterial concentration (OD_{600} = 200 for *Ecc15*).
9. Store bacterial pellet at 4°C for up to one week.

3.3 Fly Genetics

1. $Gal80^{ts}$ stocks (*esg-Gal4*^{ts} and *esg*$^{F/O}$) are raised at 18°C and shifted to 29°C 2 days prior to infection for activation of Gal4 mediated expression.
2. Stocks using FLP/FRT mediated recombination and *hsFLP* (*tub-FRT-lacZ, MARCM* and *Twin-spot MARCM* systems) are crossed appropriately for F1 progeny to carry all required transgenes (for precise crosses, see ***8, 11, 12***). The F1 progenies are raised at 18°C, then heat shocked for 40 min at 38°C, and used 2 days post clonal induction.
3. Flies of the proper genotype are sorted on a CO_2 pad prior to infection (**Fig. 2.3A**).

3.4 Oral Infection

1. Flip experimental flies into empty fly tubes and put at 29°C for 2 hrs (*see* **Note 11**).
2. Prepare 2.5% and 5% sucrose dilutions in sterile water. Mix the 5% sucrose solution with an equal volume of the bacterial pellet (at OD_{600} = 200 for *Ecc15*) to create the infection mix.
3. Set up labeled standard fly tubes with diet. Place an absorbent pad into a tube and push it down until it contacts the diet. The pad should completely cover the diet. Immediately add 150µL of either 2.5% sucrose, for controls, or sucrose and bacteria mix, for infections. Repeat for all tubes.

4. Flip flies into appropriate tubes for infection and controls (sucrose). Incubate flies at proper infection temperature for required infection time (*see* **Note 12**).

3.5 Gut Dissection

1. Prepare a clean multi-well glass spot plate and place under a dissection scope (*see* **Note 13**).
2. Anaesthetize flies using CO_2 source.
3. Transfer flies to a spot plate well containing 70% ethanol and briefly submerge (see **Note 14**).
4. Remove ethanol and replace with 1x PBS.
5. Use forceps to create a drop of PBS on a flat portion of the spot plate and transfer a fly into the droplet. There should be enough PBS covering the fly that the gut remains submerged during dissection.
6. Using two pairs of forceps, decapitate the fly with a clean stroke across the 'neck.' Ensure that the esophagus is completely severed.
7. Carefully separate the thorax from the abdomen by bracing one pair of forceps against the thorax while using the other to hold the first abdominal segment, and pull it away from the thorax. Stop once the two are separated and the gut is visible between them.
8. Sever the last two abdominal segments by pinning the end of the abdomen down with one pair of forceps and slicing across it with the other. Carefully pull the remainder of the abdomen away from the thorax and off of the gut. If the gut remains attached, either in the thorax or the abdomen, locate the crop and use it to gently pull the gut away from these segments.
9. Use the forceps to puncture the crop without removing it (*see* **Note 15**).
10. Store the gut in 1X PBS and proceed to **3.6** or **3.7**.

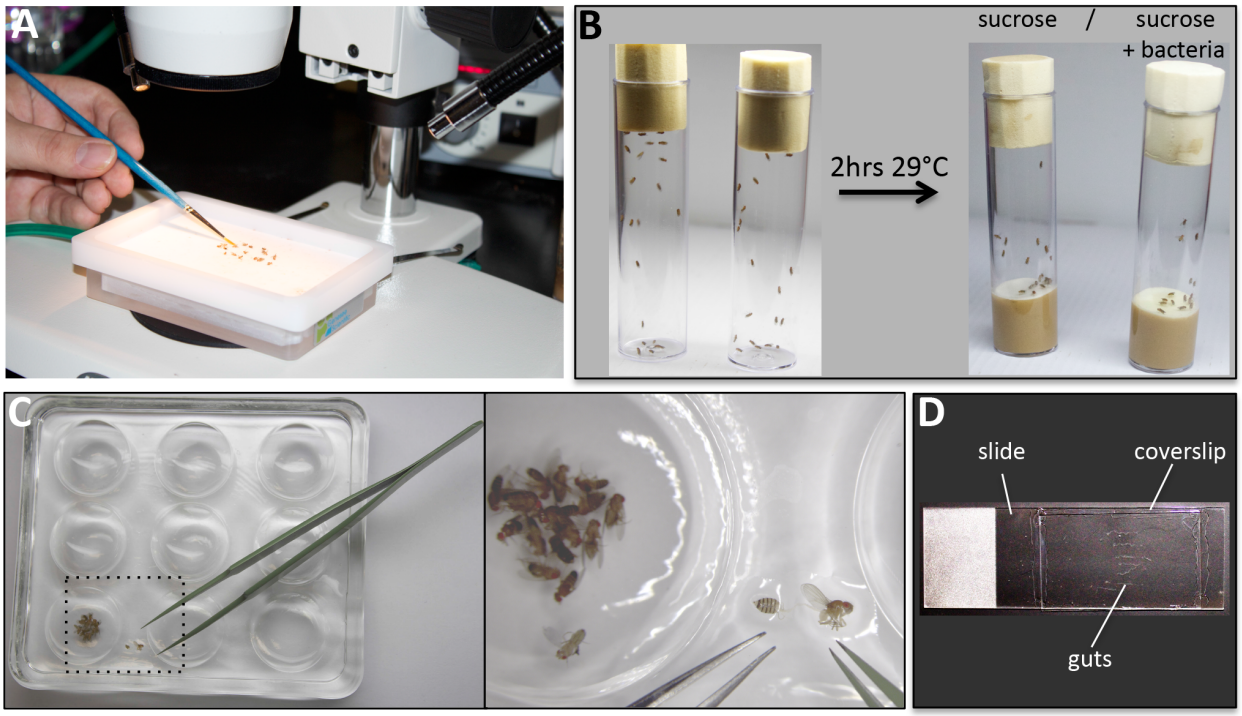

Figure 2.3. Steps in studying Intestinal Stem Cells using *Drosophila*. (**A**) Fly pushing and sorting on a CO_2 pad to obtain the desired genotype/phenotype. (**B**) Flies are starved at 29°C for 2 hrs in empty tubes before being transferred onto filter pads with sucrose (control) or bacteria and sucrose mixes. (**C**) Dissection of midguts from anaesthetized flies in PBS, on a spot plate. (**D**) Guts positioned on a slide with mounting solution under a coverslip.

3.6 Live Imaging

1. Dissect guts for live imaging, as described in **Subheading 3.5**.
2. Transfer 3-6 guts into a 1.5mL centrifuge tube with 0.5-1mL of DAPI staining solution. Incubate guts at room temperature for 10-15 min.
3. Rinse 3 times with 1X PBS. First and second washes are quick (1 min). The last wash is 5 min.
4. Mount guts on microscope slides in mounting solution or PBS/glycerol.
5. Carefully lay a coverslip over the sample in mounting solution. Carefully remove any excess that oozes from between the slide and coverslip with a Kimwipe.
6. Seal the slide with nail polish.
7. Guts are now ready for analysis using fluorescent or laser confocal microscopy (**Fig. 2.3D**).

3.7 Immunostaining

8. Dissect guts to be stained, as described in **Subheading 3.5**.
9. Transfer 3-6 guts into a 1.5mL centrifuge tube with 1mL of 4% PFA fixative in PBT. Fix guts at room temperature for 30 min in PFA/PBT.
10. Wash 2 to 3 times in PBT. First and second washes are quick (1 min). Last wash is 5-10 min.
11. Tissues may be stored in the dark and at 4°C at this stage before continuing with staining, but only for 1-2 days.
12. Block the epitopes by incubation with PBTA for one hour.
13. Remove PBTA and incubate in primary antibody hybridization solution overnight in the dark at 4°C. The hybridization solution is made by diluting the antibody to the proper concentration in PBTA (*see* **Note 16**).
14. Rinse in PBTA, 3 times 10 min each.
15. Incubate guts with the secondary antibody in PBTA and counterstain. Typical nucleus counterstain is DAPI or TO-PRO-3 (Invitrogen). Depending on the type of staining, this step may occur from 2 hrs of incubation to a new overnight treatment.
16. Wash 3 times in PBT, 10 to 30 min each.
17. Mount and image guts **(see Subheading 3.6, steps 4-6).**

4. Notes

1: Acid Mix is made by combining a solution of 8.3mL phosphoric acid in 91.7mL dH_2O and a solution of 83.6mL propionic acid in 16.4mL dH_2O.

2. Mix yeast, sucrose, cornmeal, and agar into the water and autoclave on a liquid cycle to dissolve. Add Moldex and acid mix to the diet once it is cool enough to handle with bare hands. Dispense the diet rapidly into empty fly tubes.

3. *Ecc15* is used to induce non-lethal oral infections, in which flies are able to repair and recover from damage ***(6, 15)***. Oral infections with *P. entomophila* are non-lethal at low doses but ultimately lethal at high doses and associated with high levels of Reactive Oxygen Species (ROS) and pore-forming bacterial toxins ***(15-18)***. Oral infections with *S. marcescens* are lethal due to the ability of the bacteria to cross the epithelial barrier of the gut and establish a systemic infection ***(19-21)***. *Pseudomonas aeruginosa* induces cell death in the gut and promotes ISC proliferation ***(22)***.

4. The basis of the *Gal4/UAS* transgenic system is the generation of transgenic flies that bear either Gal4 expressing transgenes that express the Gal4 yeast transcription factor in a cell specific manner (dependent of the promoter cloned in front of *Gal4*) or inducible transgenes that are controlled by Gal4 target sites: Upstream Activation Sequence (*UAS*) enhancers. The *UAS* transgene can induce the expression of a fluorescent reporter such as *GFP* or *RFP*. Flies with *UAS* and *Gal4* transgenes are crossed together and, in the F1 progeny, the *UAS* transgene is bound and transactivated by Gal4 only in cells with active *Gal4* expression. This system is further implemented by incorporation of $Gal80^{ts}$, encoding a thermosensitive form of Gal80, which acts as a Gal4 antagonist. The addition of ubiquitously expressed $Gal80^{ts}$ to the *Gal4/UAS* constructs allows the expression of the transgene in flies to be induced by incubation at 29°C, a temperature at which $Gal80^{ts}$ is inactivated (**Fig. 2.2A**). The promoter of *delta* is used to drive expression in ISCs (*delta-Gal4*), the promoter of *Su(H)* is used for EBs (*Su(H)-Gal4*), *Myo1A* for ECs (*Myo1A-Gal4*) ***(23)***, *prospero* for EE cells (*prospero-Gal4*), and *escargot* for expression in both ISCs and EBs (*esg-Gal4*) ***(4)***.

5. The *tub-FRT-lacZ* clone system makes use of a heat shock-induced, FLP recombinase-dependent, chromosome recombination that results in a heritable expression of *tub-lacZ* in the progeny of a cell ***(8)***. Two homologous chromosomes bear FRT sites (FLP recombination targets), one containing the ubiquitous promoter of *tubulin* (*tub-FRT*) and one containing the gene encoding β–galactosidase (*FRT-lacZ*). The two stocks are crossed and the F1 progeny is collected. Upon heat shock at 38°C, *hsFLP* is expressed in the F1 progeny, triggering *FRT* mediated recombination and reactivation of *lacZ* expression by joining the *tubulin* promoter to *lacZ* (*tub-lacZ*), thereby inducing *lacZ* expression in all daughter cells.

6. The $esg^{F/O}$ system (*esg-Gal4, Gal80^{ts}, UAS-FLP, act>CD2>Gal4, UAS-GFP*) uses a temperature sensitive inducible *Gal4*, driven in progenitor cells (*esg-Gal4, Gal80^{ts}*) to express FLP recombinase (*UAS-FLP*) in all intestinal progenitors. In this line, FLP removes an FRT-flanked CD2 cassette, allowing *Gal4* to be heritably expressed under the control of a ubiquitous promoter (*actin*). Expression of *Gal4* transactivates the expression of *UAS-GFP*, thereby causing all progenitor cells and their progeny to inherit GFP expression. This system allows for monitoring of midgut renewal in varying conditions (**Fig. 2.2B**).

7. Under basal conditions, about 90% of *Drosophila* ISC divisions occur asymmetrically, resulting in one daughter cell committed to differentiation and a second daughter cell that retains pluripotency ***(12, 13, 24)***. The remaining 10% are symmetric divisions, yielding either two differentiating cells or two ISCs, leading to the loss or expansion of stem cell clones in the gut. Twin-spot MARCM (Mosaic Analysis with a Repressible Cell Marker) allows labeling of the two daughter cells of an ISC with distinct fluorescent markers (GFP or RFP) (**Fig. 2.2C**). In the case of asymmetrical division, one daughter will differentiate and give rise to a single differentiated cell, whereas the other daughter will have ISC fate, and generate a clonal population. In the case

of symmetrical division, either two single differentiated cells will be generated, or two ISCs that will generate two clones labeled in GFP and RFP.

8. Sucrose can be stored at 25% concentration and at -20°C in 1-2mL aliquots.

9. Steps 1-3 should always be performed using sterile techniques.

10. *Ecc15, P. entomophila,* and *S. marcescens* are grown at 29°C, *P. aeruginosa* is grown at 37°C.

11. Two hours of starvation at 29°C is required to ensure that the flies will rapidly feed on the prepared sucrose and infection mix.

12. Flies infected by *Ecc15* are damaged in the first 4 hrs, which triggers ISC proliferation (massive from 8 hrs to 16 hrs) and gut repair (up to 5 days).

13. Special care should be taken in each step to ensure that the midgut is never handled directly by the forceps. Pinching or even holding the guts with metal forceps will puncture or tear the tissue.

14. This removes cuticular hydrocarbons that will otherwise cause flies to float on PBS and not mix. This also further anaesthetizes the flies.

15. The crop is often filled with bacteria prior to oral infection and this step is often necessary to prevent guts from floating during further processing, and to reduce the presence of free-floating bacteria during imaging.

16. Usual antibody dilutions in PBTA found in the literature: anti-GFP = 1:1000, anti-RFP = 1:250, anti-PH3 = 1:1000, anti-Prospero = 1:500, anti-PDM1 = 1:500, Alexa-anti-mouse = 1:500, Alexa-anti-rabbit = 1:500.

Acknowledgements

Photography for figures was performed by lab technician Aurélien Guillou. We thank our colleagues Peter Newell, David Duneau, Katia Sotelo-Troha, and Robert Houtz for comments on the chapter.

References

1. M. Demerec (1994) Biology of Drosophila, Cold Spring Harbor Laboratory Pr.

2. N. Buchon, N.A. Broderick, and B. Lemaitre (2013) Gut homeostasis in a microbial world: insights from Drosophila melanogaster, Nature reviews Microbiology. 11, 615–626.

3. B. Ohlstein and A. Spradling (2006) The adult Drosophila posterior midgut is maintained by pluripotent stem cells, Nature. 439, 470–474.

4. C.A. Micchelli and N. Perrimon (2006) Evidence that stem cells reside in the adult Drosophila midgut epithelium, Nature. 439, 475–479.

5. B. Ohlstein and A. Spradling (2007) Multipotent Drosophila intestinal stem cells specify daughter cell fates by differential notch signaling, Science (New York, N.Y.). 315, 988–992.

6. N. Buchon, N.A. Broderick, M. Poidevin, et al. (2009) Drosophila intestinal response to bacterial infection: activation of host defense and stem cell proliferation, Cell Host & Microbe. 5, 200–211.

7. H. Jiang, P.H. Patel, A. Kohlmaier, et al. (2009) Cytokine/Jak/Stat signaling mediates regeneration and homeostasis in the Drosophila midgut, Cell. 137, 1343–1355.

8. D.A. Harrison and N. Perrimon (1993) Simple and efficient generation of marked clones in Drosophila, Current biology : CB. 3, 424–433.

9. T. Lee and L. Luo (1999) Mosaic analysis with a repressible cell marker for studies of gene function in neuronal morphogenesis, Neuron. 22, 451–461.

10. J.S. Wu and L. Luo (2006) A protocol for mosaic analysis with a repressible cell marker (MARCM) in Drosophila, Nature Protocols. 1, 2583–2589.

11. S.R. Singh, M.K. Mishra, M. Kango-Singh, et al. (2012) Generation and staining of intestinal stem cell lineage in adult midgut, Methods Mol Biol. 879, 47–69.

12. H.-H. Yu, C.-H. Chen, L. Shi, et al. (2009) Twin-spot MARCM to reveal the developmental origin and identity of neurons, Nature neuroscience. 12, 947–953.

13. J. de Navascués, C.N. Perdigoto, Y. Bian, et al. (2012) Drosophila midgut homeostasis involves neutral competition between symmetrically dividing intestinal stem cells, The EMBO journal. 31, 2473–2485.

14. K. Beebe, W.-C. Lee, and C.A. Micchelli (2010) JAK/STAT signaling coordinates stem cell proliferation and multilineage differentiation in the Drosophila intestinal stem cell lineage, Developmental biology. 338, 28–37.

15. N. Buchon, N.A. Broderick, S. Chakrabarti, et al. (2009) Invasive and indigenous microbiota impact intestinal stem cell activity through multiple pathways in Drosophila, Genes & Development. 23, 2333–2344.

16. N. Vodovar, M. Vinals, P. Liehl, et al. (2005) Drosophila host defense after oral infection by an entomopathogenic Pseudomonas species, Proceedings of the National Academy of Sciences of the United States of America. 102, 11414–11419.

17. P. Liehl, M. Blight, N. Vodovar, et al. (2006) Prevalence of local immune response against oral infection in a Drosophila/Pseudomonas infection model, PLoS Pathogens. 2, e56.

18. O. Opota, I. Vallet-Gely, R. Vincentelli, et al. (2011) Monalysin, a novel ß-pore-forming toxin from the Drosophila pathogen Pseudomonas entomophila, contributes to host intestinal damage and lethality, PLoS Pathogens. 7, e1002259.

19. N.T. Nehme, S. Liégeois, B. Kele, et al. (2007) A model of bacterial intestinal infections in Drosophila melanogaster, PLoS Pathogens. 3, e173.

20. S.J.F. Cronin, N.T. Nehme, S. Limmer, et al. (2009) Genome-wide RNAi screen identifies genes involved in intestinal pathogenic bacterial infection, Science (New York, N.Y.). 325, 340–343.

21. M. Chatterjee and Y.T. Ip (2009) Pathogenic stimulation of intestinal stem cell response in Drosophila, Journal of cellular physiology. 220, 664–671.

22. Y. Apidianakis, C. Pitsouli, N. Perrimon, et al. (2009) Synergy between bacterial infection and genetic predisposition in intestinal dysplasia, Proceedings of the National Academy of Sciences of the United States of America. 106, 20883–20888.

23. X. Zeng, C. Chauhan, and S.X. Hou (2010) Characterization of midgut stem cell- and enteroblast-specific Gal4 lines in drosophila, Genesis (New York, NY : 2000). 48, 607–611.

24. L.E. O'Brien, S.S. Soliman, X. Li, et al. (2011) Altered modes of stem cell division drive adaptive intestinal growth, Cell. 147, 603–614.

CHAPTER III

HIPPO, TGF-B, AND SRC-MAPK PATHWAYS REGULATE TRANSCRIPTION OF THE *UPD3* CYTOKINE IN *DROSOPHILA* ENTEROCYTES UPON BACTERIAL INFECTION

This chapter represents an article published in PLOS Genetics, entitled "Hippo, TGF-β, and Src-MAPK pathways regulate transcription of the upd3 cytokine in Drosophila enterocytes upon bacterial infection" (2017) by Philip Houtz, Alessandro Bonfini, Xi Liu, Jonathan Revah, Aurélien Guillou, Mickael Poidevin, Korneel Hens, Hsin-Yi Huang, Bart Deplancke, Yu-Chen Tsai, and Nicolas Buchon.

Abstract

Cytokine signaling is responsible for coordinating conserved epithelial regeneration and immune responses in the digestive tract. In the *Drosophila* midgut, Upd3 is a major cytokine, which is induced in enterocytes (EC) and enteroblasts (EB) upon oral infection and initiates intestinal stem cell (ISC) dependent tissue repair. To date, the genetic network directing *upd3* transcription remains largely uncharacterized. Here, we have identified the key infection-responsive enhancers of the *upd3* gene and show that distinct enhancers respond to various stresses. Furthermore, through functional genetic screening, bioinformatic analyses and yeast one-hybrid screening, we determined that the transcription factors Scalloped (Sd), Mothers against dpp (Mad), and D-Fos are principal regulators of *upd3* expression. Our study demonstrates that *upd3* transcription in the gut is regulated by the activation of multiple pathways, including the Hippo, TGF-β/Dpp, and Src, as well as p38-dependent MAPK pathways. Thus, these essential pathways, which are known to control ISC proliferation cell-autonomously, are also activated in ECs to promote tissue turnover the regulation of *upd3* transcription.

Author Summary

Tissue regeneration is a fundamental process that maintains the integrity of the intestinal epithelium when faced with chemical or microbial stresses. In both healthy and diseased conditions, pro-regenerative cytokines function as central coordinators of gut renewal, linking inflammation to stem cell activity. In *Drosophila*, the upstream events that stimulate the production of the primary cytokine Unpaired 3 (Upd3) in response to indigenous or pathogenic microbes have yet to be elucidated. In this study, we demonstrate that *upd3* expression is driven in different cell types by separate microbe-responsive enhancers. In enterocytes (ECs), cytokine induction relies on the Yki/Sd, Mad/Med, and AP-1 transcription factors (TFs). These TF complexes are activated downstream of the Hippo, TGF-β and Src-MAPK pathways, respectively. Inhibiting these pathways in ECs impairs *upd3* transcription, which in turn blocks intestinal stem cell proliferation and reduces the survival rate of adult flies following enteric infections. Altogether, our study identifies the major microbe-responsive enhancers of the *upd3* gene and sheds light on the complexity of the gene regulatory network required in ECs to regulate tissue homeostasis and stem cell activity in the digestive tract.

Introduction

The digestive tract is uniquely challenged by its high degree of exposure to the external environment. The transit of nutrients through the gastrointestinal (GI) tract is accompanied by frequent introduction of biotic and abiotic stresses. In particular, digestive tissue is constantly exposed to a high density of microbes, including benign microbiota and invasive pathogens [1]. The gut epithelium performs a multifaceted role in maintaining the barrier between the host and its environment through immune responses and the maintenance of a continuous cellular monolayer [2], while digesting and absorbing nutrients. Preservation of epithelial integrity in the GI tract requires continual tissue turnover by coordinated shedding of epithelial cells along with division and differentiation of intestinal stem cells (ISCs) [1,3]. Disorders in epithelial regeneration or intestinal immunity lead to intestinal maladies including inflammatory bowel disease (IBD) and colorectal cancer [4]. Cytokines, which are central to gut homeostasis, are produced by epithelial and immune cells to properly orchestrate immune and repair responses [2,3]. The control of cytokine signaling in the digestive tract is complex, and characterizing the regulators of cytokine expression is a critical step towards fully understanding the mechanisms underlying intestinal homeostasis.

Drosophila melanogaster has emerged as a powerful model to study gut homeostasis, epithelial immunity and ISC regulation [1,5], and acts as a model for intestinal infection and pathology [6]. Like the mammalian intestine, the midgut of *Drosophila* contains ISCs that divide and differentiate to replace the absorptive, polyploid enterocytes (ECs) and secretory enteroendocrine cells (EEs) [5]. During division, midgut ISCs self-renew and give rise to a pool of transient, differentiating precursor cells called enteroblasts (EBs), which terminally differentiate into ECs. Similarly, EE cells are replaced via ISCs that divide and give rise to pre-EE progenitors

[7]. Also like the mammalian intestine, the *Drosophila* midgut is regionalized. Specifically, it can be divided into five main regions: the cardia (at the foregut-midgut junction), R1 and R2 composing the anterior midgut, R3 also known as the copper cell region, and R4 and R5 that constitute the posterior midgut [8,9].

In response to infection by microbial pathogens or, to a lesser extent, ingestion of dietary microbes, the midgut activates multiple layers of innate immunity. Among these are the induced synthesis of reactive oxygen species (ROS) by the NADPH oxidases Dual oxidase (Duox) and NADPH oxidase (Nox), and the production of antimicrobial peptides under the regulation of the immune deficiency (Imd) and JAK-STAT pathways [10-13]. Imd pathway activation is triggered by the detection of bacteria via peptidoglycan recognition receptors (PGRP-LE and PGRP-LC) [14,15] while JAK-STAT pathway activation results from the expression and secretion from the gut epithelium of *Drosophila* IL-6 family cytokines: Unpaired 3 (Upd3) and Unpaired 2 (Upd2) [16].

In addition to immune activation, enteric infections also stimulate EC delamination and tissue turnover resulting in ISC-dependent tissue repair [12,17,18]. This regenerative process has been shown to depend strongly upon the activation of multiple pathways in progenitor cells, including the Hippo, Wingless, JAK-STAT and EGFR pathways [13,17,19,20]. Bacterial infection, as well as genetically induced apoptosis in ECs, triggers the transcription and secretion of Upd3 in ECs and EBs [13,17], which subsequently initiates a homeostatic feedback loop and ultimately activates ISC-mediated regeneration. The Upd cytokines activate the JAK-STAT pathway in progenitor cells and visceral muscles, which in turn stimulates the release of epidermal growth factors (EGFs) by these cells [19,21,22]. Upd3-dependent secretion of the Epidermal Growth Factors (EGFs) Vein from visceral muscle and Spitz from EBs stimulates the EGFR

pathway in ISCs to promote proliferation. Upd3-mediated JAK-STAT activity is also required to promote rapid EB differentiation, thus accelerating epithelium turnover upon infection [13,17]. Cytokines, such as Upd3, therefore act as master regulators of intestinal homeostasis, as they are both required and sufficient to trigger immunity and tissue repair. Accordingly, the loss of Upd3 increases susceptibility to enteric infections, while ectopic induction of Upd3 induces dysplastic lesions in the gut [13,16]. However, a detailed knowledge of upstream enteric stress sensors as well as the downstream transcriptional regulatory network controlling Upd3 production in ECs remains elusive.

In this study, we initiated analysis of the transcriptional regulation of *upd3*, the primary cytokine responsible for inducing ISC proliferation and midgut renewal. We first identified two microbe-responsive enhancer sequences in the *upd3* gene that direct its expression in ECs, and an additional enhancer that regulates *upd3* induction in progenitor cells. A subsequent EC-specific RNAi knockdown screen of all the *Drosophila* transcription factors (TFs) was performed to determine which TFs govern the activity of the central infection-responsive enhancer region. From this screen, we identified 39 TFs required for enhancer induction, and 103 TFs that triggered aberrant induction when knocked down. This study was complemented by an *in vitro,* yeast one-hybrid screen as well as bioinformatic analyses of the enhancer sequence to identify TFs that may act as direct regulators of *upd3* expression. Notably, we identified the Yorkie (Yki)/Scalloped (Sd) complex, the AP-1 complex (D-Jun and D-Fos), Mad and Snail (Sna) as key regulators of *upd3* transcription. We proceeded to explore the upstream regulatory pathways that control the activity of these major TFs. We determined that transcriptional induction of *upd3* in ECs requires the Mitogen Activated Protein Kinases (MAPKs) p38b and D-ERK, downstream of Src oncogene (Src) Family Kinases (SFKs) and Raf, which converge on AP-1 activation. Surprisingly, the Stress

Activated Protein Kinase (SAPK) cascade seems to be necessary for only a minimal portion of AP-1 function in ECs. In addition, a Misshapen (Msn)-Warts (Wts)-Yki/Sd pathway, independent of Hippo (Hpo), is essential for full *upd3* expression. Finally, we found that the Decapentaplegic (Dpp) pathway is also required for *upd3* induction in ECs. Altogether, these results improve our understanding of the complex regulation of midgut tissue renewal by identifying the key TFs and pathways that control cytokine signaling in the intestinal epithelium in response to infection.

Results

Upd3 transcription is regulated by a combination of microbe-responsive, cell-specific and region-specific enhancers

Upon oral infection by entomopathogenic bacteria like *Erwinia carotovora ssp. carotovora 15* (*Ecc15*) or *Pseudomonas entomophila* (*Pe*), Upd3 acts as a signal to trigger antibacterial and reparative host responses [17,23]. We characterized this response through RT-qPCR measurements of midgut *upd3* expression, taken over the course of a week following ingestion of *Ecc15* or *Pe.* We found that *upd3* transcription was strongly induced in response to ingestion of these pathogens and peaked between 8-24h post-infection before returning to basal levels within 96h (Fig 3.1A-B). In addition, peak expression of *upd3*, as well as the time that it takes to return to basal expression, increases with bacterial dose (A-B Fig 3.1A-B). These results demonstrate that *upd3* is regulated by infection at the transcriptional level and varies with the amplitude of the given threat.

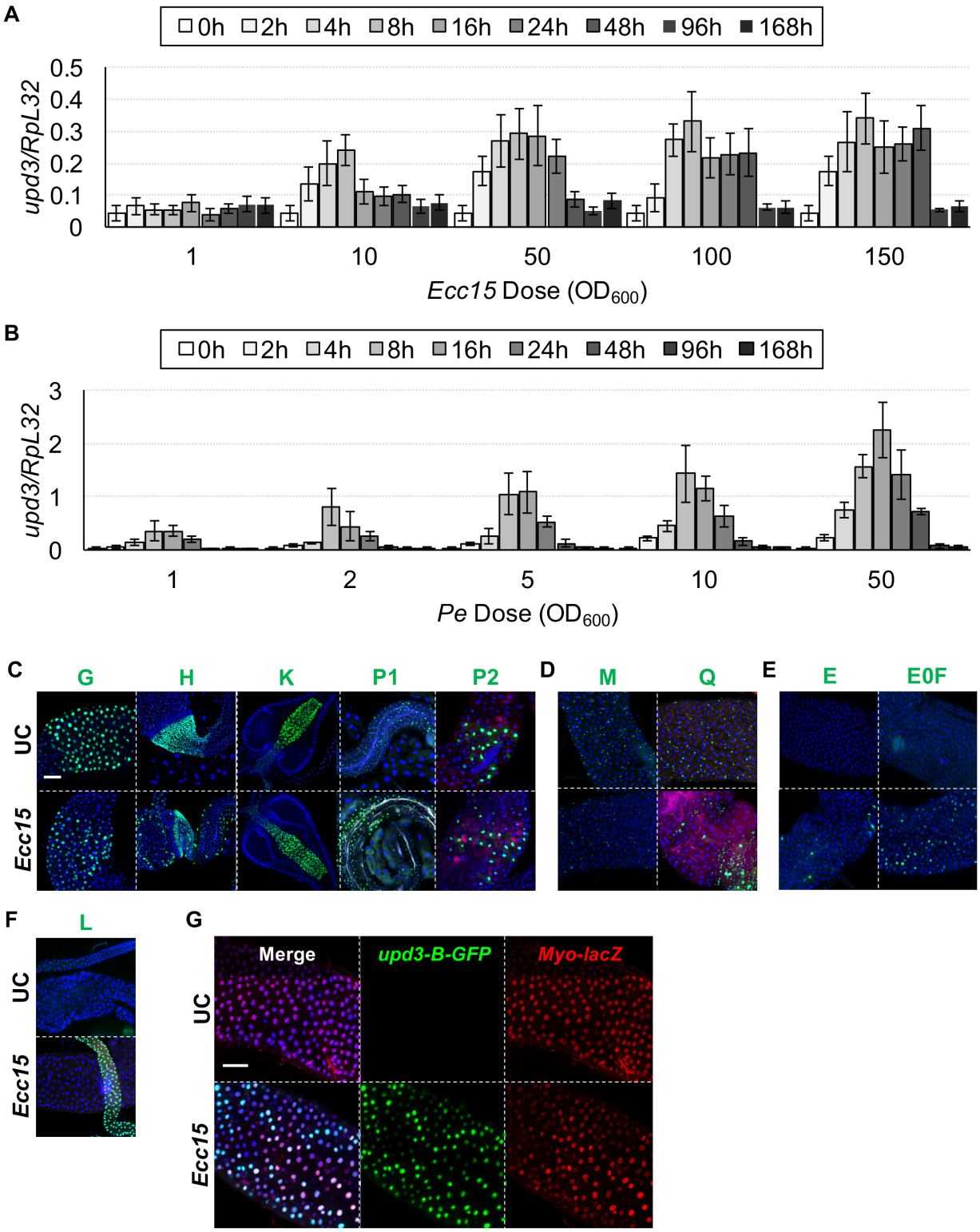

Figure. 3.1. Midgut *upd3* induction upon infection is controlled by multiple enhancer regions and is proportional to pathogen dose. (A, B) RT-qPCR measurements of *upd3* expression over multiple time points upon oral infection by *Ecc15* and *Pe,* respectively. Following either *Ecc15* or *Pe* infection, *upd3* induction peaks at 8-24h and returns to basal levels by 96h. (C) Enhancer

regions G, H, K, P1 and P2 drive expression in discrete anatomical structures of the digestive tract. For a detailed description, see S Table 3.1. (D) Enhancers M and Q induce a constant signal in small epithelial cells. (E) Enhancer regions E and E0F seem to direct transcription inconsistently in a few scattered cells along the midgut upon infection. (F) Enhancer L drives GFP expression in salivary glands in response to infection. (G) *upd3* enhancer region B drives an infection-induced, EC-specific GFP signal, similar to that of enhancer region C. Mean values of at least 3 repeats are represented ± SEM. Scale bars are 50μm.

As an initial step to characterize *upd3* regulation in the digestive tract, we sought to identify the key enhancer regions that control its expression, especially its induction in response to pathogens. To this end, we generated twenty-one GFP transcriptional reporters covering the entire *upd3* locus. Overlapping fragments of ~1-1.5Kb were cloned upstream of a GFP reporter, starting from 4.2Kb upstream of the *upd3* start site and ending 7.3Kb downstream of the gene. Reporters were designated *upd3-A-GFP* through *upd3-R-GFP* (Fig 3.2A, S Table 3.1). We first evaluated the transcriptional activity of these reporters both in unchallenged (UC) and orally infected flies. Seven lines gave no detectable signal in the digestive system under any condition (enhancers A, D, F, J, N, O1, O2, see Fig 3.2A). The remaining enhancer regions were divided into five categories based on their expression profile: seven enhancer regions drove GFP expression constitutively, with little change in response to infection by *Ecc15*. *1)* For five of these lines, the signal was limited to specific regions of the gut, including the foregut and hindgut (*upd3-H-GFP*), the foregut only (*upd3-K-GFP*), the hindgut only (*upd3-P1-GFP*), and the copper cell region (*upd3-G-GFP* and *upd3-P2-GFP*) (Fig 3.1C). *2)* The remaining two constitutive enhancer regions (*upd3-M-GFP* and *upd3-Q-GFP*) are active throughout the midgut in populations of small cells (Fig 3.1D). Interestingly, cells expressing *upd3-M-GFP* accumulate upon infection (Fig 3.2B). Overlap of the *upd3-M-GFP* signal and immunostaining of the progenitor marker *esg-lacZ* [24] revealed that the *upd3-M-GFP* reporter is specific to ISCs and EBs, and that the increase in total signal upon infection is thus secondary to progenitor cell proliferation (Fig 3.2B). *3)* Two additional enhancer

regions (*upd3-E-GFP* and *upd3-E0F-GFP*) drove GFP expression in sporadic ECs of the R2 and R4 midgut segments upon infection (S1E Fig). *4)* One enhancer drove inducible *upd3* expression only in the salivary glands (*upd3-L-GFP*, Fig 3.1F). *5)* Finally, we identified four infection-responsive enhancer regions, which show little or no GFP signal in UC conditions, but are activated upon infection: these include two overlapping regions of the *upd3* promoter (regions B-C), region I, and region R (Fig 3.2A). Enhancer lines *upd3-B-GFP*, *upd3-C-GFP*, and *upd3-I-GFP* express GFP exclusively in ECs during infection, as shown by co-immuno-staining of GFP and the EC marker *Myo-lacZ* (Fig 3.2C, D and Fig 3.1G). The *upd3-I-GFP* signal was stronger in the copper cell region and less consistent in the rest of the midgut. In contrast, *upd3-R-GFP* shows activity upon infection only in the ISC and EB cells, marked by *esg-lacZ* (Fig 3.2E). Of note, the expression patterns identified in our study recapitulate the known *upd3* signaling dynamics in the gut, including induction in ECs and progenitor cells upon stress [13,17,23], as well as robust local expression in the middle midgut and in the cardia [8], suggesting that we adequately captured the complexity of *upd3* regulation. Altogether, these results indicate that *upd3* expression is controlled by several classes of enhancers, including microbe-responsive and region and/or cell type-specific regulators.

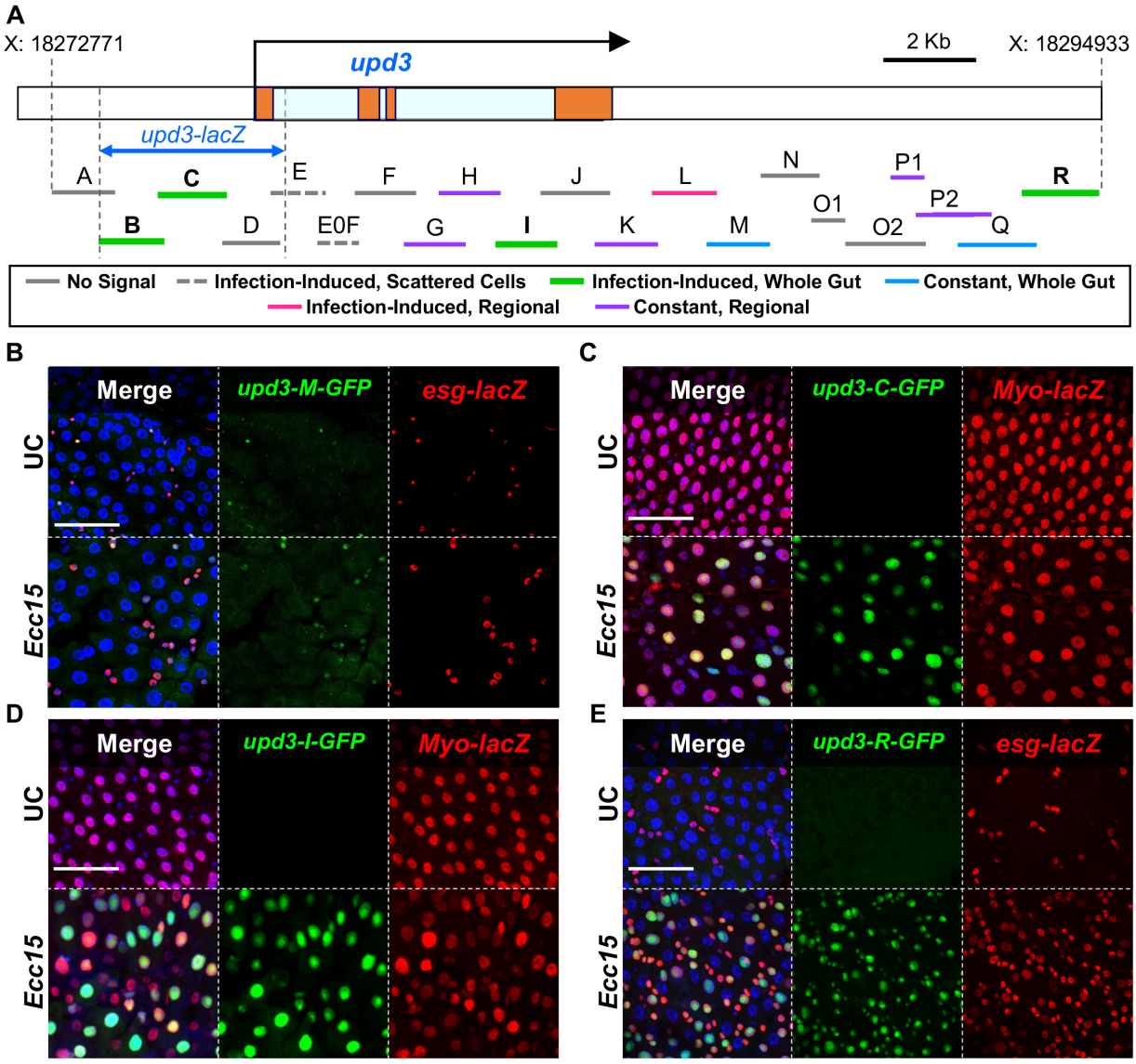

Figure 3.2. The *upd3* gene is regulated by cell-specific, region-specific and infection-responsive enhancers. (A) Schematic of the *upd3* gene and the 21 overlapping sequences used to create GFP reporter lines. The *upd3* exons are represented by orange blocks and the introns are light blue. Putative enhancer regions have been color coded by their ability to drive GFP expression as follows: Solid Grey– no midgut signal, Dashed Grey– infection induced signal in scattered cells, Green– infection-induced signal throughout the gut, Blue– constant signal throughout the gut, Pink– infection induced signal in a specific midgut region, Purple– constant signal confined to a specific midgut region. (B) Enhancer region M drives an unvarying GFP signal in *esg-lacZ* expressing cells (ISCs and EBs) in all regions. (C, D) Both the C and I enhancer region sequences drive GFP in an infection-inducible manner, specifically in *Myo*-positive cells (ECs) throughout the midgut. (E) Enhancer region R drives infection-induced GFP expression in *esg*-positive cells (ISCs and EBs). (B, C, D, E) Confocal microscopy images taken at 40x magnification with four color channels. DAPI stained nuclei in Blue, GFP in green and antibody stained β-Gal in red. Scale bars are 50µm.

Microbe-responsive *upd3* enhancers are stress-activated enhancers

Upd3 acts as a major regulator of intestinal epithelial renewal and its expression is induced by a diversity of enteric stresses, not only limited to bacterial infections [16]. For instance, feeding bleomycin (bleo), which induces gut epithelial cell loss, or dextran sulfate sodium (DSS) that disrupts basal membrane, induces *upd3* transcription in the gut (Fig 3.3A) and promotes intestinal epithelial turnover (Fig 3.3B) [25]. Furthermore, basal levels of *upd3* expression and subsequent tissue turnover have been shown to be regulated by the microbiota [16,26]. We confirmed that the guts of germ-free (GF) flies express a lower degree of *upd3* than conventionally raised (CR) flies (Fig 3.3C). These results suggest that the regulation of *upd3* expression integrates signals from multiple stimuli, including various intestinal injuries and even benign gut microbes.

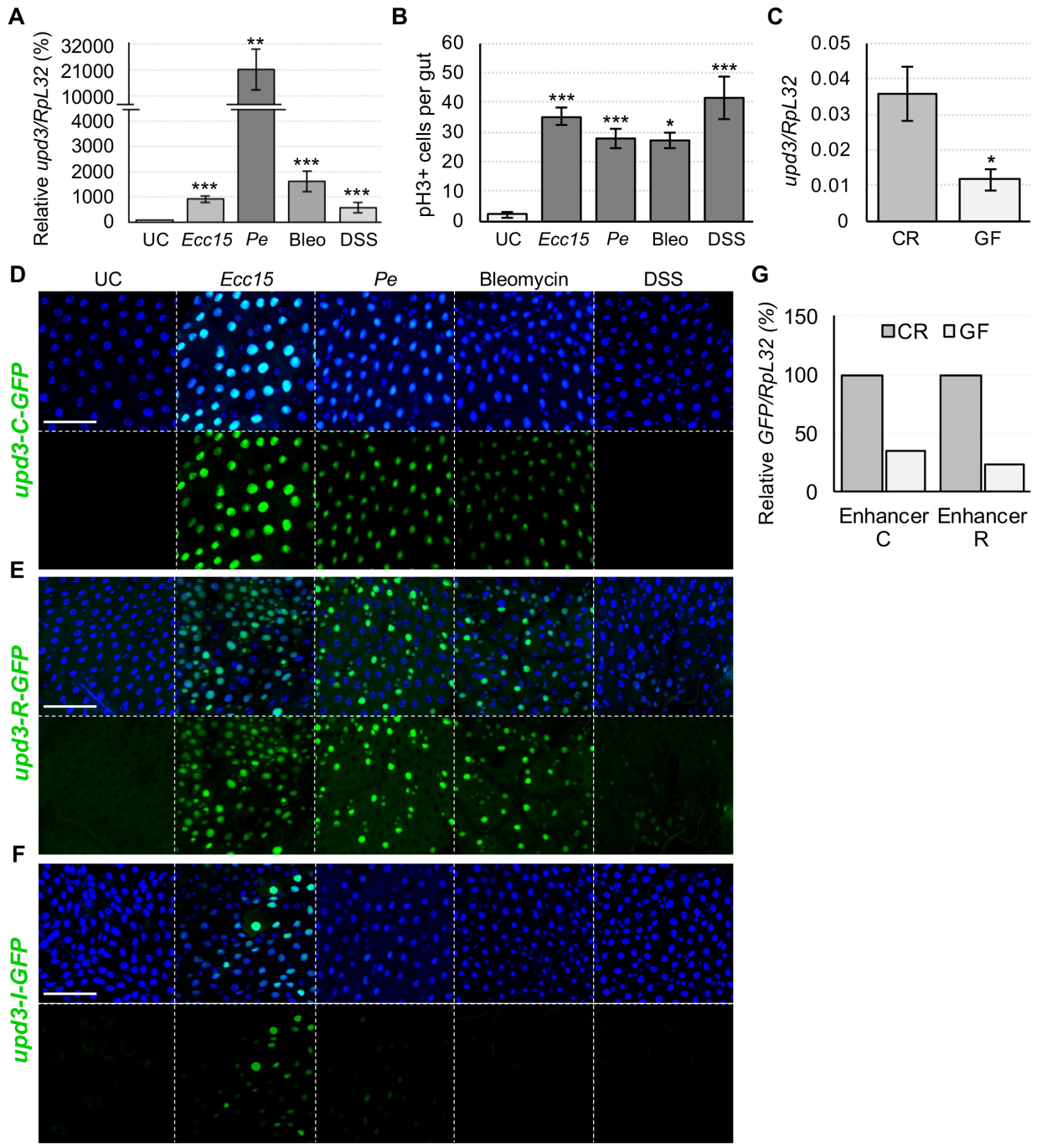

Figure 3.3. Bacterial infection, stress and the microbiota induce *upd3* through distinct enhancers. (A) RT-qPCR measured *upd3* expression is significantly induced by *Ecc15* and *Pe* infection, as well as bleomycin (bleo) treatment and DSS. (B) ISC proliferation, measured by phospho-Histone H3 (pH3) immunostaining, is triggered in response to ingestion of harmful bacteria (*Ecc15* and *Pe*) and chemical stressors (bleo and DSS). (C) RT-qPCR measurements of *upd3* transcription in the gut of germ-free (GF) flies shows reduced expression compared to their conventionally reared (CR) counterparts. (D, E) Confocal imaging shows that *upd3-C-GFP* and *upd3-R-GFP* strongly induce GFP expression in response to all presented stresses, except for DSS treatment. (F) In contrast, enhancer I responds exclusively to *Ecc15* and marginally to *Pe* infection

by GFP induction. (G) Measuring GFP expression in *upd3-C-GFP* and *upd3-R-GFP* flies by RT-qPCR, normalized to the GFP expression in each line under CR conditions, reveals a reduction in basal enhancer C and R activity in GF conditions. Scale bars are 50μm. Statistical significance: mean values of at least 3 repeats are represented ± SEM. *p<0.05, **p<0.01, ***p<0.001 (student's t-test).

We next examined whether these diverse stimuli all activate the microbe-responsive enhancers that we had previously identified. To this purpose, we fed *upd3-C-GFP*, *upd3-I-GFP*, and *upd3-R-GFP* flies damaging bacteria (*Ecc15* and *Pe*) and harmful chemicals (DSS and bleo) at doses that trigger comparable epithelium renewal rates. *Upd3-C-GFP* induced GFP expression in response to every treatment except DSS (Fig 3.3D). Enhancer region R responded to *Ecc15*, *Pe*, bleo, and weakly to DSS by inducing GFP in progenitor cells (Fig 3.3E). In *upd3-I-GFP* flies, a GFP signal was only detected upon infection with *Ecc15*, and mostly in the copper cell region, while little signal was detected in response to *Pe* and no significant signal was observed in response to bleo or DSS treatment (Fig 3.3F). Our findings imply that different stresses (i.e. DSS vs other stressors) may be interpreted through distinct cellular mechanisms and thus stimulate cytokine production via separate enhancers. They also suggest that all stressors that affect ECs (*Ecc15*, *Pe*, bleo) stimulate *upd3* expression mainly through enhancer region B-C.

We next investigated whether the infection responsive enhancers C and R also react to the presence of microbiota. To this end, we generated CR and GF *upd3-C-GFP* and *upd3-R-GFP* flies and monitored their levels of GFP (Fig 3.3G and Fig 3.4A-B). The basal GFP signals of CR flies is already very low with few GFP-positive cells detectable microscopically per midgut, rendering qualitative analysis challenging. We therefore estimated enhancer C and R activity by quantifying GFP levels by RT-qPCR. This revealed a significant reduction in enhancer C and R-driven GFP expression in GF midguts compared to CR ones (Fig 3.3G). Our results demonstrate that both indigenous and pathogenic bacteria, as well as chemical stressors like bleo, all regulate *upd3*

expression through enhancers C and R, albeit to differing degrees. Altogether, these data suggest that enhancers C and R are microbe-responsive and act as stress sensing enhancers.

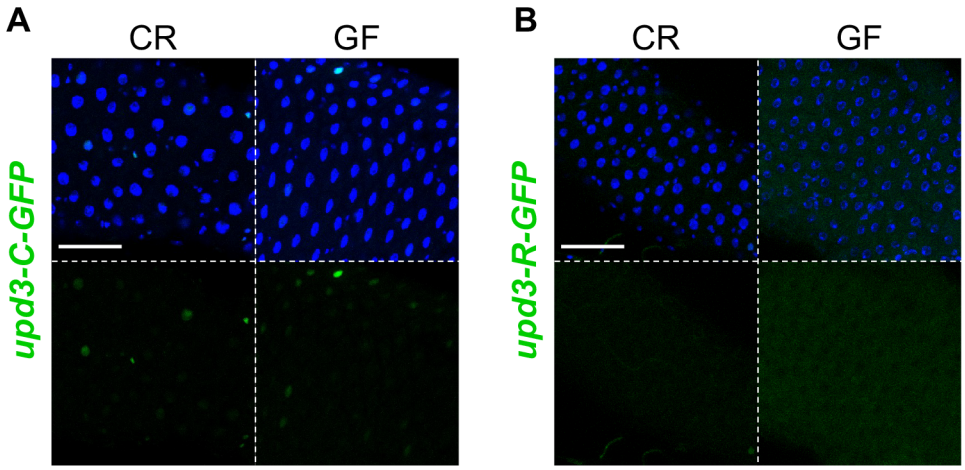

Figure 3.4. Qualitative comparison of visible *upd3-C-GFP* and *upd3-R-GFP* signals in CR and GF flies. (A, B) Enhancer regions C and R display no obvious difference in visible GFP signal between CR and GF conditions. Scale bars are 50µm.

in vivo, *ex vivo* and *in silico* screens to identify key TFs regulating infection-induced *upd3* transcription

We next aimed to identify the molecular mechanisms that control *upd3* transcription in response to infection. As *upd3* transcription is induced by infection in both ECs (enhancers B-C and I in Fig 3.2C-D, Fig 3.1G and [12,16,17]) and EBs (enhancer R in Fig 3.2E and [23]), we began by determining which cell type contributes the most to global *upd3* production in the midgut upon infection. RT-qPCR analysis of *upd3* expression in guts in which *upd3* was knocked-down by RNAi in ECs (*Myo-Gal4^{TS}>UAS-upd3-IR*) or EBs (*Su(H)-Gal4^{TS}>UAS-upd3-IR*) confirmed that ECs are the principal source of *upd3* in the gut upon infection with *Ecc15* or *Pe* (Fig 3.5A-B). In agreement with this, knockdown of *upd3* in ECs strongly reduced ISC proliferative activity (Fig 3.5C). This suggests that the key enhancers controlling the levels of Upd3 in the gut are those functional in ECs (regions B, C and I). As *upd3-I-GFP* responds only moderately to infection by

Ecc15, but not *Pe* (Fig 3.3F), we decided to focus on enhancer regions B and C, which respond strongly to infectious bacteria and cellular stress. To further investigate the importance of the B-C enhancer region in activating *upd3* expression in response to infection we created two new reporter lines, one that comprises the entire *upd3* locus (all enhancers included) and encodes an NLS-GFP-tagged Upd3 protein (full locus) (Fig 3.6A), and one in which the B-C sequence was deleted from the full locus (full locus – (B+C)) (Fig 3.6A). While the complete *upd3* sequence was able to direct an infection-induced GFP signal in the midgut, deletion of the B-C region eliminated all signal (Fig 3.6B) demonstrating that enhancers B and C are central to *upd3* regulation. In addition, quantification of *upd3-C-GFP* signal revealed that the kinetics of GFP induction upon infection is in accordance with total gut *upd3* expression (Figs 3.1A and 3.5D). Finally, the promoter of the *upd3* reporter construct, *upd3-lacZ*, which covers regions B and C (Fig 3.2A), drove a strong and consistent signal in the same cells that are marked by *upd3-C-GFP* (Fig 3.5E). We conclude that the regulation of enhancer regions B and C (and thus of *upd3-lacZ*) is sufficient to induce *upd3* with a faithful EC expression pattern during enteric infection.

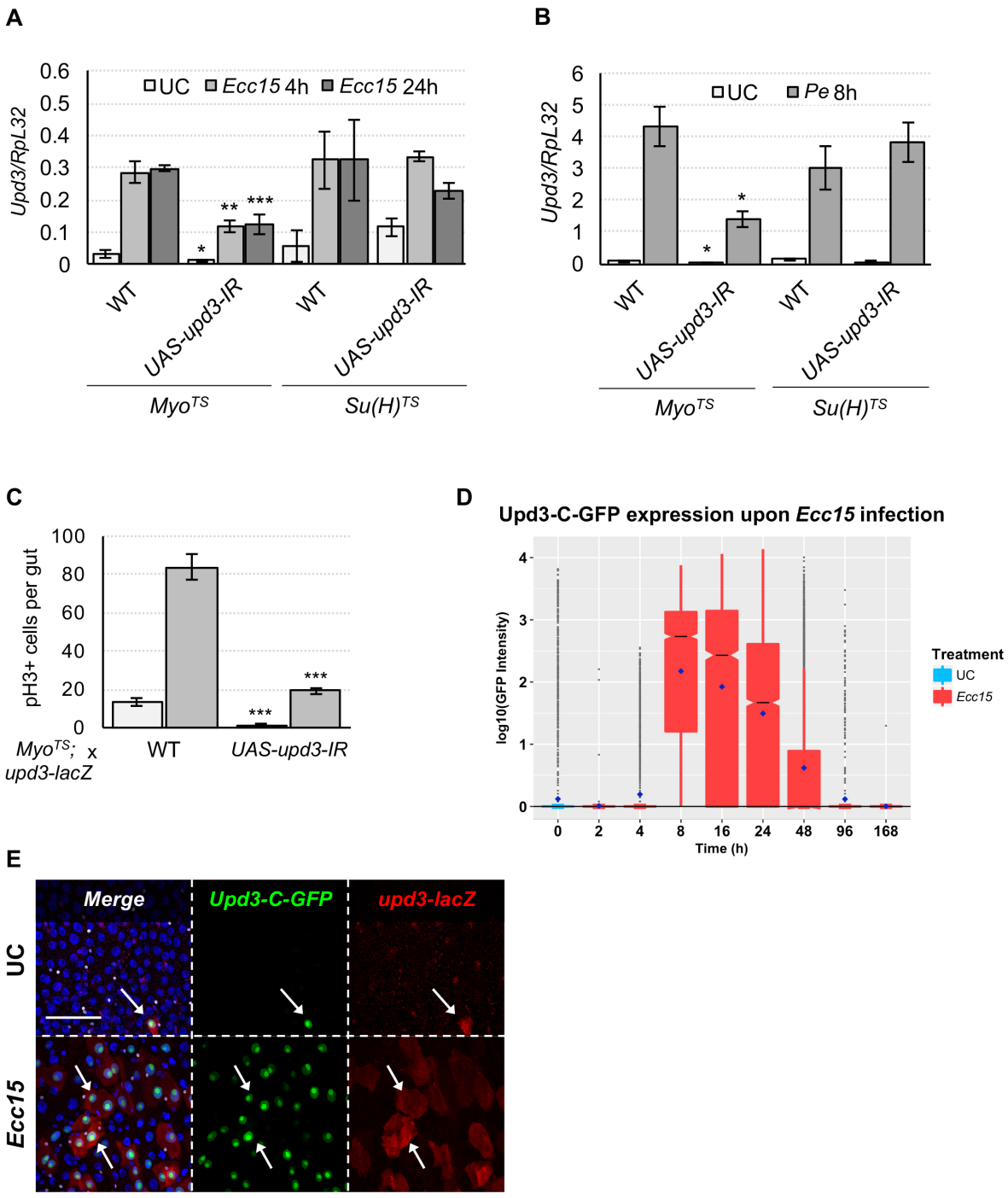

Figure 3.5. Infection-induced *upd3* transcription occurs specifically in ECs and closely matches the *upd3-C-GFP* and *upd3-lacZ* signals. (A, B) RT-qPCR measurements of total gut *upd3* expression following EC (*Myo*) or EB (*Su(H)*)-specific knockdown of *upd3*, and *Ecc15* (A) or *Pe* (B) infection, indicates that most *upd3* induction is derived from ECs. (C) Accordingly, knockdown of *upd3* specifically in ECs (*Myo-Gal4*^{TS} driven UAS-RNAi) is adequate to strongly inhibit ISC proliferation in the midgut, as revealed by pH3+ cell counting. (D) A measure of GFP intensity in the cells of *upd3-C-GFP* guts for multiple time-points following *Ecc15* infection shows a peak in intensity at 8-24h and a return to basal levels by 96h. Black bars represent the median

and blue diamonds represent the mean GFP intensity for each time point. (E) The signals driven by *upd3-C-GFP* and *upd3-lacZ* are induced upon *Ecc15* infection and overlap in the same ECs. White arrows indicate cells in which *upd3-C-GFP* and *upd3-lacZ* expression overlap. Statistical significance: mean values of at least 3 repeats are represented ± SE. *p<0.05, **p<0.01, ***p<0.001 (student's t-test). Scale bar is 50µm.

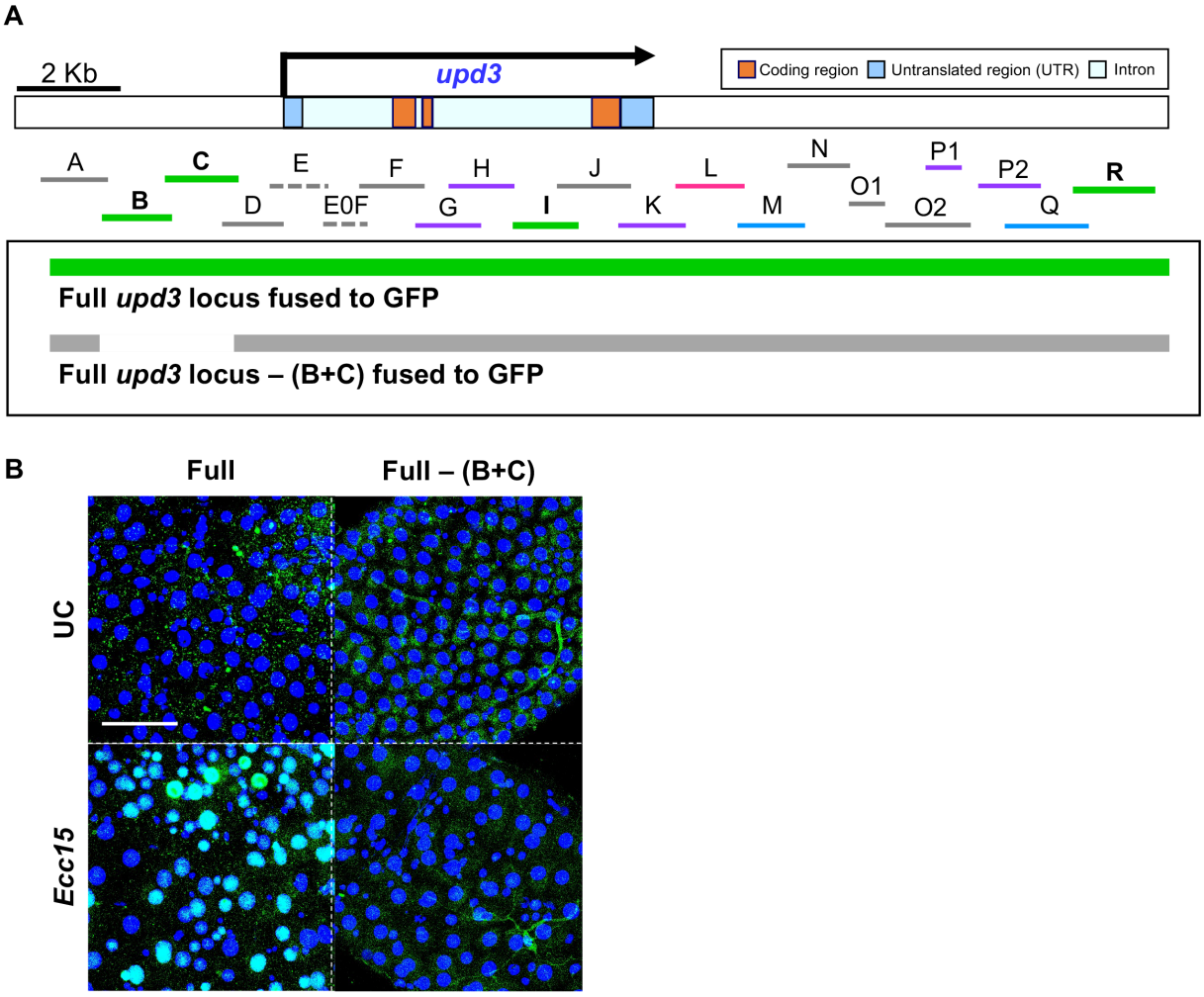

Figure 3.6. Enhancer sequence B-C is critical for driving infection-induced expression of genes using the *upd3* locus. (A) Schematic of the *upd3* gene and the 21 overlapping sequences used to create GFP reporter lines. The *upd3* exons are represented by orange blocks and the introns are light blue. Putative enhancer regions have been color coded by their ability to drive GFP expression as follows: Solid Grey– no midgut signal, Green– infection-induced signal throughout the gut. (B) A sequence covering the *upd3* locus is capable of directing an infection-induced GFP signal in the midgut, but is unable to after the deletion of enhancer sequence B-C. Scale bars are 50µm.

In order to identify the key regulators of *upd3* acting through enhancers B and C, we initiated a comprehensive set of *in vivo*, *ex vivo* and *in silico* screens. First, a functional RNAi screen was performed by driving RNAi-mediated knockdown of 632 TFs (84% of all known and predicted TFs of *D. melanogaster*) using all available *UAS-RNAi* transgenic lines of the TRiP collection (Transgenic RNAi Project, Fig 3A) [27]. The Gal4/Gal80^{TS} system (*Myo-Gal4^{TS}, upd3-lacZ*) allowed us to express RNAi specifically in the ECs of adult flies, thus minimizing developmental or systemic side effects. When available, two different *UAS-RNAi* lines were tested (see S Table 3.2), bringing the total number of lines to 755. Following one week of RNAi induction, five guts were dissected from both unchallenged (UC) and *Ecc15* orally infected flies, and ß-galactosidase enzymatic activity levels were measured as a read-out of *upd3* induction. F1 progeny (*Myo-Gal4^{TS}, upd3-lacZ>UAS-RNAi*) with *upd3-lacZ* activity that was, compared to controls, increased or decreased by 40% upon infection and/or increased or decreased by 50% in UC conditions (see methods section and Fig 3.8A-B) were selected as positive hits. We further estimated the strength of the positive hit phenotypes by calculating their z-score compared to the entire population of crosses tested under the same conditions (UC or *Ecc15* infected) (S Table 3.2). Based on these criteria, we identified 149 lines with significantly altered *upd3-lacZ* expression in either challenged or unchallenged conditions. Positive hits were retested at least twice and 138 TFs were found to significantly alter *upd3-lacZ* expression when suppressed (Fig 3.7A-B, S Table 3.2). Specifically, RNAi against 17 TFs in ECs resulted in reduced basal *upd3-lacZ* in UC flies, and knockdown of 66 TFs increased *upd3-lacZ* under the same UC conditions (Fig 3.7A and 3.8C-D). Furthermore, 24 TFs seemed required for *upd3-lacZ* expression upon infection while RNAi against 53 TFs increased *Ecc15*-induced *upd3-lacZ* activity (Fig 3.7A and 3.8C-D). These results indicate that the knockdown of many TFs results in *upd3-lacZ* induction rather than inhibition. This is in

agreement with the fact that disrupting gut homeostasis by modulating key TFs such as *GATAe*, *Ptx1*, *Activating transcription factor 3* (*Atf3)*, *X box binding protein-1 (Xbp1)*, either in normal or stressed conditions, can indirectly result in higher expression levels of *upd3* [8]. Based on EC-specific transcriptomic data obtained by Fluorescence-Activated Cell Sorting (FACS) of ECs coupled to RNA-seq, we established that 92% of TFs identified as positive hits by our screen are expressed in ECs (RPKM $\geq$ 0.1) and 63% of the TFs required for *upd3-lacZ* expression are transcriptionally regulated (fold RPKM induction $\geq$ 1.5 or $\leq$ -1.5) upon *Pe* infection (Fig 3.8E) [28,29]. This indicates that most of the TFs identified as *upd3* regulators by our screen are expressed in ECs and regulated upon enteric infection, and serves as an indirect control of our screen quality. Surprisingly, TFs that alter *upd3-lacZ* expression in basal conditions or upon infection are poorly correlated with one another (R^2=0.24, Fig 3.8F), suggesting that different mechanisms regulate *upd3* expression in basal homeostasis and upon infection. Interestingly, positive hits in our screen were enriched for TFs involved in animal development and tissue growth rather than stress or immune responses, again suggesting that epithelial morphogenesis and dynamics are critical to *upd3* regulation (Fig 3.8G). Altogether, our functional genetic screen identified multiple TFs that have the capacity to modulate the expression of *upd3-lacZ*, particularly in response to infection.

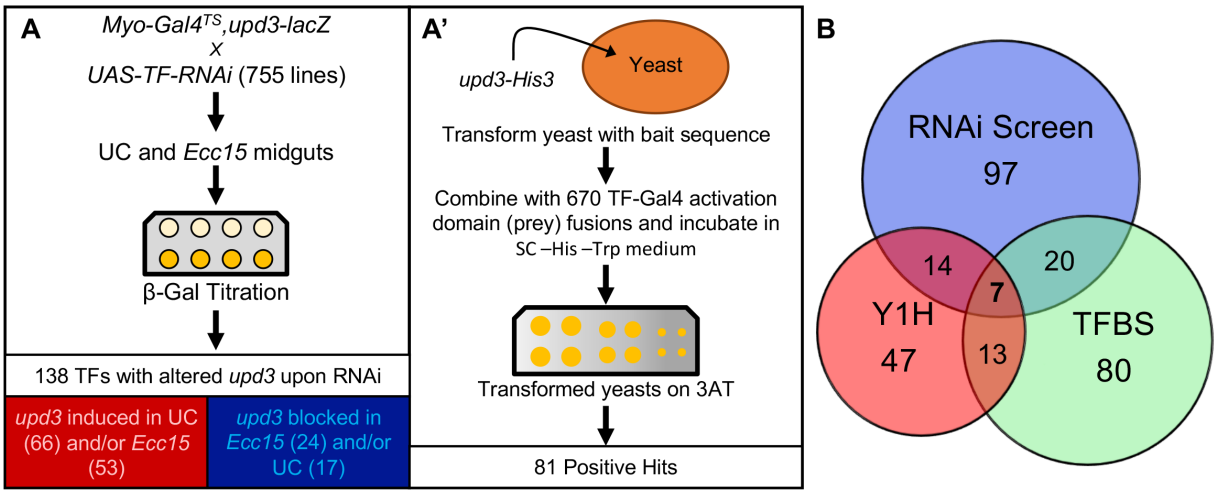

C

Gene Acronym	Rel lacZ UC	Z-score UC	Rel lacZ Ecc15	Z-score Ecc15	TFBS	Y1H	EC expr (RPKM)	EC reg (fold)
POSITIVE REGULATORS OF UPD3 (DIRECT)								
kay	0.45	-1.89	0.32	-3.46	yes	++	40.11	1.43
sd	0.57	-1.32	0.38	-2.91	yes	+/-	2.50	1.66
Trl	0.68	-0.90	0.39	-2.84	yes	+	0.43	-4.65
pan	0.68	-0.91	0.52	-1.80	yes	++	0.28	-5.55
gt	0.47	-1.75	1.21	1.02	yes	++	0.61	-1.48
ADDITIONAL POSITIVE REGULATORS OF UPD3								
sna	0.59	-1.24	0.43	-2.43	yes	-	1.51	130.55
Jra	0.76	-0.64	0.57	-1.51	no	-	26.87	4.30
yki	0.69	-0.85	0.59	-1.40	no	-	11.24	-1.36
Mad	0.41	-2.11	0.64	-1.12	yes	-	11.11	-1.46
Rx	0.84	-0.40	0.52	-1.85	yes	-	0.01	switched on
Ubx	0.84	-0.39	0.60	-1.36	yes	-	0.01	-30.17
CG33213	0.64	-1.05	0.59	-1.39	no	-	1.63	12.14
GLOBAL EPIGENETIC REGULATORS								
CtBP	0.73	-0.73	0.49	-2.05	no	-	18.31	2.56
TRR	1.36	0.76	0.49	-2.02	no	-	0.51	-1.41
MBD-like	1.06	0.16	0.59	-1.39	no	-	9.23	4.42
color legend	<0.9x UC, <0.7x Ecc15				<0.5x UC, <0.6 Ecc15			

Gene Acronym	Rel lacZ UC	Z-score UC	Rel lacZ Ecc15	Z-score Ecc15	TFBS	Y1H	EC expr (RPKM)	EC reg (fold)
NEGATIVE REGULATORS OF UPD3 (DIRECT)								
Ptx1	1.58	1.11	1.88	2.49	yes	++	2.94	-5.90
achi	2.03	1.71	1.33	1.33	yes	+	0.83	1.44
aop	1.53	1.04	1.56	1.87	no	+	1.86	3.99
CrebB-17A	4.04	3.34	1.43	1.56	no	+	2.34	2.81
lola	3.58	3.06	0.86	-0.14	no	+	2.62	-1.27
Atf3	2.25	1.95	0.80	-0.40	no	++	33.47	-1.03
NEGATIVE REGULATORS OR ALTERING GUT HOMEOSTASIS								
GATAe	8.74	5.18	2.02	2.73	no	-	6.76	-1.58
Xbp1	4.80	3.75	1.60	1.94	no	-	133.93	-2.53
dwg	2.35	2.05	1.89	2.50	no	-	4.24	4.87
hang	1.93	1.59	1.74	2.23	no	-	1.26	1.30
GLOBAL EPIGENETIC REGULATORS								
MBD-R2	8.24	5.04	2.93	3.98	no	+	3.67	1.31
Tip60	2.80	2.47	1.59	1.93	no	++	1.62	4.16
chm	3.67	3.11	2.47	3.41	no	-	0.89	1.21
dom	9.43	5.36	1.84	2.41	no	-	1.59	-1.69
trx	1.75	1.35	0.80	-0.38	no	-	0.89	1.57
color legend	>1.5x UC, >1.3x Ecc15				>2.0x UC, >1.5x Ecc15			

D

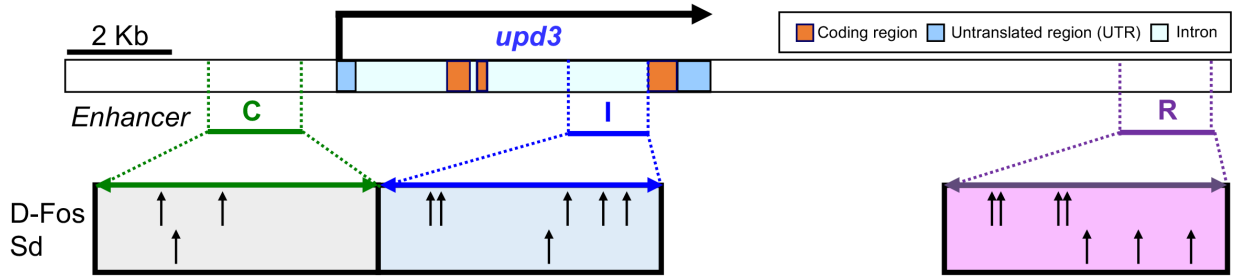

Figure 3.7. Combination of *in vivo*, *in vitro*, and *in silico* TF screens identifies direct and indirect regulators of *upd3* transcription. (A) Basic schematics of the RNAi (A) and yeast one-hybrid screens (A') along with the number of positive TF hits for each. (B) Venn diagram displaying the number of positive hit TFs identified by each screen and identified by multiple approaches. (C) Summary table of important TF hits organized by whether they induced or suppressed *upd3* induction, as well as by their TF category: putative direct regulators of *upd3* that likely bind to enhancer regions of the gene, indirect regulators that lack evidence for direct binding potential but have strong phenotypes and probable cause for controlling *upd3*, and epigenetic regulators that may influence *upd3* expression by modifying genomic DNA structure. The seven

genes that were positive hits for all three screens are indicated by red text. (D) Schematic representation of D-Fos and Sd binding motifs present in *upd3* enhancer regions C (Green), I (Blue), and R (Purple).

Figure 3.8. The regulation of Upd3 differs in basal and infected conditions. (A-B) The relative *upd3-lacZ* values for each of the 718 lines used in our screen in either UC conditions (A) or upon infection (B) are depicted here. Three controls are used in these experiments (*Myo-Gal4^{TS}; upd3-lacZ* x *attP2, attP40* and *Cs*) and their variation across 66 sets of experiments is depicted (brown, vertical line of points). The distribution of these control values due to inter-experimental variation was used to establish thresholds for determining positive hits (yellow dotted line is the threshold for increased expression and blue dotted line is the threshold for decreased expression). (C-D) Venn diagrams representing the overlap between TF hits inducing (C) or reducing (D) *upd3-lacZ* activity when knocked-down in ECs, in both basal condition and upon infection, showing only minor overlap between the two conditions. (E) Venn diagram showing the overlap between TFs considered as positive hits in our screen and their expression in ECs and/or regulation upon oral infection (based on [28]). Positive hits in the screen are enriched in genes that are expressed and regulated in ECs. (F) A scatter plot representing the relative effect of each TF on basal (x-axis) and infected (y-axis) conditions demonstrates that TFs modulating *upd3-lacZ* activity in UC and infected conditions are not correlated. Control samples are represented by orange points. (G) Gene Ontology Enrichment analysis demonstrates that the positive hit TFs identified in our screen are strongly enriched for involvement in development and epithelium morphogenesis as shown in this table. Statistical significance: mean values of at least 3 repeats are represented ± SE. *$p<0.05$, **$p<0.01$, ***$p<0.001$ (student's t-test).

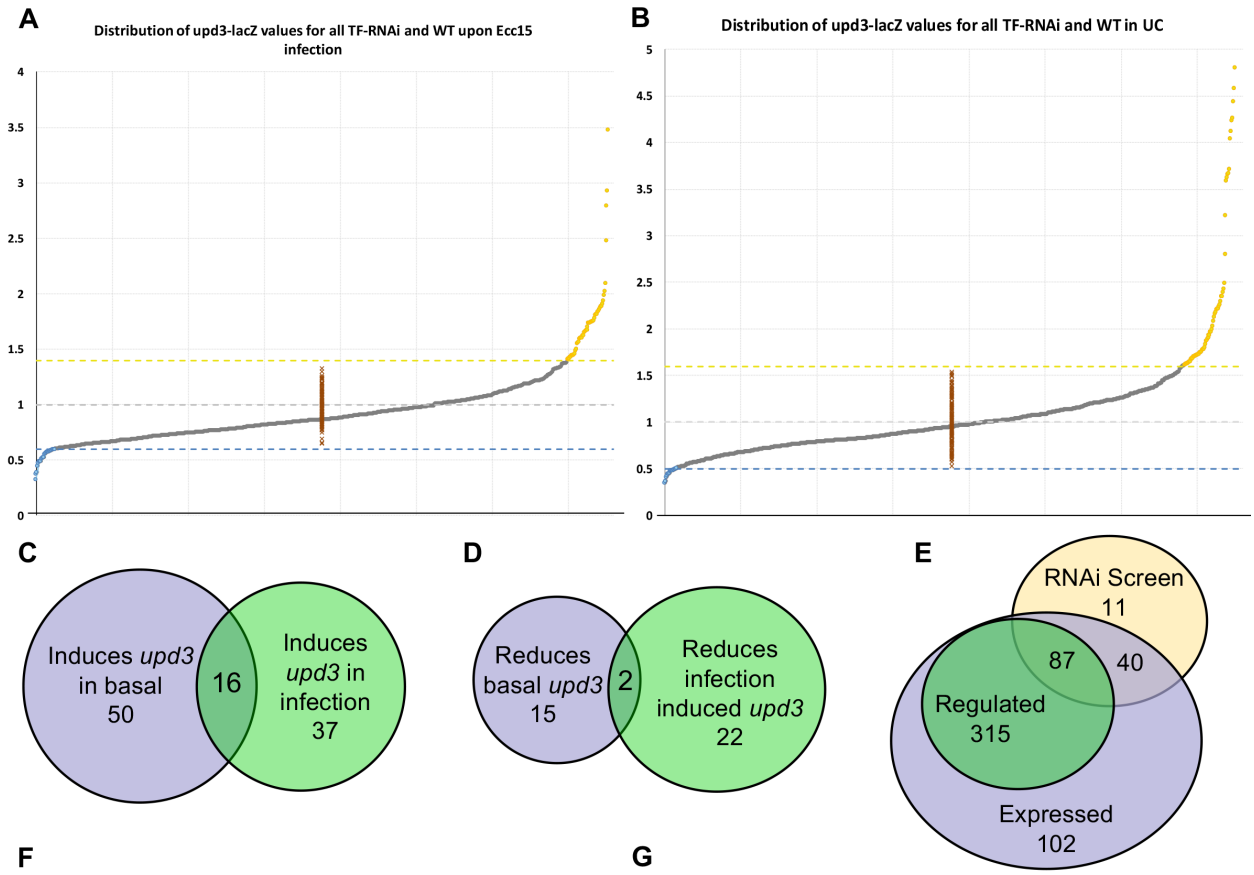

Description	P-value	FDR q-value	Enrichment (N, B, n, b)
developmental process involved in reproduction	3.93E-06	4.67E-03	2.13 (79,18,35,17)
anatomical structure development	7.51E-06	4.46E-03	1.37 (79,47,48,39)
single-organism developmental process	7.74E-06	3.06E-03	1.41 (79,48,42,36)
developmental process	8.31E-06	2.47E-03	1.37 (79,51,43,38)
anatomical structure morphogenesis	8.92E-06	2.12E-03	1.62 (79,36,38,28)
animal organ development	1.77E-05	3.50E-03	1.65 (79,32,39,26)
morphogenesis of an epithelium	4.05E-05	6.86E-03	2.32 (79,12,34,12)
tissue morphogenesis	4.05E-05	6.00E-03	2.32 (79,12,34,12)
regulation of multicellular organismal development	6.84E-05	9.02E-03	2.43 (79,13,30,12)
post-embryonic morphogenesis	7.74E-05	9.19E-03	1.97 (79,20,34,17)
cellular developmental process	2.60E-04	2.80E-02	1.49 (79,39,38,28)
organ morphogenesis	4.44E-04	4.40E-02	2.14 (79,13,34,12)
single-organism cellular process	4.88E-04	4.46E-02	1.40 (79,45,39,31)
sensory organ development	4.99E-04	4.23E-02	2.77 (79,15,19,10)
regulation of developmental process	5.24E-04	4.15E-02	1.98 (79,16,35,14)
cell fate commitment	5.28E-04	3.91E-02	3.05 (79,9,23,8)
reproductive process	7.53E-04	5.26E-02	1.77 (79,23,35,18)
post-embryonic appendage morphogenesis	9.90E-04	6.53E-02	2.01 (79,15,34,13)

RNAi knockdown of TFs in ECs can influence *upd3-lacZ* expression in multiple ways: TFs could be acting via direct regulation of the *upd3* promoter region, indirect regulation through secondary genes or even non-cell-autonomously through changes in gut physiology that subsequently alter *upd3* expression. To complement our RNAi screen and identify the direct regulators of *upd3* transcription, we thus undertook two parallel approaches. First, we performed a yeast one-hybrid screen to assess the direct interaction between the *upd3* promoter and all *Drosophila* TFs (Fig 3.7A'). This additional screen identified 81 yeast one-hybrid-positive TFs (S Table 3.3). Among these, 21 (more than 25%) showed altered *upd3-lacZ* expression when knocked down, suggesting a role in *upd3* gene regulation (Fig 3.7B). To further indicate the binding potential of TFs of interest, an *in silico* search for known TF-binding sites (TFBS) was performed in the same genomic region using the JASPAR and RedFly databases (Fig 3.7B-C and S Table 3.2) [30,31]. We identified seven TFs that are positive for all three approaches, thus specifying them as direct regulators of *upd3*: *D-Fos* or *kayak*, *sd*, *Trithorax-like (Trl)*, *pangolin (pan)*, *giant*, *Ptx1*, *achintya (achi*) (Fig 3.7B-C). Knockdown of two of these TFs caused abnormal induction of *upd3-lacZ* (*Ptx1* and *achi*). The five others were found to be required for *upd3-lacZ* expression either basally (*giant*) or both during infection and in basal conditions *(D-Fos*, *sd, Trl and*, *pan*) (Fig 3.7C). Of note, Sd and D-Fos have multiple binding sites in infection-responsive enhancers (Fig 3.7D), and are critical for *upd3* transcription in both UC and infected conditions (Fig. 3.7C). We therefore propose that these TFs act as direct, master regulators of *upd3* expression in the gut.

Next, we examined TFs that strongly alter *upd3-lacZ* expression upon knockdown but lack evidence for binding potential to the *upd3* promoter region. These important TFs required for *upd3-lacZ* induction include: Sna, a key regulator of epithelial to mesenchymal transition (EMT); Jra (D-Jun), the partner of D-Fos in the AP-1 transcriptional complex; Yki, the transcriptional

partner of Sd in the Hippo pathway; Mad, a transcription factor that mediates TGF-β/Dpp signaling; and one thus far uncharacterized TF (CG33213) (Fig 3.7C and S Table 3.2). Surprisingly, we found that the homeodomain TFs, Retinal Homeobox (Rx) and Ultrabithorax (Ubx) are also required for *upd3-lacZ* activity, primarily upon infection (Fig 3.7C), suggesting these TFs could be involved in tissue repair. Among these TFs, Sna, Mad, Rx and Ubx were not found to bind to the *upd3* promoter by the yeast one-hybrid assay, although there are some binding sites in the *upd3* promoter region for these TFs according to the JASPAR database (Fig 3.7C). This suggests that there is a possibility that they could act directly. Finally, global regulators of transcription such as the transcriptional corepressor CtBP, the H3K4 methyl-transferase Trithorax-Related (Trr) and MBD-like, a member of the NuRD complex also influenced the regulation of *upd3-lacZ* (Fig 3.7C).

On the opposite side of the spectrum, we also identified TFs that cause increased *upd3-lacZ* expression when knocked-down. For instance, Ptx1, a master regulator of middle midgut identity, has TFBS sites in *upd3*, interacts with *upd3* in the one-hybrid screen and its knockdown strongly induces *upd3-lacZ* in both UC and infected guts (Fig 3.7C) [28]. This indicates that Ptx1 could act as a direct negative regulator of *upd3* in the middle midgut. The TFs Anterior open (Aop), Cyclic-AMP response element binding protein-17A (CrebB-17A), Longitudinals lacking (Lola), Atf3, and Achi also show potential to bind to the *upd3* promoter region in our one-hybrid screen and trigger *upd3-lacZ* induction when depleted in ECs. RNAi against *GATAe*, *Xbp1*, *deformed wings* (*dwg*), and *hangover* (*hang*) results in elevated levels of *upd3-lacZ* in both *Ecc15* infected and UC conditions, but the absence of TFBS and association in our one-hybrid screen suggests that this is likely an indirect effect due to disruption of intestinal homeostasis. We also found a distinct set of epigenetic factors that strongly increase *upd3-lacZ* activity when knocked-down.

Among these, there are known positive regulators of transcription such as MBD-R2 (NSL complex); the Tip60 acetylase; the histone acetyl-transferase Chameau (Chm), Domino (Dom) of the SWI-SNF complex and Trl of the eponymous TRL complex. In summary, our combination of *in vivo*, *in vitro*, and *in silico* screens allowed us to identify putative direct positive and negative regulators of *upd3* induction, as well as key transcriptional regulators of gut homeostasis.

Indirect positive regulators of *upd3* include the transcriptional repressor Snail, which is induced in ECs upon infection.

Among our positive hit TFs that are strongly required for *upd3-lacZ* induction, we took note of Sna, as well as the homeodomain TFs, Rx and Ubx, and the epigenetic regulator, Trl. Despite the fact that Trl was the only one with a yeast one-hybrid predicted TFBS, knockdown of any of these TFs blocked infection-induced *upd3-lacZ* activity by 40% or more (Fig 3.7C and Fig 3.9A). RT-qPCR measurements of *upd3* mRNA levels upon *Ecc15* infection further confirmed the requirement of these TFs for proper *upd3* transcriptional upregulation (Fig 3.9B).

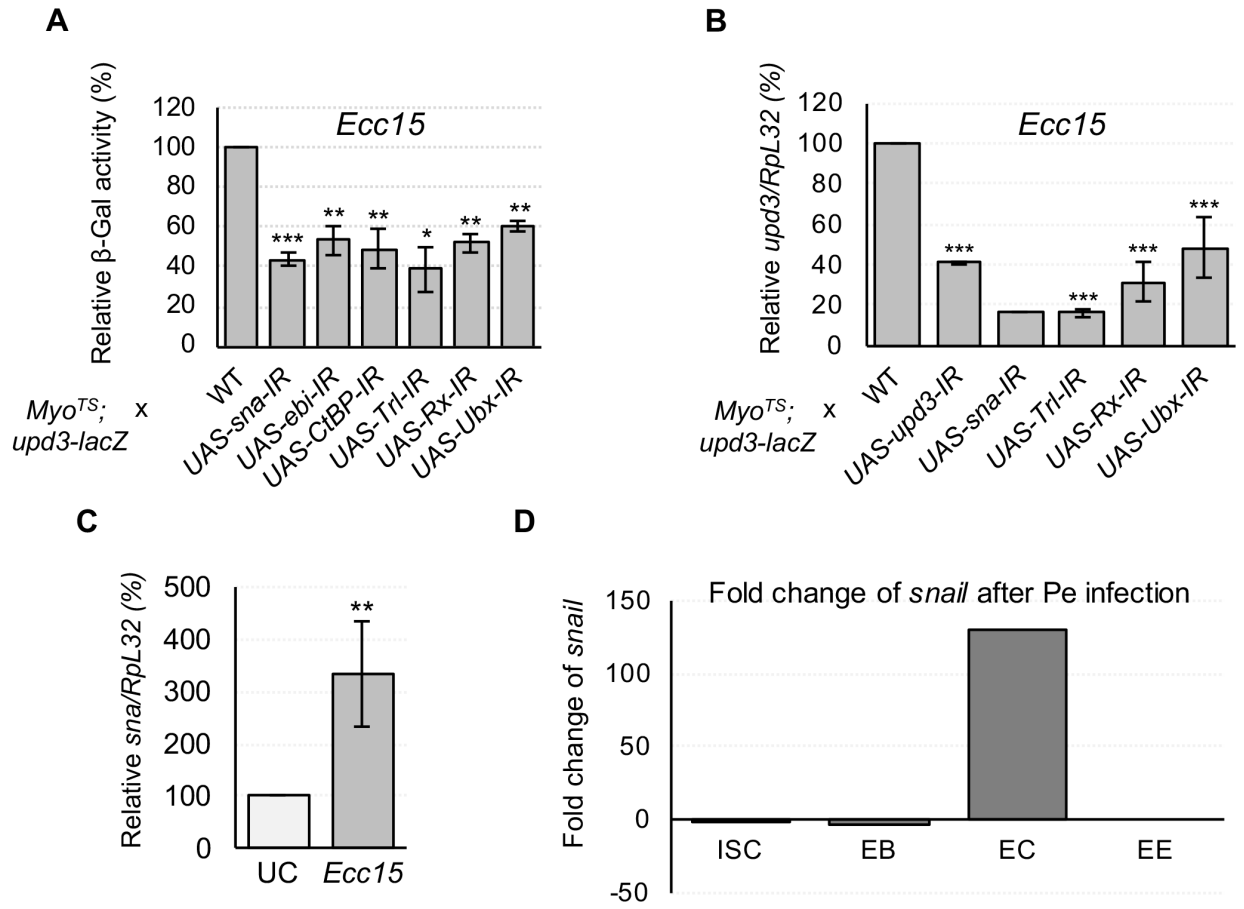

Figure 3.9. Infection-induced *upd3* expression in ECs requires the indirect functions of Snail and its transcriptional co-repressors, as well as homeodomain TFs and epigenetic regulators. (A) Induction of *upd3-lacZ* by *Ecc15* infection is impeded by RNAi-mediated knockdown of Snail (Sna), its corepressors Ebi and CtBP, the epigenetic regulator Trl, and the homeodomain TFs, Rx and Ubx. (B) RT-qPCR measurements of total midgut *upd3* expression corroborate *upd3-lacZ* results. (C) RT-qPCR measurements of *sna* expression reveal that the gene is transcriptionally upregulated in the midgut following *Ecc15* infection. (D) Cell-specific midgut RNA-Seq data reveals that *sna* is transcriptionally induced specifically in ECs during oral infections by *Pe*. Statistical significance: mean values of at least 3 repeats are represented ± SEM. *p<0.05, **p<0.01, ***p<0.001 (student's t-test).

Sna classically acts as a repressor of transcription [32,33], suggesting that its positive effect on *upd3* expression is indirect. We further confirmed that EC-specific RNAi against CtBP or Ebi, the co-repressors recruited by Sna to mediate transcriptional repression [34,35], also suppressed *upd3-lacZ* activity during *Ecc15* infection (Fig 3.9A). It is notable that these phenotypes were found in ECs, despite the fact that Sna has been described as a marker and regulator of progenitors

in the *Drosophila* midgut [28]. Surprisingly, we found that Sna itself is transcriptionally upregulated in response to both *Ecc15* (Fig 3.9C) and *Pe* (Fig 3.9D) infections. In addition, most of its upregulation occurs in ECs (Fig 3.9D). Altogether, our results suggest that, in response to infection, Sna is upregulated in ECs, and in turn promotes *upd3* upregulation through an indirect mechanism.

The Hippo pathway controls *upd3* induction in response to infection through the TFs Yorkie and Scalloped

The Hippo pathway consists of a kinase cascade resulting in the phosphorylation of Wts, which in turn phosphorylates and inhibits the transcription factor Yki [36]. When released from phosphorylation-induced restraint, Yki is transported to the nucleus, where it dimerizes with other TFs to promote transcription of target genes [37]. Hippo regulation plays an important role in tissue regeneration and growth. In addition, Yki has been shown to control epithelium turnover, acting cell-autonomously in ISCs via a Hpo/Wts/Yki pathway and non-cell-autonomously in EBs via the Msn/Wts/Yki pathway [38].

As previously mentioned, Yki and its partner Sd were found in our TF RNAi screen to be required in ECs for *upd3* transcription in both basal and *Ecc15*-infected conditions (Fig 3.7C and 3.10A-B). In addition, Sd was found to interact with the *upd3* promoter by yeast one-hybrid, suggesting that the Hippo pathway may be directly involved in basal and infection-induced *upd3* expression. We also noted that Trr, a major constituent of the TRR histone H3 lysine 4 (H3K4) methyltransferase complex, and Trl, which are both required for full Yki-Sd mediated transcription [39,40], are also required during infection for *upd3-lacZ* induction (Fig 3.10A). Conversely, overexpressing Yki, or knockdown of either *wts* or its activator, *msn,* in ECs was enough to induce

the transcription of *upd3-lacZ* (Fig 3.10C). However, RNAi mediated depletion of *hpo*, which encodes another Wts phosphorylating kinase, had no significant effect on *upd3-lacZ* (Fig 3.11). Finally, overexpressing *msn* in ECs inhibited usual *upd3-lacZ* activity in *Ecc15* infected and unchallenged midguts (Fig 3.10A-B). We confirmed the requirement of the Hippo pathway TF, Sd, for *upd3* transcription in ECs during enteric infection by RT-qPCR (Fig 3.10D). Our results suggest that the Hippo pathway, which has been shown to be important for *upd3* regulation under basal conditions and in response to abiotic stress [41,42], is additionally required in ECs for *upd3* expression in response to oral infection by *Ecc15*.

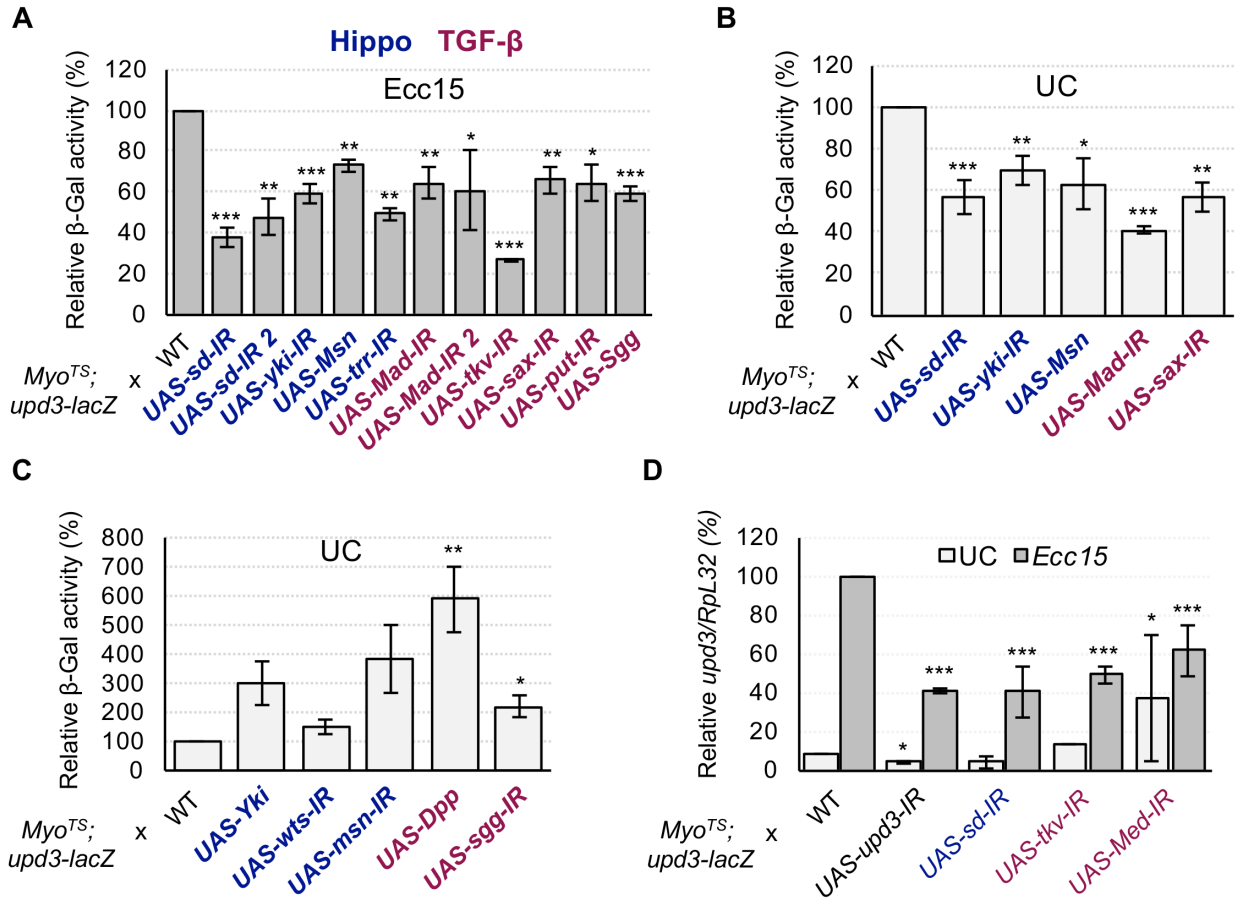

Figure 3.10. Infection-induced expression of *upd3* in ECs requires the Hippo and Dpp pathways. (A-C) Measurements of midgut *upd3-lacZ* activity under *Ecc15* infected and UC conditions during EC-specific knockdown or overexpression of Hippo and Dpp pathway components. Depletion of the Hippo TFs *sd* or *yki*, or overexpression of an upstream inhibitor (Msn) blocks basal and infection-induced *upd3-lacZ* expression. Likewise, knockdown of *trr*, an epigenetic enhancer of Yki/Sd activity, also inhibits infection-induced *upd3-lacZ*. Alternatively,

overexpression of Yki or knockdown of its upstream inhibitors *wts* and *msn* is sufficient to induce *upd3-lacZ*. Knockdown of the Dpp pathway TF *Mad*, either of the three Dpp pathway receptors, *tkv*, *sax*, or *put*, or overexpression of the *Mad* inhibitor, Sgg all blocked *upd3-lacZ* activity. Overexpression of Dpp itself or knockdown of *sgg* induced *upd3-lacZ*. (D) RT-qPCR was used to directly measure *upd3* transcription levels, and confirm that the function of the Hippo and Dpp pathway TFs are required for *upd3* induction. Statistical significance: mean values of at least 3 repeats are represented ± SEM. *p<0.05, **p<0.01, ***p<0.001 (student's t-test).

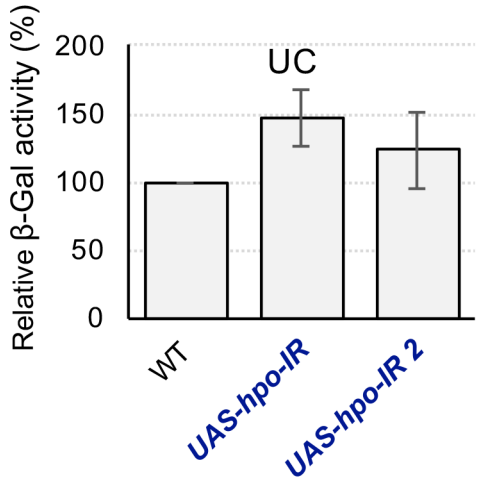

Figure 3.11. Knockdown of the Yki inhibitor, Hippo, is not sufficient to induce *upd3*. Basal *upd3* expression, as reported by *upd3-lacZ* activity, is not significantly induced by EC-specific knockdown of *hippo*. Statistical significance: mean values of at least 3 repeats are represented ± SE. *p<0.05, **p<0.01, ***p<0.001 (student's t-test).

The TGF-β/Dpp pathway is required for *upd3* induction in response to infection

The TGF-β/Dpp pathway has emerged as a major regulator of intestinal homeostasis in *Drosophila*, as it has been found to be involved in diverse processes including ISC proliferation, ISC quiescence, EC differentiation and EC protection [43-48]. Mad, a TF downstream of the Dpp pathway was found in our screen to be necessary for wild-type *upd3-lacZ* levels upon ingestion of *Ecc15* as well as in basal conditions (Fig 3.10A-B). Thus, we explored whether ECs require a fully functional Dpp pathway to regulate the transcription of *upd3*. EC-specific RNAi against the Dpp type-1 receptors, *thickveins* (*tkv*) and *saxophone* (*sax*), or the type-2 co-receptor *punt* (*put*), all decreased infection-responsive *upd3-lacZ* activity (Fig 5A). Furthermore, overexpression of Dpp

triggered aberrant induction of *upd3-lacZ* (Fig 3.10C). We additionally tested the Dpp pathway via manipulation of the glycogen-synthase-3-kinase Shaggy (Sgg), which has been shown to negatively regulate Mad through phosphorylation of linker serines [49]. Overexpression of *sgg* in ECs blocked *upd3-lacZ* induction, while *sgg* knockdown increased *upd3-lacZ* basal activity (Fig 3.10A and C). A role for the Dpp pathway in regulating *upd3* was further supported by RT-qPCR of *upd3* in flies expressing EC-specific RNAi against *tkv* or *Medea* (*Med*), a TF that acts together with Mad [50], as both led to decreased induction of *upd3* upon *Ecc15* infection (Fig 3.10D). Altogether, our data demonstrate that the Dpp pathway is required for proper *upd3* transcription in response to infection.

Src-Raf-Dsor1-ERK and Licorne-p38 pathways converge to regulate *upd3* transcription upon infection

D-Fos and D-Jun were among the TFs in our screen that most strongly impacted *upd3-lacZ* activity upon infection. When activated by upstream kinases these two TFs act together as the AP-1 transcription factor complex [51]. D-Fos also interacts *ex vivo* (in our Y1H screen) with the *upd3* promoter, suggesting that AP-1 acts as a direct regulator of *upd3* transcription. Accordingly, RNAi against *D-Fos* or *D-Jun*, or the expression of a dominant negative D-Jun (*UAS-Jra*^{DN}) significantly decreased *upd3-lacZ* activity (Fig 3.12A-B). As an additional confirmation of these results, we found that RNAi mediated knockdown of *D-Fos* in ECs prevented infection-responsive *upd3* expression as measured by RT-qPCR (Fig 3.12C).

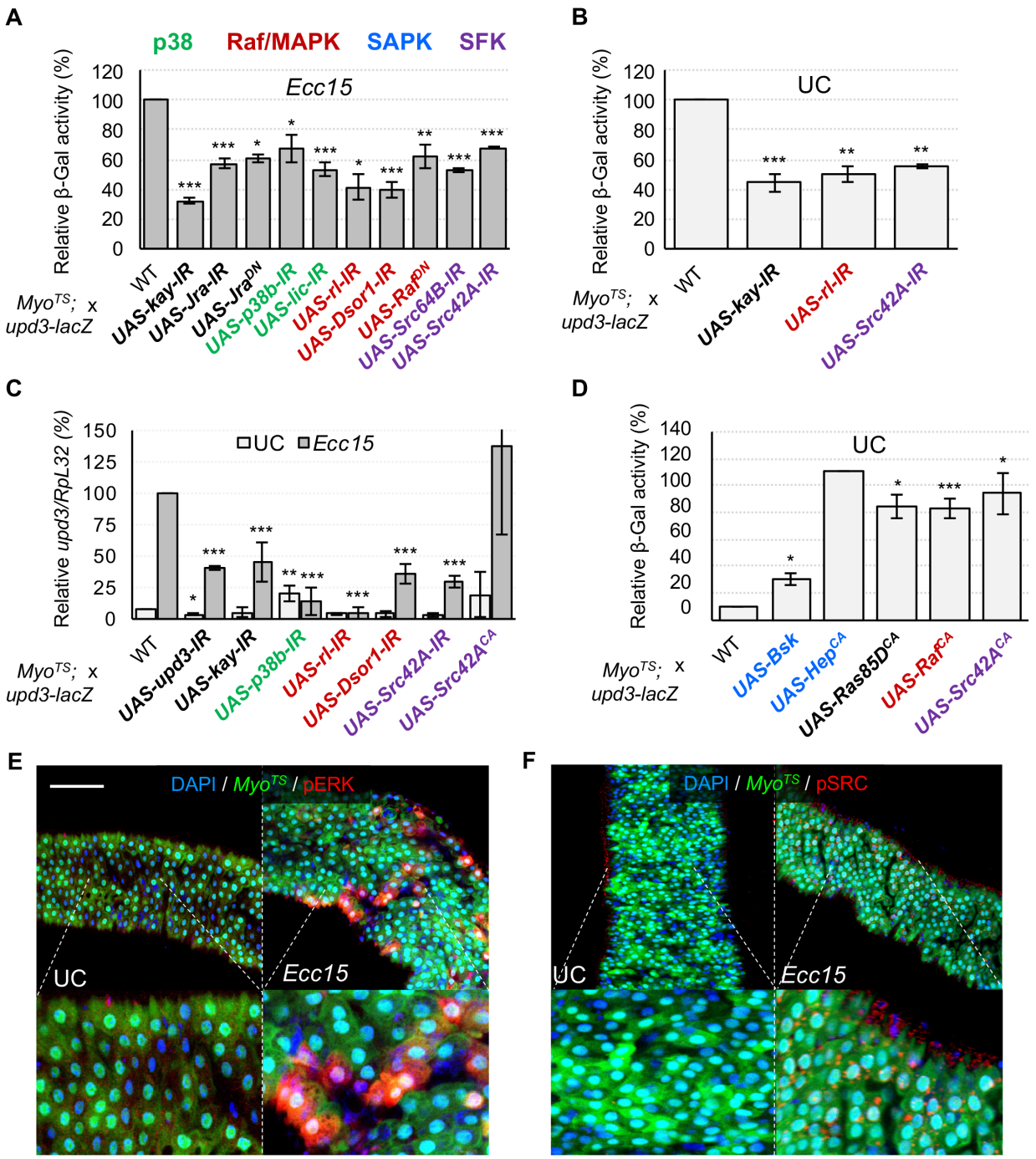

Figure 3.12. Infection-induced *upd3* expression in ECs requires the TFs D-Jun and D-Fos, activated by upstream Src-MAPK pathways. (A-B) Knockdown by RNAi of multiple constituents of MAPK pathways, as well as Src kinases or the TFs D-Jun (Jra) and D-Fos (Kay) inhibits *upd3-lacZ* activity under *Ecc15* infection or UC conditions. (C) RT-qPCR measurements of total midgut *upd3* expression corroborate *upd3-lacZ* results. (D) In addition to their requirement for *upd3-lacZ* activity, activation of the MAPKs and SFKs can also induce *upd3-lacZ* expression in UC conditions. SAPKs can also induce this activity when stimulated. (E, F) Immunostaining against phosphorylated forms of ERK and Src reveals that these kinases are activated in response

to infection in ECs. Scale bar is 100μm. Statistical significance: mean values of at least 3 repeats are represented ± SEM. *p<0.05, **p<0.01, ***p<0.001 (student's t-test).

We next aimed to identify the upstream pathway(s) that regulate(s) D-Fos and D-Jun in response to *Ecc15* infection. Phosphorylation and subsequent activation of the AP-1 complex is carried out by both Stress Activated Protein Kinases (SAPKs) and Mitogen Activated Protein Kinases (MAPKs) [52]. SAPKs and MAPKs act in phosphorylation cascades that result in the activation of terminal kinases such as JNK, Basket (Bsk), p38 and ERK (Fig 3.14F). It has been previously shown that artificial activation of the *Drosophila* SAPK, Bsk, by overexpression of Hemipterous (Hep) induces *upd3* transcription in the gut, possibly through the activation of apoptosis or by directly regulating AP-1 [17,19]. We first evaluated whether apoptosis is required for *upd3* expression in response to microbes. To this end, we manipulated the expression of caspase and autophagy genes in ECs and measured the resulting *upd3-lacZ* activity. Our results confirmed that promotion of autophagy or apoptosis, by overexpression of *Autophagy-related 1 (Atg1)* or Death regulator Nedd2-like caspase (*Dronc*), respectively, induced *upd3* (Fig 3.13A). However, inhibiting either pathway by RNAi against *Dronc, Death-associated APAF1-related killer (Dark), Atg1, Atg7* or *Atg18*, or by overexpression of the caspase inhibitor P35 (*UAS-P35*), had no significant negative effect on *upd3-lacZ* levels during infection (Fig 3.13B). Furthermore, detection of caspase activity in ECs by the *UAS-Apoliner* system (Fig 3.13C) [53], in conjunction with immunostaining for *upd3-lacZ*-derived β-galactosidase, revealed that cytokine production during enteric infection is not restricted to ECs with increased caspase activity (Fig 3.13D). Altogether these data suggest that apoptosis and autophagy are not the key inducers of *upd3* expression upon infection.

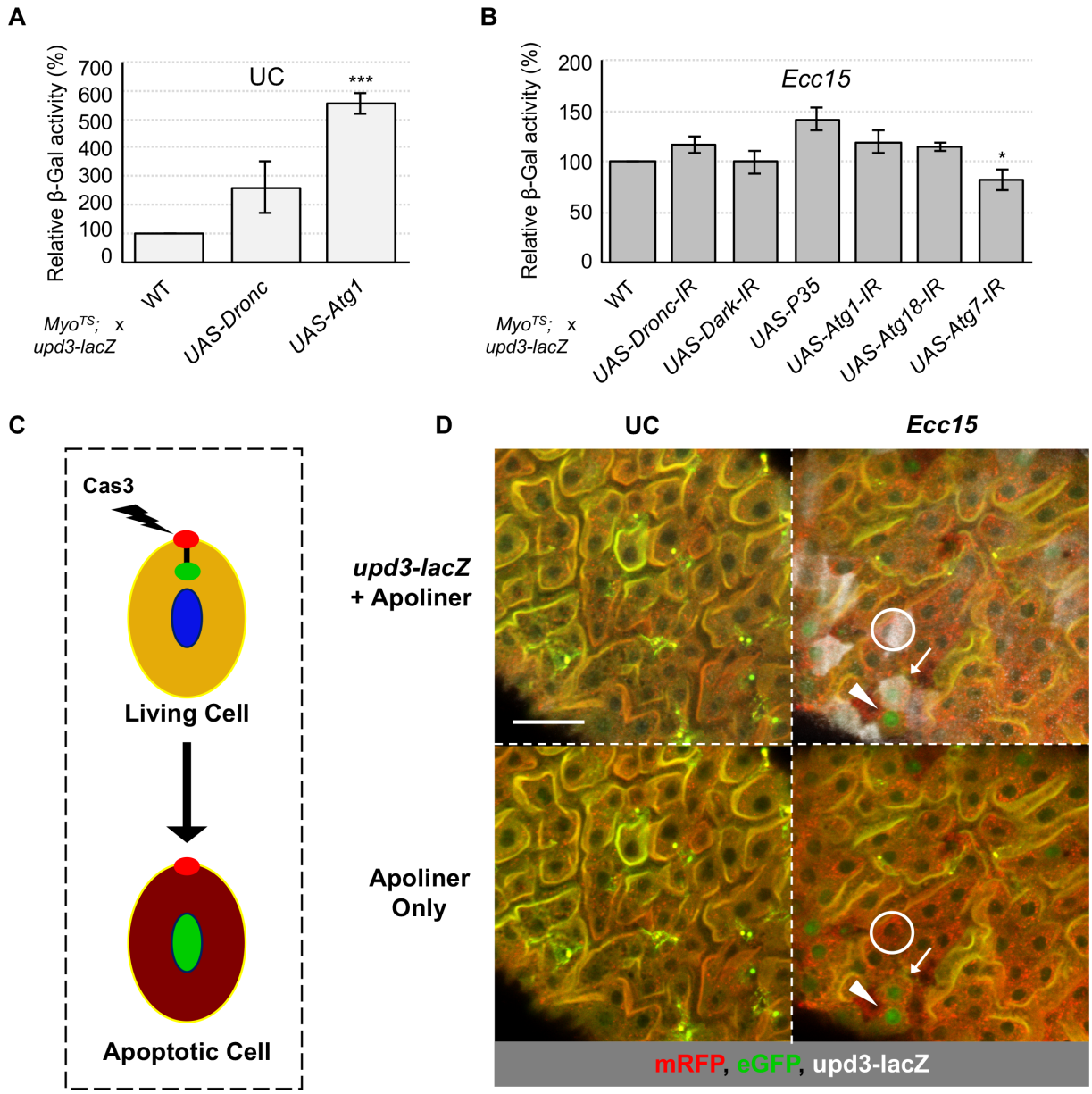

Figure 3.13. *upd3* expression in ECs is not dependent on apoptosis or autophagy._(A, B) Overexpression of caspases or autophagy genes is sufficient to induce *upd3* expression, as measured by *upd3-lacZ* (A). However, blocking apoptosis or autophagy by RNAi against caspases or autophagy genes, or overexpression of P35, does not impede *Ecc15*-induced *upd3* transcription (B). (C, D) The Apoliner construct expresses a membrane-bound mRFP fluorophore with a caspase sensitive site attached to an intracellular eGFP fluorophore. Caspase 3 (Cas3) cleaves this linker region, releasing the GFP fluorophore and allowing it to re-localize to the nucleus (C). *UAS-Apoliner,* driven by *NP1-Gal4,* marks apoptotic ECs with GFP localized to the nucleus (D). In *Ecc15* infected guts, we observe ECs that are caspase active and *upd3*-negative (white arrowhead), caspase inactive and *upd3*-positive (white circle), and both caspase-active and *upd3*-positive (white arrow). Scale bars are 25µm. Statistical significance: mean values of at least 3 repeats are represented ± SE. *p<0.05, **p<0.01, ***p<0.001 (student's t-test).

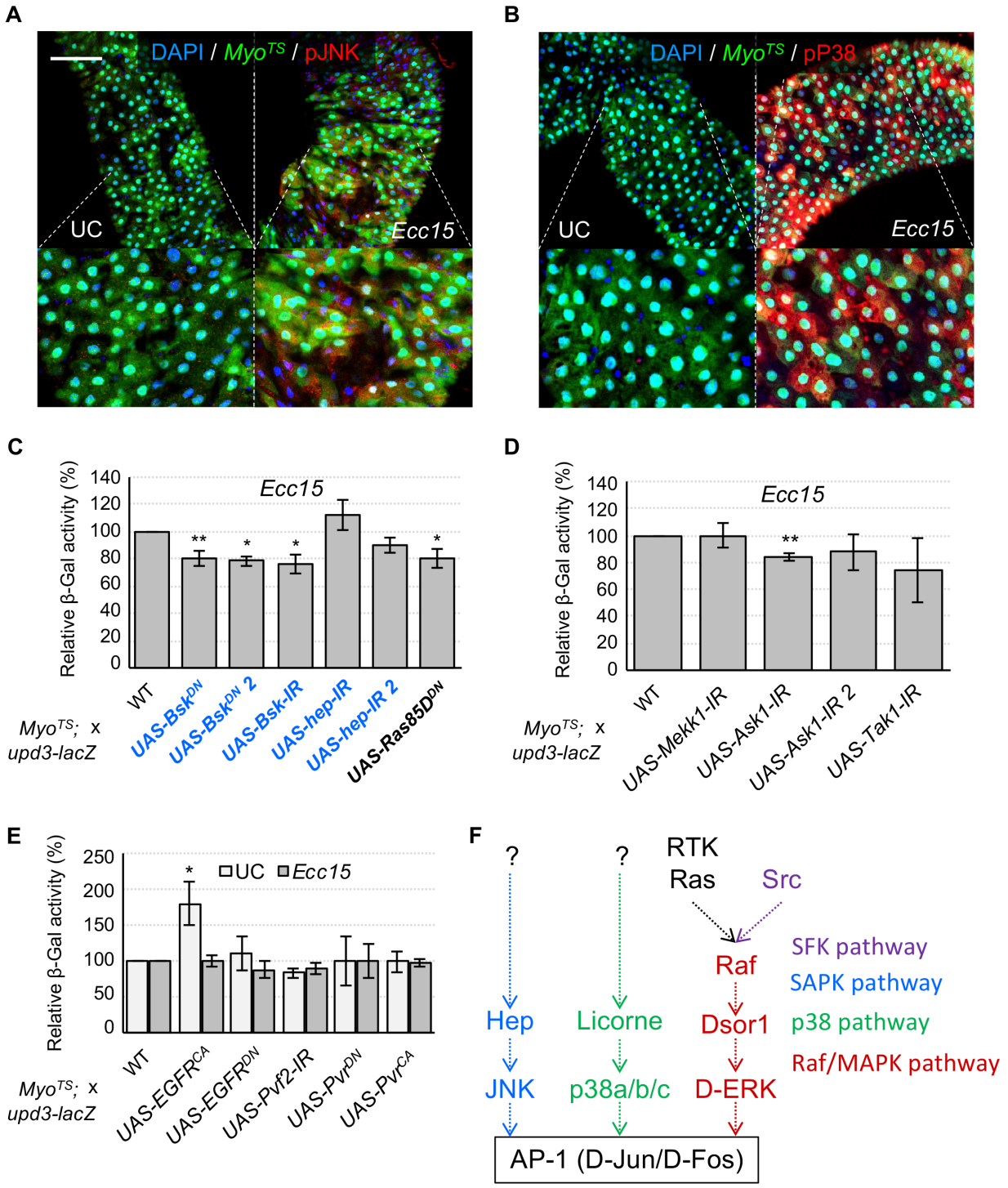

Figure 3.14. Activation of JNK, Hep, Ras and major RTKs induce *upd3* expression but are not required for infection-induced expression. (A, B) Immunostaining against phosphorylated forms of JNKand p38 reveals that these kinases are activated in response to infection in ECs. (C) EC-specific inhibition of Bsk, Hep, or Ras, by RNAi or by expression of dominant negative forms has minimal effect on *Ecc15*-induced *upd3* expression. (D) EC-specific depletion of the MAPKKKs, MEKK1, ASK1, and TAK1 has no major effect on *Ecc15*-induced *upd3* expression. (E) Finally, EC-specific inhibition of EGFR, Pvr, or Pvf2 has no negative effect on *upd3-lacZ*

activity, although activation of EGFR in ECs is sufficient to trigger *upd3-lacZ* expression. (F) Schematic of the SAPK/MAPK network. The AP-1 complex (D-Jun and D-Fos) is regulated by both Stress Activated Protein Kinase (SAPKs) and Mitogen Activated Protein Kinases (MAPKs). SAPKs lead to the activation of JNK, and MAPKs result in the activation of terminal kinases, including p38 and ERK. Statistical significance: mean values of at least 3 repeats are represented ± SE. *p<0.05, **p<0.01, ***p<0.001 (student's t test).

We next sought to evaluate the contribution of JNK to *upd3* induction upon infection with *Ecc15*. We first verified whether *Ecc15* infection triggers JNK activation in ECs, via co-immunostaining of the phosphorylated form of JNK and an EC marker (*Myo-Gal4^{TS}>UAS-GFP*) (Fig 3.14A). In agreement with previous publications, ectopic activation of the JNK pathway in ECs, by overexpressing Bsk or a constitutively active form of Hep, strongly promoted *upd3-lacZ* transcription (Fig 3.12D). However, EC-specific expression of a dominant negative form of Bsk (*UAS-Bsk^{DN}*), or knockdown of *bsk* expression, decreased *upd3-lacZ* activity following oral infection by only 20% (Fig 3.14C). Additionally, RNAi knockdown of *hep* did not decrease *upd3-lacZ* induction significantly (Fig 3.14C). This suggests that JNK only plays a minor role in *upd3* regulation, and thus additional stress pathways may be responsible for stimulating AP-1 in response to oral bacterial infection.

Another possible candidate for AP-1 regulation is the p38 family of stress responsive MAPKs. The p38 kinases can regulate the AP-1 complex (Fig 3.14C), and have been shown to be involved in the response to oral infection in *Drosophila* [54]. Immunostaining for phosphorylated p38 kinases revealed a substantial increase in p38 phosphorylation in ECs upon infection (Fig 3.14B). To investigate the role of the p38 pathway further, we knocked down the three p38 kinases of *Drosophila* (*p38a*, *p38b* and *p38c),* independently. Only knockdown of *p38b* gave a mild, but significant (p<0.05) decrease in *upd3-lacZ* induction upon infection (Fig 3.12A). We similarly tested the involvement of the upstream p38 MAPKK, Licorne (Lic), and found that knockdown of

lic in ECs also blocks increased *upd3-lacZ* transcription in response to oral infection. These experiments suggest that the stress in ECs caused by enteric infection triggers activation of a Lic/p38b pathway that mediates part of the induction of *upd3-lacZ*.

In addition to JNK and p38 kinases, the D-ERK kinase is also able to activate the AP-1 complex (Fig 3.14F) [51]. Thus, we decided to investigate whether the MAPK/D-ERK pathway could also act upstream of AP-1 to regulate *upd3* upon infection. Immunostaining for the phosphorylated form of Rolled (Rl), the *Drosophila* homologue of ERK, revealed that infection with *Ecc15* triggers D-ERK activation in ECs within two hours (Fig 3.12E). Furthermore, RNAi knockdown of *rl* in ECs resulted in a strong decrease in *upd3-lacZ* activity upon infection (Fig 3.12A), suggesting that the MAPK/ERK pathway is necessary for infection-regulated *upd3* induction. MAPKs are activated in a phosphorylation cascade downstream of MAPKKs and MAPKKKs (Fig 3.14F). Two of the four *Drosophila* MAPKKs (Lic and Hep) were previously tested for a role in *upd3* regulation, and thus we proceeded to test the remaining two: Downstream of raf1 (Dsor1) and MAP kinase kinase 4 (Mkk4). As for ERK, Dsor1 was critical for full induction of *upd3-lacZ* upon infection (Fig 3.12A). Accordingly, expressing a dominant negative form of the upstream MAPKKK, Raf, in ECs also decreased *upd3-lacZ* regulation by infection, while blocking other MAPKKKs, TGF-β activated kinase 1 (TAK1), Apoptotic signal-regulating kinase 1 (ASK1) and MEKK1, did not (Fig 3.12A and 3.14D). Furthermore, constitutively active Raf expression is sufficient to induce *upd3-lacZ* activity (Fig 3.12D). These data together suggest the possibility of a Raf/Dsor1/ERK pathway that regulates *upd3* expression via AP-1 in response to midgut infection or damage. Activation of Raf by phosphorylation is typically accomplished via Ras, downstream of growth factor receptors (Fig 3.14F). However, although overexpression of constitutively active Ras is sufficient to induce *upd3* (Fig 3.12D), blocking Ras itself (Fig 3.14C)

or signaling through the key Receptor Tyrosine Kinases (RTKs) EGFR and PDGF- and VEGF-receptor related (Pvr) (*UAS-Ras*^{DN}, *UAS-EGFR*^{DN}, *UAS-Pvr-*^{DN}) did not impair *upd3-lacZ* activity (Fig 3.14E). Likewise, RNAi knockdown of the Pvr ligand, PDGF- and VEGF-related factor 2 (Pvf2), had no effect on *upd3-lacZ* regulation. Raf signaling can occur downstream of additional tyrosine kinases, including the Src family kinases (SFKs, Fig 3.14F) [55,56]. Immunostaining for the phosphorylated form of Src kinases revealed that infection with *Ecc15* triggers Src activation in ECs (Fig 3.12F). To determine if the Src complex is also required for *upd3* regulation, we knocked down *Src42A* and *Src64B* by RNAi in ECs (Fig 3.12A). Depletion of either *Src42A* or *Src64B* decreased *upd3-lacZ* induction upon infection. Conversely, the expression of a constitutively active form of Src42A in ECs triggered *upd3-lacZ* induction in absence of infection, suggesting that a Src/Raf/Dsor1/MAPK pathway is sufficient to activate *upd3* transcription. We further confirmed our results by RT-qPCR of *upd3* in response to infection while blocking expression of *Dsor1*, *p38b* and *Src42A* in ECs by RNAi, as well as by activating the pathway by expression of a constitutively active form of Src42A (Fig 3.12C). In summary, our results demonstrate that multiple kinase cascades (Licorne-p38b and Src/Raf/Dsor1/ERK) are activated in ECs following oral *Ecc15* infection and converge on the regulation of *upd3*.

Impairment of *upd3* regulatory TFs or their upstream activators in ECs reduces ISC proliferation and compromises adult lifespan

We next aimed to evaluate the physiological consequences of modulating in ECs the pathways that control *upd3* transcription. The number of mitotically active ISCs (phospho-Histone H3 positive cells) following *Ecc15* ingestion was significantly reduced by knockdown of AP-1 and Sd, as well as the MAPK, Rl, the Dpp receptor, Tkv, and the epigenetic regulator, Trl, using the temperature

sensitive, EC specific driver line (Myo^{TS}) (Fig 3.15A). This suggested that pathways required for EC-derived Upd3 production are required for proper ISC activity upon infection. We therefore monitored the survival of flies expressing EC-specific RNAi against pathway components of the Hippo, Dpp and SFK/MAPK/AP-1 pathways as well as putatively indirect regulators (Sna, Trl, Rx, Ubx) of *upd3* upon infection. These flies had significantly shorter lifespans following *Ecc15* infection compared to wild-type controls, and LT50 values lower than controls by at least two days (Fig 3.15B-D, S Table 3.4). In addition, we also found that, under UC conditions, these knockdown flies have significantly shorter lives than wild-type ones, and correspondingly lower LT50 values (Fig 3.16A-C, S Table 3.4), implying that the knockdown of these genes, or the subsequent reduction in basal Upd3 levels compromises midgut epithelial homeostasis. We further confirmed our results by altering the expression of our candidate genes in ECs using multiple independent transgenic *UAS-RNAi* lines for each gene and monitoring their survival in both infected and unchallenged conditions (S Table 3.4). Altogether, our experiments demonstrated that the Hippo, Dpp and SFK/MAPK/AP-1 pathways are required in ECs for survival to oral infection and for normal aging.

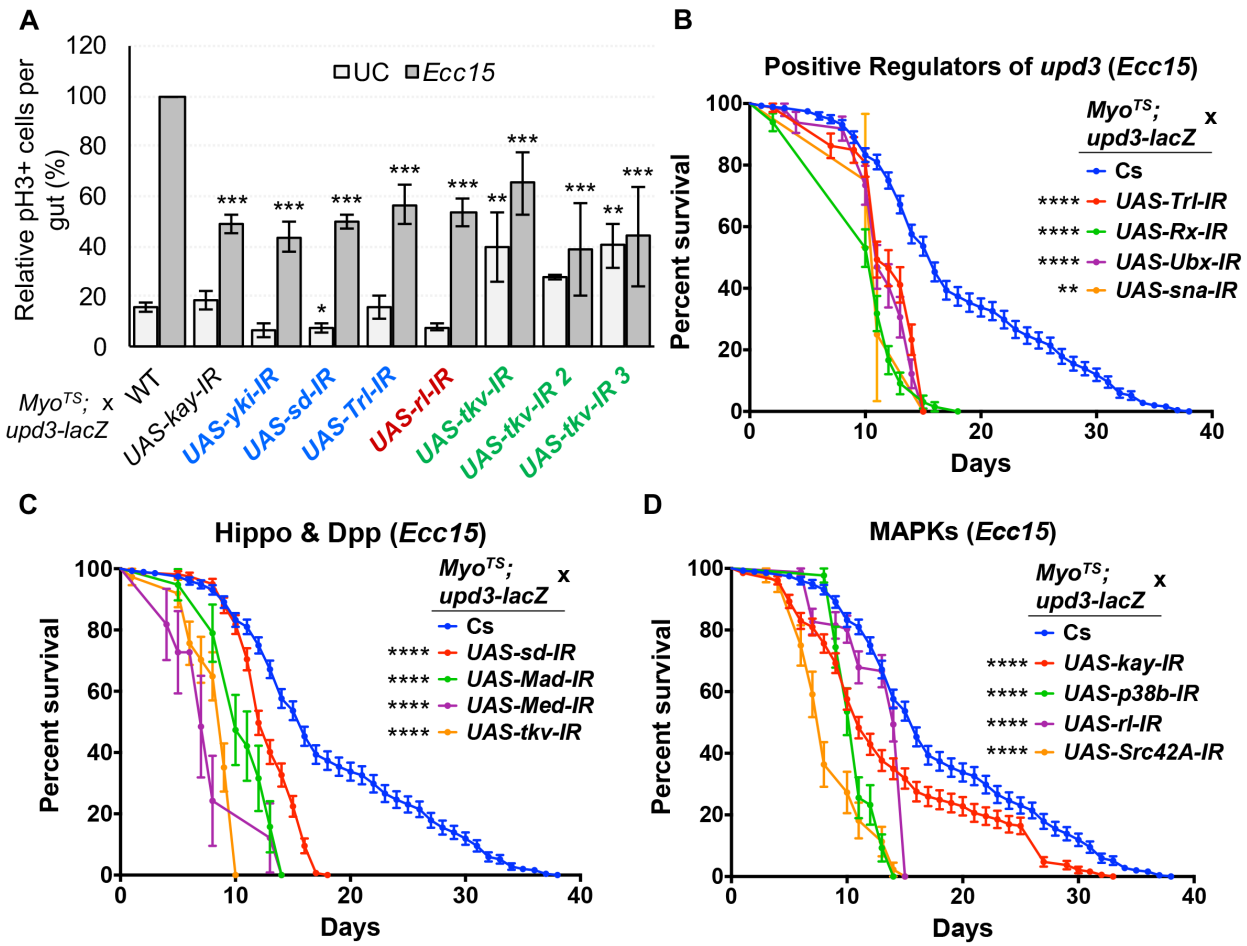

Figure 3.15. ISC proliferation and survival following *Ecc15* infection are compromised by inhibition of the TFs and pathways that are required for *upd3* induction. (A) Total pH3+ cell counts in unchallenged and *Ecc15* infected guts demonstrate that knockdown in ECs of *D-Fos*, *yki*, *sd*, *Trl*, and *sna* as well as upstream components of the MAPK and Dpp pathways is accompanied by a decrease in ISC mitotic activity. Statistical significance: mean values of at least 3 repeats are represented ± SEM. *p<0.05, **p<0.01, ***p<0.001 (student's t test).
(B-D) Survival curves of flies orally infected with *Ecc15* alongside RNAi-induced knockdown of indirect *upd3* regulators (B), Hippo and Dpp pathways components (C), or MAPK pathway factors (D). Curves represent averaged survival ± SE. Statistical significance: *p<0.0332, **p<0.0021, ***p<0.0002, ****p<0.0001 (Log-rank test).

Figure 3.16. Knockdown of positive regulators of *upd3* identified from screening reduces lifespan. (A-C) RNAi mediated knockdown of epigenetic regulators and homeobox genes (A), Hippo and Dpp pathway genes (B), or SAPK and MAPK constituents (C) reduces the lifespan of unchallenged flies. Curves represent averaged survival ± SE. *p<0.0332, **p<0.0021, ***p<0.0002, ****p<0.0001 (Log-rank test).

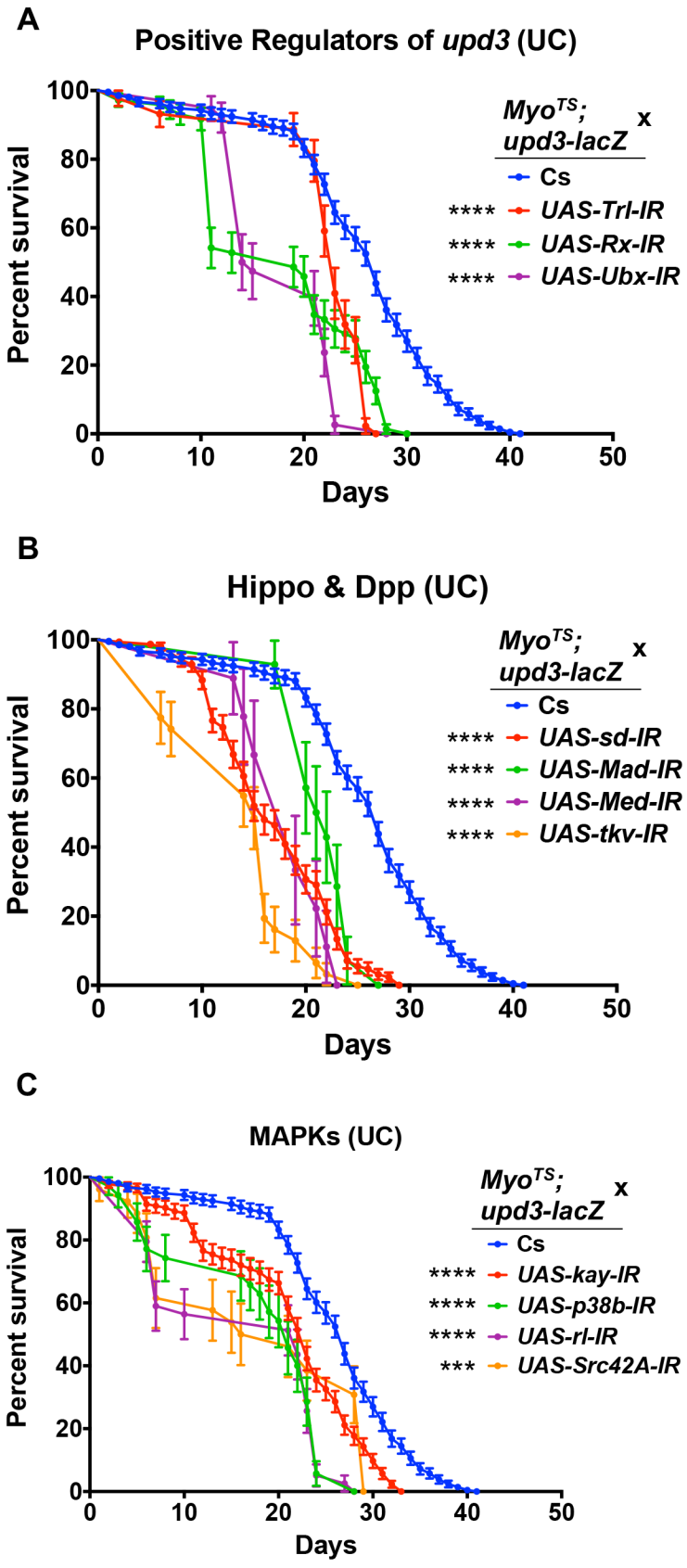
A
Positive Regulators of upd3 (UC)
Percent survival
Days
Myo^TS; upd3-lacZ x
Cs
**** UAS-Trl-IR
**** UAS-Rx-IR
**** UAS-Ubx-IR
B
Hippo & Dpp (UC)
Percent survival
Days
Myo^TS; upd3-lacZ x
Cs
**** UAS-sd-IR
**** UAS-Mad-IR
**** UAS-Med-IR
**** UAS-tkv-IR
C
MAPKs (UC)
Percent survival
Days
Myo^TS; upd3-lacZ x
Cs
**** UAS-kay-IR
**** UAS-p38b-IR
**** UAS-rl-IR
*** UAS-Src42A-IR

Discussion

The *Drosophila* Unpaired ligands, as well as mammalian type I family cytokines, such as IL-6, play an essential role in activating JAK-STAT and other signaling pathways upstream of tissue renewal. Our study provides insight into the complex regulation of Upd3, a cytokine that is transcriptionally induced in response to pathogenic and endogenous microbes, and initiates immune activation and stem cell proliferation.

Microbe-responsive enhancers as DAMP sensors

We found that the *upd3* gene is regulated by three classes of enhancers: region-specific, cell-specific and stress/microbe-responsive. This complexity likely reflects the multiple roles of the JAK-STAT pathway in the *Drosophila* midgut, where it acts to stimulate ISC proliferation, promote differentiation and serves as a regional determinant of cell identity, notably in the middle midgut [8,12,17,57]. We propose that the different functions of *upd3* are therefore regulated independently by the diverse enhancer regions we identified. We further identified microbial responsive enhancers that are active either in ECs (B-C and I) or in progenitor cells (enhancer R), supporting a distinct regulation of *upd3* in different cell types. Interestingly, the progenitor-specific enhancer R is the only one to be induced by DSS feeding (and only to a low degree), while the EC specific enhancers B-C and I do not promote transcription in these conditions. It has been speculated that DSS elicits stem cell proliferation through alteration of the basal lamina rather than by direct damage to ECs [25], such as that caused by *Ecc15* infection or by bleo treatment. This suggests that different cell-type specific enhancers allow for induction of *upd3* expression in response to a broad variety of stresses.

The regulation of host gene expression by bacteria in *Drosophila* relies mostly on dedicated pathways, Toll and Imd, that trigger effector induction in response to the detection of microbial patterns (MAMPs), such as bacterial derived peptidoglycan [58]. The microbe-responsive enhancers of *upd3* are activated by both pathogenic and benign microbes, such as *Ecc15* and the gut microbiota, but are also stimulated by toxic chemicals such as bleo or DSS. This result suggests that cytokine production in the gut is primarily triggered in response to damage associated molecular patterns (DAMPs) rather than the detection of microbes alone. Considering that dietary microbes and the microbiota are constantly associated with the gut tissue, triggering perpetual, low-level Imd activation, responding to DAMPs could be a strategy to couple immune activation and tissue repair to the presence of pathogens rather than beneficial or commensal microbes. Accordingly, we found that *upd3* activation is less pronounced by the microbiota than by pathogens. These pathways have been shown to be activated by various stresses and are central to *upd3* regulation in ECs. A major source of stress in response to microbes, is the production of ROS, partly induced by NADPH oxidases Nox and Duox of the host immune response [59,60]. Notably, SAPKs and Src kinases are both sensitive to ROS and their activity is modulated by oxidative stress, indicating that a NADPH oxidase, ROS, Src, SAPK/MAPK axis could be involved in *upd3* regulation. Future work should determine the link between infection-induced ROS, Src/SAPK activation and the control of gut homeostasis.

upd3 integrates signals from multiple signaling pathways

We further focused on identifying the key TFs that regulate *upd3* in the midgut. We found that altering the expression of 138 over the 708 *Drosophila* TFs significantly altered *upd3* expression in the midgut. This number is surprisingly high, as it implies that a quarter of *Drosophila* TFs

directly or indirectly regulate *upd3* transcription. We interpret this high number as an indication that *upd3* acts as a stress marker, and that any physiological alteration in the gut will result in a rupture of gut homeostasis and consequently in the induction of *upd3* [8]. We therefore propose that *upd3* acts as a global sensor of gut stress and in turn initiates a stereotypical immune and homeostatic program.

This poses the question of how multiple stresses can converge on the activation of *upd3* transcription. Our results suggest that in ECs, stresses are mostly integrated by one *upd3* enhancer (B-C) that responds to both chemical and biotic stresses. Integration could occur either because all stresses result in one simple damage signal, for instance cell loss in the epithelium, or as a consequence of multiple types of gut damage. Interestingly, the TFs altering *upd3* expression in basal and infected conditions are not the same, indicating that different cascades regulate *upd3* expression under different conditions. Upon infection, our data show that the Dpp, Hippo, SAPK and MAPK pathways are all involved in the regulation of *upd3*. We therefore propose a model in which the diverse transcriptional regulation of *upd3* is required for its multiple roles in homeostatic regulation.

The different transduction pathways we identified all respond to different cues. We find that the Dpp pathway is likely involved in the activation of enhancer B-C in the *Drosophila* midgut. The Dpp pathway is furthermore essential for EC differentiation, growth, survival to infection, and injury-induced Dpp negatively controls midgut homeostasis [43,45]. Upon enteric infection, the Dpp pathway displays complex behavior. In an early response, Dpp released from hemocytes has been shown to stimulate ISC proliferation, but in a second phase, the Dpp pathway promotes the reestablishment of a quiescent state in these same cells [61]. Our results suggest that upon infection with *Ecc15*, the Dpp pathway also plays a role in ECs by promoting *upd3* transcription, which

could synergize with the early proliferative role of this pathway in ISCs. It remains unclear whether Dpp acts directly or indirectly on the *upd3* promoter. We identified Mad and Med as required for *upd3* expression, and TFBS for Mad are found in the promoter region of *upd3*; however, our yeast one-hybrid screen did not detect a direct interaction between these two components.

We did find evidence of direct regulation of the *upd3* gene by transcription factors downstream of the Hippo pathway and SAPK/SFK/MAPK cascades. The Hippo pathway regulates ISC proliferation in the midgut both cell-autonomously and non-cell-autonomously [42,62,63]. The upstream regulators of Hippo signaling remain uncharacterized in the midgut, but the MAPKKKK Msn has been shown to control Wts in progenitor cells [64]. Our data suggest that the Yki/Sd complex directly regulates *upd3* in ECs upon infection, and that Msn, but not Hpo, is involved in that process. We furthermore identified D-Fos and D-Jun (AP-1) as direct regulators of *upd3* transcription, acting downstream of Src-Raf-Dsor1-ERK and Licorne-p38b kinase cascades. Stress responsive kinases, as well as SFKs, are key regulators of AP-1 [55]. It remains unclear whether the upstream stimuli inducing SAPK/SFK/MAPKs to regulate *upd3* upon infection include oxidative stress, cytoskeletal modification or a combination of both, but all these stimuli occur upon infection and are possible candidates. We propose that the role of SFKs, MAPKs and SAPKs in the regulation of cytokine expression and cell proliferation is conserved across organisms. Indeed, AP-1 and these conserved pathways have been demonstrated to have an important role in the regulation of cytokine secretion and tumorigenesis [65,66]. Src kinases have been previously shown to be important for wound healing in multiple models, potentially downstream of ROS production [67,68], suggesting that conserved pathways are used in both tissue repair and gut regeneration. Interestingly, the pathways we identified in our study are known to work cooperatively in other systems. For example, mammalian JNK kinases are capable of

phosphorylating YAP (Yki homologue), and can inhibit multiple constituents of the Hippo pathway during tumorigenesis [69]. In addition, mammalian Src has been shown to regulate YAP during inflammation [70]. Finally, it was recently found that binding sites for Yap/Taz/Tead (Yki/Sd in *Drosophila*) and AP-1 are associated genome-wide with enhancers of genes involved in oncogenic growth. Altogether, these results and our own suggest that the SAPK/SFK/MAPK pathways in coordination with Hippo and TGF-β pathways work together in a conserved regulatory network that controls tissue growth and repair.

Cell loss, Upd3 regulation and tissue renewal

The maintenance of gut tissue homeostasis relies on the induction of ISC proliferation to compensate for the loss of cells in the epithelium in a homeostatic feedback loop. A simple model of homeostasis would hold that cell death directly triggers *upd3* expression and subsequent ISC proliferation in a coupled manner. In agreement with this model, induction of apoptosis in ECs is sufficient to induce *upd3* expression and trigger ISC proliferation [17]. However, a recent study using oral infection with a low dose of pathogenic bacteria in *Drosophila* demonstrated that cytokine-induced ISC proliferation can be elicited even by infections that do not induce epithelial cell death [71]. This indicates that the coupling of ISC proliferation with cell loss is not complete. In agreement with these results, we found that neither apoptosis nor autophagy alone appear to be necessary for *Ecc15*-induced *upd3* expression. Rather, the results of Loudhaief *et al.* (2017) and our study suggest that cytokine signaling results from stress detection rather than cell death, and that regenerative processes can occur independently of apoptosis [71]. This is also in agreement with the fact that the gut microbiota, which induces basal levels of epithelial stress but does not induce massive cell death in the gut, also stimulates basal cytokine production [3,13,16,26].

Pathways such as Hippo regulate both cell death and apoptosis, as well as cytokine production in the gut. We therefore propose that coupling between cell death and cell renewal is a consequence of cross-talk between regulatory pathways, rather than renewal as a direct consequence of cell death.

Another hypothesis is that cell loss without death is coupled to tissue repair. Accordingly, infection induces the loss of ECs from the epithelium prior to anoikis [19]. It is therefore possible that EC delamination, rather than death, is a key signal for regeneration as evidenced by the observation that loss of EC contact with the basal lamina of the midgut epithelium can trigger Upd3 production [72]. EMT is a process of tissue morphogenesis reminiscent of cell delamination, in which epithelial cells detach and are extruded from the epithelial sheet whereupon they migrate as loosely associated mesenchymal tissue. Curiously, our study shows that the transcription factor Sna, a main regulator of *Drosophila* EMT and a marker of progenitor cells in the midgut, is both transcriptionally induced in ECs upon infection and required for *upd3* transcription [8,73]. Sna's role as a negative regulator of transcription implies that this phenotype is likely a secondary effect. We thus propose that *upd3* expression may be downstream of Sna-dependent, EMT-like shedding of ECs in response to enteric stresses. In such a scenario, cell loss would require an EMT like regulation in ECs and indirectly trigger *upd3* transcription. Epithelial structure and tension modulated by delamination could also result in Src and Hippo pathway activation, and ultimately in *upd3* induction. Future work will determine how ECs are extruded from the epithelial sheet and how cell loss modulates Upd3 production.

Regulatory networks are reused in multiple epithelial cell types to coordinate tissue repair

The regulatory pathways that we find upstream of *upd3* transcription in ECs appear to be the same pathways required in ISCs to control their proliferation. For instance, inactivation of the Hippo pathway or induction of the Dpp pathway in ISCs is sufficient to stimulate stem cell proliferation in the *Drosophila* midgut [42] [61]. Similarly, the MAPK pathway has been demonstrated to be critical in ISCs for division and differentiation downstream of EGFR [19]. However, the regulation of these pathways is not always identical between cell types: while the SAPK kinase cascade is strongly required cell-autonomously for ISC activity [13], its effect on *upd3* induction in ECs is only marginal. Along these lines, MAPKs act downstream of growth factor receptors in ISCs, while we found that Src kinases trigger their activation in ECs. We thus propose that a single regulatory network controls ISC proliferation both cell-autonomously and cell non-autonomously and that the two processes are linked by the secretion of cytokines and growth factors.

Conclusions

Altogether, the results of our study illustrate key aspects of the regulation of cytokine expression by intestinal cells in the gut. We identify microbe-responsive enhancers in the promoter of *upd3* that act as stress sensors, thanks to the cooperative regulation by multiple pathways. Dpp, Hippo, Src, SAPK and MAPK pathways all converge on the transcriptional regulation of *upd3*, thus acting together as a genetic network dedicated to damage detection and response. Strikingly, this genetic network controls both proliferation in stem cells, as well as the expression of cytokines in ECs to subsequently induce ISC proliferation. This genetic regulatory network therefore links stem cell proliferation and cytokine production in one common molecular framework, and paves the way for future studies to decrypt the link between inflammation and cancer in the gut.

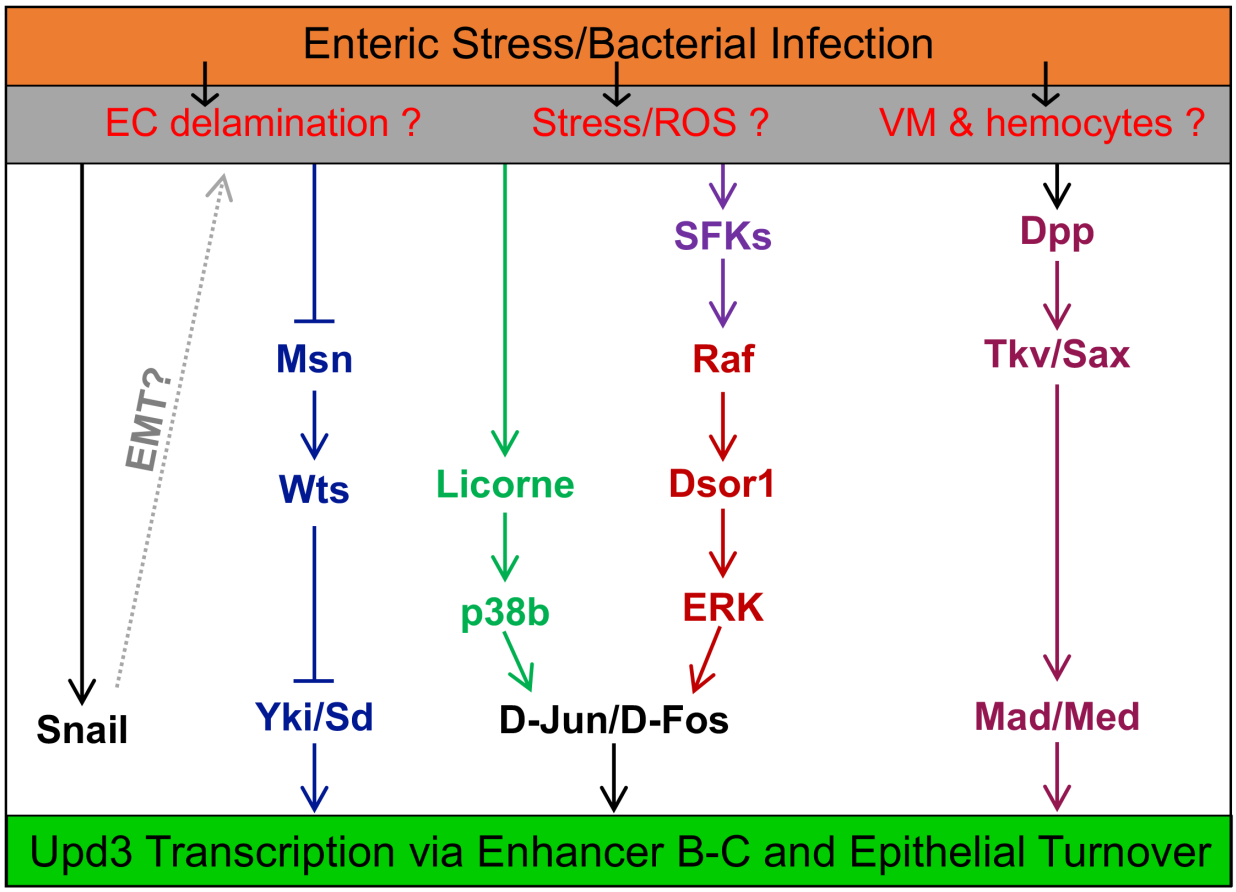

Figure 3.17. Model of Upd3 regulation in midgut ECs in response to enteric stress. Schematic representation of the pathways that control *upd3* transcription in ECs during intestinal trauma. Biotic and abiotic stresses, as well as the responsive ROS production, induce epithelial cell extrusion and cell death. The Sna TF may act as an integral component of cellular extrusion by negatively regulating cellular adhesion. SFK and MAPK pathways are activated by cellular stress, and converge on the activation of D-Fos and D-Jun TFs. The Hippo pathway likely responds to tissue loss in the midgut by removing the inhibition of the Yki and Sd TF complex.

Materials and methods

Fly stocks and Husbandry

Drosophila stocks were maintained at room temperature (~23°C) on standard fly medium (sucrose, cornmeal, yeast, and agar). Control lines: as controls, we used the F1 progeny of the driver line crossed to wild-type stocks such as Canton-S (Cs) (BDSC: 64349), and background matched stocks such as *attp2* (BDSC: 36303) and *attp40* (BDSC: 36304). Gal4 Drivers: *Myo1A-Gal4, UAS-GFP, tub-Gal80^{TS}; upd3-lacZ* (*Myo^{TS}*, EC-specific), *Su(H)GBE-Gal4;UAS-GFP, tub-Gal80^{TS}*

(*Su(H)^{TS},* EB-specific) [17]. Conditional *Gal4^{TS}* flies were obtained by crossing virgin females of the driver strain with males of the *UAS-transgene* line. For RNAi and overexpression experiments, F1 progenies (*driver > UAS-transgene*) were raised at 18°C until 3 days after emergence, to allow for full gut development. Flies were then switched to 29°C for a week to allow for maximum transgene expression and RNAi-mediated gene knockdown. UAS-transgene stocks: RNAi transgenic fly lines were obtained from Bloomington (TRiP lines), VDRC (Vienna) or NIG (Japan), as specified in S Table 3.2. *UAS-Atf3 3xHA* was obtained from FlyORF. *UAS-Src42A*, *UAS-Src42A^{YF}*, *UAS-Src64B*, *UAS-Src64B^{YF}* were generously provided by professor Tian Xu [74]. *UAS-bsk^{DN}; IF/CyO* (BDSC: 6409), *UAS-Src42A-IR* (NIG-FLY: 7873R-2), *UAS-Src42A-IR* (NIG-FLY: 7873R-3), *UAS-Src64B-IR* (VDRC: 35252), *UAS-Src64B-IR* (NIG-FLY: 7524R-1)/*CyO; MKRS/TM6B*, *UAS-Src42A^{YF5382B}*, *sb/TM6B, UAS-Src64B^{YF161}*; *sb/TM6B, yw;;Src64B^{YU1332}* (BDSC: 7342)*, w-; IF/CyO; UAS-csk/TM6B, w-; UAS-cpb7/Cyo; MKRS/TM6B, w-; IF/CyO; UAS-cpa attB/TM6B* [75], *w-; UAS-cpa-IRC10* [75], *w-; IF/CyO; UAS-cpb-IR/TM6B* (VDRC: 46668), *w-;;; zyx^{D41}* [76], were generously provided by Florence Janody. *UAS-Apoliner* and *Tub-Apoliner* were both generously provided by Jean-Paul Vincent [53]. Reporter lines: *upd3.1-lacZ*, *esg-lacZ, Myo-lacZ,* [17]. A complete list of the TRiP UAS-RNAi lines used in the TF screen can be found in S Table 3.2. A list of the additional transgenic lines used in this report can be found in S Table 3.5.

Generation of Upd3 enhancer trap lines

Overlapping fragments of ~1.5Kb were cloned in front of GFP, starting from 4.2Kb upstream of the *upd3* start site and ending 7.3Kb downstream of the gene. These sequence fragments were designated putative *upd3* enhancer regions A-R and cloned into T vector followed by pH-stinger

[77] to create 21 enhancer trap GFP vectors. Each vector was used to generate at least two enhancer trap GFP fly lines (to account for insertion position effects), which were then screened for capacity to drive GFP expression in the adult midgut under both basal conditions as well as *Ecc15* infection. In addition, two reporter transgenes expressing NLS-GFP, fused to the Upd3 protein and driven under the control of the full *upd3* locus and endogenous promoter (from 4.2Kb upstream of the *upd3* start site, up to 7.3Kb downstream of the gene), as well as the same reporter with enhancer B and C sequence regions deleted, were created and inserted at the *attP2* insertion site.

Bacterial cultures and Oral Infection

Erwinia carotovora ssp. carotovora 15 (*Ecc15*) *and Pseudomonas entomophila (Pe)* are two Gram-negative bacteria, pathogenic to the *Drosophila* midgut when ingested [1]. Bacteria were maintained on standard LB agar plates and *Pe* was plated from glycerol stocks for each experiment. Bacteria were cultured in LB broth at 29°C for 16 hours. Oral infection was performed as previously described [12]: flies were starved in empty vials for 2 hours at 29°C, then moved to fly vials in which the standard food was completely covered by a filter paper disc containing 150µl of either 2.5% sucrose solution (control), or 5% sucrose solutions mixed in equal volume with OD_{600} = 200 bacterial pellet, or a solution of 500µg/ml of bleomycin or 6% DSS. Orally treated flies were incubated at 29°C until dissection.

Generation of Axenic flies

3 to 5 day old flies were transferred on fresh fruit juice agar plates. After 1 day of habituation, flies were allowed to lay eggs for 4-6 hours. Eggs were first suspended in 1X PBS, rinsed in 70% EtOH for 1 minute and dechorionated using 10% bleach for ~10min. Eggs were then transferred under a

sterile flow hood and further rinsed 3 times with sterile ddH_2O. The eggs were finally transferred into sterile fly vials with sterilized fly food. Flies were tested for presence of bacteria after each experiment, by plating homogenates on MRS agar plates.

Immunohistochemistry and fluorescence imaging

After dissection, *Drosophila* midguts were fixed in 4% paraformaldehyde in 1X PBS for 45 to 90 minutes and successively washed 3 times with 0.1% TritonX in PBS. Guts to be immunostained were then incubated for an hour in blocking solution (1% bovine serum albumin, 1% normal donkey serum, and 0.1% Triton X-100 in PBS). Overnight primary antibody staining was performed at RT. Guts were washed 3 times with 0.1% TritonX in PBS and ≥2 hour secondary antibody staining was performed in PBS. Primary antibodies used: rabbit anti-pH3 (1:000, EMD Millipore), rabbit anti-β-Galactosidase (1:1000, MP Biomedicals), and mouse anti-Prospero (1:100, DSHB). Secondary antibodies used: donkey anti-rabbit-555 (1:2000, Thermo Fisher), donkey anti-mouse-488 (1:2000, Thermo Fisher), and donkey anti-mouse-647 (1:1000, Thermo Fisher). DNA was stained in 1:50,000 DAPI (Sigma-Aldrich) in PBS and 0.1% TritonX for 30min, and samples received a final three washes in PBS before mounting in antifade medium (Citifluor AF1). Imaging was performed on a Zeiss LSM 700 fluorescent/confocal inverted microscope.

β-Galactosidase Titration Assay

Myo-Gal4^{TS}; Upd3-lacZ driver/reporter flies were crossed to RNAi or overexpression lines and their adult progeny were induced at 29°C for seven days, then treated with either sucrose (control) or *Ecc15* for 16 hours. Five midguts were dissected for each sample and homogenized in 100µl Z-buffer (60mM Na_2HPO_4, 60mM NaH_2PO_4, 10mM KCl, 1mM $MgSO_4$, 50mM β-mercaptoethanol,

adjusted pH to 8 with NaOH). Homogenates were then centrifuged and 40µl of supernatant was mixed with 250µl of 0.35mg/ml ONPG (o-nitrophenol-β-D-galactoside) in Z-buffer solution in the wells of a 96-well plate. Absorbance was then measured at 420nm in a plate-reader (spectra max plus, Molecular Devices) every minute for one hour at 37°C. Because the amount of ONPG added to the reaction is sufficient to saturate the β-Gal in the samples, the reaction rate (absorbance vs time) is proportional to the quantity of β-Gal in each sample, and thus the maximum reaction rate (V_{max}) was used as a measure of the relative β-Gal quantity in each sample. For each experiment, the average of three controls was used as a reference and relative *upd3-lacZ* activity was calculated (S Table 3.2). The three controls used were: progeny of *Myo-Gal4^{TS}; upd3-lacZ* virgins crossed to either the wild type strain, *Canton-S* (Cs), or the controls "*attP2"* and "*attP40"*. The *attP2* and *attP40* lines are background controls for the TRiP *UAS-RNAi* stocks, while Cs is a standard, laboratory wild-type fly line. We used the variation in *upd3-lacZ* activity between the three controls (S5A-B Fig) to determine a confidence interval and select positive hits in the screen results (lower than 0.6 and higher than 1.4 upon infection, lower than 0.5 and higher than 1.6 in UC conditions). We further confirmed the significance of these results by the calculation of z-scores for each RNAi knockdown tested (S Table 3.2).

Survival experiments

Myo-Gal4^{TS}; upd3-lacZ driver/reporter flies were crossed to the *UAS-RNAi* lines and their progeny were raised at 18°C. At 3-days post eclosure, 20 adult females were shifted to 29°C, the temperature at which all survival experiments were done to allow constant expression of the RNAi constructs. Day seven post-induction was considered day 0 of the survival studies. The controls used were the F1 progeny of crosses between our driver and the wild-type stock Cs, as well as the

background-matched lines "*attP2*" and "*attP40*". To evaluate possible background or off-target effects, multiple RNAi lines were used for each gene and the survival of all parental lines alone was also monitored. Survival was recorded in unchallenged (UC) conditions, in which flies were kept on standard cornmeal medium, and upon constant exposure to *Ecc15* (flies were transferred to new tubes with fresh *Ecc15* every 3 days). Deaths were monitored daily and plotted using the GraphPad Prism 7.0c software. Results of survival experiments are aggregates of 3 to 9 biological replicates and error bars represent standard errors. LT50s were determined using PROBIT analysis in R.

RT-qPCR

Total RNA was extracted from 15 to 20 female fly midguts following standard protocol with Trizol (Invitrogen). Reverse transcription (RT) was performed using the qScript cDNA synthesis kit (Quanta) and quantitative PCR with SsoAdvanced Universal SYBR Green Supermix (Bio-Rad) and a CFX96 TouchTM Real-Time PCR Detection System (Bio-Rad). Measured mRNA quantities were normalized to control *Rp49* (*RpL32*) mRNA values.

Yeast One-Hybrid

The *upd3-lacZ* sequence was cloned into 4 fragments fused to the *HIS3* reporter to generate baits further tested in yeast one-hybrid. *HIS3* encodes an imidazoleglycerol-phosphate dehydratase, that catalyzes histidine synthesis, and the inhibitor 3-amino-1,2,4-triazole (3AT) competitively inhibits this activity. The higher the level of 3AT in the medium is, the higher *HIS3* expression needs to be to insure yeast growth, thus testing the strength of transactivation of the *bait-HIS3* in response to multiple TFs. Prior to the TF/bait interaction test, a self-activation test was performed to assess

whether natural *S. cerevisiae* TFs are sufficient to induce basal *HIS3* expression. This test was performed by measuring the growth of eight independently transformed yeasts for each bait on SC-His plates with varying concentrations of 3AT (0, 10, 20, 40, 60, 80mM). For each bait, a transformant yeast that can grow on SC-His medium, but is unable to grow on medium supplemented with 3AT was selected.

The yeast one-hybrid assay was performed as previously described [27,78,79]. Briefly, *upd3-HIS3* baits were integrated in the genome of *Saccharomyces cerevisiae* and transformed with a collection of 670 plasmids containing *Drosophila* TF open reading frames fused to the Gal4 activation domain. Each colony was plated on synthetic complete medium lacking Histidine (to select for the *upd3*-His construct) and Tryptophan (to select for the presence of the TF vector). Plates were incubated at 30°C for 3, 7, and 10d and imaged using a Bio-Rad gel doc system. Yeasts not transformed with any TF prey and yeasts transformed with the Gal4 activation domain alone served as negative control. Plate images were analyzed using the R package Gitter, that estimates colony surface and circularity. Sets of quadruplicate colonies that showed growth above background levels were deduced to have a direct interaction between the TF prey and the DNA bait, and the strength of the interaction was estimated and ranked (from +/- to +++) by the ability of each yeast colony to grow on increasing concentrations of the HIS3 inhibitor 3AT as previously described [27,79].

Acknowledgements

We would like to thank Florence Janody, Bruce Edgar, Jean-Paul Vincent, Matthew Freeman and Tian Xu for stocks and reagents. We also thank members of the Buchon lab for helpful comments on the manuscript. We thank the TRiP at Harvard Medical School (NIH/NIGMS R01-GM084947)

for providing transgenic RNAi fly stocks and/or plasmid vectors used in this study. Stocks obtained from the Bloomington Drosophila Stock Center (NIH P40OD018537) were used in this study.

References

1. Buchon N, Broderick NA, Lemaitre B. Gut homeostasis in a microbial world: insights from Drosophila melanogaster. Nat Rev Micro. 2013;11: 615–626. doi:10.1038/nrmicro3074

2. Peterson LW, Artis D. Intestinal epithelial cells: regulators of barrier function and immune homeostasis. Nat Rev Immunol. 2014;14: 141–153. doi:10.1038/nri3608

3. Karin M, Clevers H. Reparative inflammation takes charge of tissue regeneration. Nature. 2016;529: 307–315. doi:10.1038/nature17039

4. Radtke F, Clevers H. Self-renewal and cancer of the gut: two sides of a coin. Science. 2005;307: 1904–1909. doi:10.1126/science.1104815

5. Bonfini A, Liu X, Buchon N. From pathogens to microbiota: How Drosophila intestinal stem cells react to gut microbes. Dev Comp Immunol. 2016;64: 22–38. doi:10.1016/j.dci.2016.02.008

6. Apidianakis Y, Rahme L. Drosophila melanogaster as a model for human intestinal infection and pathology. Dis Model Mech. 2011;4: 21–30. doi:10.1242/dmm.003970

7. Zeng X, Hou SX. Enteroendocrine cells are generated from stem cells through a distinct progenitor in the adult Drosophila posterior midgut. The Company of Biologists Limited; 2015;142: 644–653. doi:10.1242/dev.113357

8. Buchon N, Osman D, David FPA, Yu Fang H, Boquete J-P, Deplancke B, et al. Morphological and molecular characterization of adult midgut compartmentalization in Drosophila. Cell Rep. 2013;3: 1725–1738. doi:10.1016/j.celrep.2013.04.001

9. Marianes A, Spradling AC, Brand A. Physiological and stem cell compartmentalization within the Drosophila midgut. elife. eLife Sciences Publications Limited; 2013;2. doi:10.7554/eLife.00886

10. Ryu J-H, Ha E-M, Oh C-T, Seol J-H, Brey PT, Jin I, et al. An essential complementary role

of NF-kappaB pathway to microbicidal oxidants in Drosophila gut immunity. EMBO J. 2006;25: 3693–3701. doi:10.1038/sj.emboj.7601233

11. Ha E-M, Lee K-A, Seo YY, Kim S-H, Lim J-H, Oh B-H, et al. Coordination of multiple dual oxidase-regulatory pathways in responses to commensal and infectious microbes in drosophila gut. Nat Immunol. 2009;10: 949–957. doi:10.1038/ni.1765

12. Buchon N, Broderick NA, Poidevin M, Pradervand S, Lemaitre B. Drosophila intestinal response to bacterial infection: activation of host defense and stem cell proliferation. Cell Host Microbe. 2009;5: 200–211. doi:10.1016/j.chom.2009.01.003

13. Buchon N, Broderick NA, Chakrabarti S, Lemaitre B. Invasive and indigenous microbiota impact intestinal stem cell activity through multiple pathways in Drosophila. Genes Dev. Cold Spring Harbor Lab; 2009;23: 2333–2344. doi:10.1101/gad.1827009

14. Bosco-Drayon V, Poidevin M, Boneca IG, Narbonne-Reveau K, Royet J, Charroux B. Peptidoglycan Sensing by the Receptor PGRP-LE in the Drosophila Gut Induces Immune Responses to Infectious Bacteria and Tolerance to Microbiota. Cell Host Microbe. 2012;12: 153–165. doi:10.1016/j.chom.2012.06.002

15. Neyen C, Poidevin M, Roussel A, Lemaitre B. Tissue- and Ligand-Specific Sensing of Gram-Negative Infection in Drosophila by PGRP-LC Isoforms and PGRP-LE. J Immunol. 2012. doi:10.4049/jimmunol.1201022

16. Osman D, Buchon N, Chakrabarti S, Huang Y-T, Su W-C, Poidevin M, et al. Autocrine and paracrine unpaired signaling regulate intestinal stem cell maintenance and division. J Cell Sci. The Company of Biologists Ltd; 2012;125: 5944–5949. doi:10.1242/jcs.113100

17. Jiang H, Patel PH, Kohlmaier A, Grenley MO, Mcewen DG, Edgar BA. Cytokine/Jak/Stat signaling mediates regeneration and homeostasis in the Drosophila midgut. Cell. 2009;137: 1343–1355. doi:10.1016/j.cell.2009.05.014

18. Chatterjee M, Ip YT. Pathogenic stimulation of intestinal stem cell response in Drosophila. J Cell Physiol. 2009;220: 664–671. doi:10.1002/jcp.21808

19. Buchon N, Broderick NA, Kuraishi T, Lemaitre B. Drosophila EGFR pathway coordinates stem cell proliferation and gut remodeling following infection. BMC Biol. BioMed Central Ltd; 2010;8: 152. doi:10.1186/1741-7007-8-152

20. Cordero JB, Stefanatos RK, Scopelliti A, Vidal M, Sansom OJ. Inducible progenitor-derived Wingless regulates adult midgut regeneration in Drosophila. EMBO J. 2012. doi:10.1038/emboj.2012.248

21. Biteau B, Jasper H. EGF signaling regulates the proliferation of intestinal stem cells in Drosophila. 2011;138: 1045–1055. doi:10.1242/dev.056671

22. Jiang H, Grenley MO, Bravo M-J, Blumhagen RZ, Edgar BA. EGFR/Ras/MAPK signaling mediates adult midgut epithelial homeostasis and regeneration in Drosophila. Cell Stem Cell. 2011;8: 84–95. doi:10.1016/j.stem.2010.11.026

23. Zhou F, Rasmussen A, Lee S, Agaisse H. The UPD3 cytokine couples environmental challenge and intestinal stem cell division through modulation of JAK/STAT signaling in the stem cell microenvironment. Dev Biol. 2013;373: 383–393. doi:10.1016/j.ydbio.2012.10.023

24. Karpac J, Biteau B, Jasper H. Misregulation of an adaptive metabolic response contributes to the age-related disruption of lipid homeostasis in Drosophila. Cell Rep. 2013;4: 1250–1261. doi:10.1016/j.celrep.2013.08.004

25. Amcheslavsky A, Jiang J, Ip YT. Tissue damage-induced intestinal stem cell division in Drosophila. Cell Stem Cell. 2009;4: 49–61. doi:10.1016/j.stem.2008.10.016

26. Broderick NA, Buchon N, Lemaitre B. Microbiota-induced changes in drosophila melanogaster host gene expression and gut morphology. MBio. American Society for Microbiology; 2014;5: e01117–14. doi:10.1128/mBio.01117-14

27. Hens K, Feuz J-D, Isakova A, Iagovitina A, Massouras A, Bryois J, et al. Automated protein-DNA interaction screening of Drosophila regulatory elements. Nat Meth. 2011. doi:10.1038/nmeth.1763

28. Dutta D, Dobson AJ, Houtz PL, Gläßer C, Revah J, Korzelius J, et al. Regional Cell-Specific Transcriptome Mapping Reveals Regulatory Complexity in the Adult Drosophila Midgut. Cell Rep. 2015;12: 346–358. doi:10.1016/j.celrep.2015.06.009

29. Dutta D, Buchon N, Xiang J, Edgar BA. Regional Cell Specific RNA Expression Profiling of FACS Isolated Drosophila Intestinal Cell Populations. Curr Protoc Stem Cell Biol. Hoboken, NJ, USA: John Wiley & Sons, Inc; 2015;34: 2F.2.1–2F.2.14. doi:10.1002/9780470151808.sc02f02s34

30. Mathelier A, Zhao X, Zhang AW, Parcy F, Worsley-Hunt R, Arenillas DJ, et al. JASPAR 2014: an extensively expanded and updated open-access database of transcription factor binding profiles. Nucleic Acids Research. 2014;42: D142–7. doi:10.1093/nar/gkt997

31. Gallo SM, Gerrard DT, Miner D, Simich M, Soye Des B, Bergman CM, et al. REDfly v3.0: toward a comprehensive database of transcriptional regulatory elements in Drosophila. Nucl Acids Res. 2010;39: D118–D123. doi:10.1093/nar/gkq999

32. Bothma JP, Magliocco J, Levine MS. The Snail Repressor Inhibits Release, not Elongation, of Paused Pol II in the Drosophila Embryo. Current biology : CB. NIH Public Access; 2011;21: 1571–1577. doi:10.1016/j.cub.2011.08.019

33. Chopra VS, Kong N, Levine MS. Transcriptional repression via antilooping in the Drosophila embryo. Proceedings of the National Academy of Sciences. National Acad Sciences; 2012;109: 9460–9464. doi:10.1073/pnas.1102625108

34. Qi D, Bergman M, Aihara H, Nibu Y, Mannervik M. Drosophila Ebi mediates Snail-dependent transcriptional repression through HDAC3-induced histone deacetylation. EMBO J. European Molecular Biology Organization; 2008;27: 898–909. doi:10.1038/emboj.2008.26

35. Nibu Y, Zhang H, Bajor E, Barolo S, Small S, Levine MS. dCtBP mediates transcriptional repression by Knirps, Krüppel and Snail in the Drosophila embryo. The EMBO Journal. European Molecular Biology Organization; 1998;17: 7009–7020. doi:10.1093/emboj/17.23.7009

36. Huang J, Wu S, Barrera J, Matthews K, Pan D. The Hippo signaling pathway coordinately regulates cell proliferation and apoptosis by inactivating Yorkie, the Drosophila Homolog of YAP. Cell. 2005;122: 421–434. doi:10.1016/j.cell.2005.06.007

37. Staley BK, Irvine KD. Hippo signaling in Drosophila: Recent advances and insights. Singh A, Irvine KD, editors. Dev Dyn. 2011;241: 3–15. doi:10.1002/dvdy.22723

38. Li Q, Li S, Mana-Capelli S, Roth Flach RJ, Danai LV, Amcheslavsky A, et al. The Conserved Misshapen-Warts-Yorkie Pathway Acts in Enteroblasts to Regulate Intestinal Stem Cells in Drosophila. Dev Cell. 2014;31: 291–304.

39. Qing Y, Yin F, Wang W, Zheng Y, Guo P, Schozer F, et al. The Hippo effector Yorkie activates transcription by interacting with a histone methyltransferase complex through Ncoa6. elife. 2014;3: 1260. doi:10.7554/eLife.02564

40. Bayarmagnai B, Nicolay BN, Islam ABMMK, Lopez-Bigas N, Frolov MV. Drosophila GAGA factor is required for full activation of the dE2f1-Yki/Sd transcriptional program. Cell Cycle. 2012;11: 4191–4202. doi:10.4161/cc.22486

41. Shaw RL, Kohlmaier A, Polesello C, Veelken C, Edgar BA, Tapon N. The Hippo pathway regulates intestinal stem cell proliferation during Drosophila adult midgut regeneration. 2010;137: 4147–4158. doi:10.1242/dev.052506

42. Staley BK, Irvine KD. Warts and Yorkie mediate intestinal regeneration by influencing stem cell proliferation. Curr Biol. 2010;20: 1580–1587. doi:10.1016/j.cub.2010.07.041

43. Guo Z, Driver I, Ohlstein B. Injury-induced BMP signaling negatively regulates Drosophila midgut homeostasis. J Cell Biol. 2013;201: 945–961. doi:10.1083/jcb.201302049

44. Tian A, Jiang J. Intestinal epithelium-derived BMP controls stem cell self-renewal in Drosophila adult midgut. 2014;3: e01857. doi:10.7554/eLife.01857

45. Zhou J, Florescu S, Boettcher A-L, Luo L, Dutta D, Kerr G, et al. Dpp/Gbb signaling is required for normal intestinal regeneration during infection. Dev Biol. 2014. doi:10.1016/j.ydbio.2014.12.017

46. Li H, Qi Y, Jasper H. Dpp signaling determines regional stem cell identity in the regenerating adult Drosophila gastrointestinal tract. Cell Rep. 2013;4: 10–18. doi:10.1016/j.celrep.2013.05.040

47. Driver I, Ohlstein B. Specification of regional intestinal stem cell identity during Drosophila metamorphosis. 2014;141: 1848–1856. doi:10.1242/dev.104018

48. Li Z, Zhang Y, Han L, Shi L, Lin X. Trachea-derived dpp controls adult midgut homeostasis in Drosophila. Dev Cell. 2013;24: 133–143. doi:10.1016/j.devcel.2012.12.010

49. Aleman A, Rios M, Juarez M, Lee D, Chen A, Eivers E. Mad linker phosphorylations control the intensity and range of the BMP-activity gradient in developing Drosophila tissues. Sci Rep. 2014;4: 6927. doi:10.1038/srep06927

50. Wisotzkey RG, Mehra A, Sutherland DJ, Dobens LL, Liu X, Dohrmann C, et al. Medea is a Drosophila Smad4 homolog that is differentially required to potentiate DPP responses. Development. 1998;125: 1433–1445.

51. Kockel L, Homsy JG, Bohmann D. Drosophila AP-1: lessons from an invertebrate. Oncogene. 2001;20: 2347–2364. doi:10.1038/sj.onc.1204300

52. Kappelmann M, Bosserhoff A, Kuphal S. AP-1/c-Jun transcription factors: regulation and function in malignant melanoma. Eur J Cell Biol. 2014;93: 76–81. doi:10.1016/j.ejcb.2013.10.003

53. Bardet P-L, Kolahgar G, Mynett A, Miguel-Aliaga I, Briscoe J, Meier P, et al. A fluorescent reporter of caspase activity for live imaging. Proceedings of the National Academy of Sciences. National Acad Sciences; 2008;105: 13901–13905. doi:10.1073/pnas.0806983105

54. Chakrabarti S, Poidevin M, Lemaitre B. The Drosophila MAPK p38c Regulates Oxidative Stress and Lipid Homeostasis in the Intestine. Garsin DA, editor. PLoS Genet. Public Library of Science; 2014;10: e1004659. doi:10.1371/journal.pgen.1004659

55. Stokoe D, McCormick F. Activation of c-Raf-1 by Ras and Src through different mechanisms: activation in vivo and in vitro. EMBO J. 1997;16: 2384–2396. doi:10.1093/emboj/16.9.2384

56. Tran NH, Frost JA. Phosphorylation of Raf-1 by p21-activated kinase 1 and Src regulates Raf-1 autoinhibition. J Biol Chem. American Society for Biochemistry and Molecular Biology; 2003;278: 11221–11226. doi:10.1074/jbc.M210318200

57. Li H, Qi Y, Jasper H. Preventing Age-Related Decline of Gut Compartmentalization Limits Microbiota Dysbiosis and Extends Lifespan. Cell Host Microbe. 2016;19: 240–253. doi:10.1016/j.chom.2016.01.008

58. Buchon N, Silverman N, Cherry S. Immunity in Drosophila melanogaster - from microbial recognition to whole-organism physiology. Nat Rev Immunol. 2014;14: 796–810. doi:10.1038/nri3763

59. Ha E-M, Lee K-A, Park SH, Kim S-H, Nam H-J, Lee H-Y, et al. Regulation of DUOX by the Galphaq-phospholipase Cbeta-Ca2+ pathway in Drosophila gut immunity. Dev Cell. 2009;16: 386–397. doi:10.1016/j.devcel.2008.12.015

60. Jones RM, Luo L, Ardita CS, Richardson AN, Kwon YM, Mercante JW, et al. Symbiotic lactobacilli stimulate gut epithelial proliferation via Nox-mediated generation of reactive oxygen species. EMBO J. 2013;32: 3017–3028. doi:10.1038/emboj.2013.224

61. Ayyaz A, Li H, Jasper H. Haemocytes control stem cell activity in the Drosophila intestine. Nat Cell Biol. 2015;17: 736–748. doi:10.1038/ncb3174

62. Karpowicz P, Perez J, Perrimon N. The Hippo tumor suppressor pathway regulates intestinal stem cell regeneration. 2010;137: 4135–4145. doi:10.1242/dev.060483

63. Ren F, Wang B, Yue T, Yun E-Y, Ip YT, Jiang J. Hippo signaling regulates Drosophila intestine stem cell proliferation through multiple pathways. Proceedings of the National Academy of Sciences. 2010;107: 21064–21069. doi:10.1073/pnas.1012759107

64. Li Q, Li S, Mana-Capelli S, Roth Flach RJ, Danai LV, Amcheslavsky A, et al. The Conserved Misshapen-Warts-Yorkie Pathway Acts in Enteroblasts to Regulate Intestinal Stem Cells in Drosophila. Dev Cell. 2014;31: 291–304. doi:10.1016/j.devcel.2014.09.012

65. Qiao Y, He H, Jonsson P, Sinha I, Zhao C, Dahlman-Wright K. AP-1 is a key regulator of proinflammatory cytokine TNFα-mediated triple-negative breast cancer progression. Journal of Biological Chemistry. American Society for Biochemistry and Molecular Biology; 2016;291: 18309–18309. doi:10.1074/jbc.A115.702571

66. Khalaf H, Jass J, Olsson P-E. Differential cytokine regulation by NF-kappaB and AP-1 in Jurkat T-cells. BMC Immunol. BioMed Central; 2010;11: 26. doi:10.1186/1471-2172-11-26

67. Yoo SK, Freisinger CM, LeBert DC, Huttenlocher A. Early redox, Src family kinase, and calcium signaling integrate wound responses and tissue regeneration in zebrafish. J Cell Biol. Rockefeller University Press; 2012;199: 225–234. doi:10.1083/jcb.201203154

68. Juarez MT, Patterson RA, Sandoval-Guillen E, McGinnis W. Duox, Flotillin-2, and Src42A Are Required to Activate or Delimit the Spread of the Transcriptional Response to Epidermal Wounds in Drosophila. PLoS Genet. 2011;7: e1002424. doi:10.1371/journal.pgen.1002424

69. Sun G, Irvine KD. Regulation of Hippo signaling by Jun kinase signaling during compensatory cell proliferation and regeneration, and in neoplastic tumors. Dev Biol. 2011;350: 139–151. doi:10.1016/j.ydbio.2010.11.036

70. Taniguchi K, Wu L-W, Grivennikov SI, de Jong PR, Lian I, Yu F-X, et al. A gp130–Src–YAP module links inflammation to epithelial regeneration. Nature. 2015;519: 57–62. doi:10.1038/nature14228

71. Loudhaief R, Brun-Barale A, Benguettat O, Nawrot-Esposito M-P, Pauron D, Amichot M, et al. Apoptosis restores cellular density by eliminating a physiologically or genetically induced excess of enterocytes in the Drosophila midgut. Development. Oxford University Press for The Company of Biologists Limited; 2017;144: 808–819. doi:10.1242/dev.142539

72. Patel PH, Dutta D, Edgar BA. Niche appropriation by Drosophila intestinal stem cell tumours. Nat Cell Biol. 2015;17: 1182–1192. doi:10.1038/ncb3214

73. Cano A, Pérez-Moreno MA, Rodrigo I, Locascio A, Blanco MJ, del Barrio MG, et al. The transcription factor Snail controls epithelial|[ndash]|mesenchymal transitions by repressing E-cadherin expression. Nat Cell Biol. Nature Publishing Group; 2000;2: 76–83. doi:10.1038/35000025

74. Pedraza LG, Stewart RA, Li D-M, Xu T. Drosophila Src-family kinases function with Csk to regulate cell proliferation and apoptosis. Oncogene. Nature Publishing Group; 2004;23: 4754–4762. doi:10.1038/sj.onc.1207635

75. Fernández BG, Jezowska B, Janody F. Drosophila actin-Capping Protein limits JNK activation by the Src proto-oncogene. Oncogene. 2013;33: 2027–2039. doi:10.1038/onc.2013.155

76. Gaspar P, Holder MV, Aerne BL, Janody F, Tapon N. Zyxin antagonizes the FERM protein expanded to couple F-actin and Yorkie-dependent organ growth. - PubMed - NCBI. Current Biology. 2015;25: 679–689.

77. Barolo S, Carver LA, Posakony JW. GFP and beta-galactosidase transformation vectors for promoter/enhancer analysis in Drosophila. BioTechniques. 2000;29: 726–728– 730– 732.

78. Hens K, Feuz J-D, Deplancke B. A High-throughput Gateway-Compatible Yeast One-Hybrid Screen to Detect Protein-DNA Interactions. Methods Mol Biol. 2012;786: 335–355. doi:10.1007/978-1-61779-292-2_20

79. Kalay G, Lusk R, Dome M, Hens K, Deplancke B, Wittkopp PJ. Potential Direct Regulators of the Drosophila yellow Gene Identified by Yeast One-Hybrid and RNAi Screens. G3 (Bethesda). Genetics Society of America; 2016;6: 3419–3430. doi:10.1534/g3.116.032607

List of Supplementary Materials

S Table 3.1. *upd3*-enhancer-GFP line summary.
This table describes the precise expression pattern of our *upd3*-enhancer-GFP lines.

S Table 3.2. TF TRiP line summary from upd3-lacZ screen.
This table describes the results of our functional screen. Relative lacZ activity values are indicated, as well as the presence of a TFBS for that transcription factor and the interaction in one hybrid screen (Y1H).

S Table 3.3. Yeast one-hybrid assay summary.
This table describes the transcription factors found to bind upd3 by one hybrid. The score reflects the intensity of the binding which results in a stronger growth on selective medium (see Mat&Met).

S Table 3.4. LT50 Values of survival experiments.
This table records the LT50 values and confidence intervals for the lines tested in survival experiments, under *Ecc15*-infected and unchallenged (UC) conditions. The first sub-table presents results associated with the main and supplementary figures (Fig 7B-D, S9A-C Fig) and the additional sub-tables present the results of independent validation experiments, showing additionally tested RNAi lines for the same genes, as well as the survival data of parental lines. Blue text represents lines that are in the *attP2* background, green text represents those that are in the *attP40* background.

S Table 3.5. Additional *Drosophila* stocks.
Lines used in this study and their provenance.

CHAPTER IV

RECRUITMENT OF ADULT PRECURSOR CELLS UNDERLIES LIMITED REPAIR OF INFECTION-INDUCED DAMAGE IN THE LARVAL DROSOPHILA MIDGUT

This chapter represents an article submitted for publication in Cell Host & Microbe, entitled "Recruitment of adult precursor cells underlies limited repair of infection-induced damage in the larval Drosophila midgut" (2018) by Philip Houtz, Alessandro Bonfini, Xiaoli Bing, and Nicolas Buchon. We are currently working on experiments and revisions for our response to reviewer critiques and suggestions.

Abstract

Surviving infection requires immune and repair mechanisms. Developing organisms face the additional challenge to integrate these mechanisms with tightly controlled developmental processes. The larval *Drosophila* midgut lacks dedicated intestinal stem cells. We show that, upon infection, larvae perform limited repair using adult midgut precursors (AMPs). AMPs differentiate in response to damage to generate new enterocytes, transiently depleting their pool. Developmental delay allows for AMPs number reconstitution, which ensures the completion of metamorphosis. Notch signaling is required for the differentiation of AMPs into peripheral cells (PCs), but not to differentiate PCs into enterocytes. Dpp signaling is sufficient, but not necessary, to induce PC differentiation into enterocytes. Infection-induced JAK/STAT pathway is both required and sufficient for differentiation of AMPs and PCs into new enterocytes. Altogether, this work highlights the constraints imposed by development on an organism's response to infection and demonstrates the transient use of adult precursors for tissue repair.

Introduction

Organisms require robust developmental processes to ensure their viable transition into adults. The tightly regulated progression of development can interfere with the regenerative capacity of maturing organisms. This suggests that the ability of developing organisms to deal with damage, injury or stress could be particularly constrained. Organisms have developed strategies to cope with such challenges. In *Drosophila melanogaster* larvae for instance, undifferentiated and fate-committed imaginal cells, which are precursor cells for adult appendages, have ingrained repair processes that allow for their reconstitution when damaged (Hariharan and Serras, 2017; Smith-Bolton, 2016; Smith-Bolton et al., 2009). Damaged imaginal tissue alters developmental timing via cellular signaling that ultimately modulates the circulating levels of hormones such as PTTH, in order to coordinate repair with developmental progression (Colombani et al., 2012; Halme et al., 2010; Jaszczak et al., 2016). However, it remains unclear whether damage to the larval tissue itself triggers a similar regenerative process and if/how it may impact development. This is especially important for intestinal epithelial tissue, which faces the unique challenge of balancing digestive and absorptive functions with its necessary role as a barrier to ingested pathogenic microbes and harmful chemicals (Buchon et al., 2013). In this study, we analyze the larval gut epithelial response after oral pathogenic infection, its impact on adult midgut precursor cells and the consequences that this has on gut and organismal development.

Preservation of tissue homeostasis and epithelial integrity in the gastrointestinal tract requires continual tissue turnover, enacted in the digestive tract via the proliferation and differentiation of dedicated intestinal stem cells (ISCs) to counter the constant loss of old, damaged or dying epithelial cells. Tissue renewal is also crucial for the gut to mend itself in response to infectious,

chemical or physical injuries (Karin and Clevers, 2016; Liu et al., 2017). The *Drosophila* larval midgut epithelium contains absorptive enterocytes (ECs) and secretory enteroendocrine cells (EEs). However, in contrast with its adult counterpart, it does not undergo continuous epithelial renewal (Jiang and Edgar, 2009; Micchelli et al., 2011). Accordingly, during larval development, the midgut does not grow in size by increasing the number of ECs, but rather by increasing the size and ploidy of a set number of larval ECs (Duronio, 1999). Additionally, the larval midgut contains undifferentiated progenitor cells, the adult midgut precursors (AMPs) that ultimately generate all of the epithelial cells in the adult midgut (Mathur et al., 2010). AMPs undergo several rounds of division over the course of larval development to form distinct structures akin to imaginal discs known as imaginal midgut islets. These islets consist of a central cluster of proliferating AMPs enclosed within the membrane(s) of one or more surrounding peripheral cells (PCs), and are dispersed throughout the larval midgut epithelium (Mathur et al., 2010). PCs act as a barrier to enclose AMPs and actively control their behavior, thus acting as a temporary niche.

The digestive tract of *Drosophila* larvae is exposed to a continuous flow of ingested material that can contain potentially pathogenic microbes, since its natural diet is composed of yeasts and other microbes growing in rotting fruits (Lemaitre and Hoffmann, 2007). Most bacteria are non-infectious upon ingestion and are rapidly eliminated from the digestive tract, but a few pathogens have been identified that can persist in the larval midgut, elicit a systemic immune response, and perturb epithelial homeostasis. These include *Erwinia carotovora ssp carotovora 15* (*Ecc15*), a gram-negative plant pathogen, that was discovered to also be pathogenic to *Drosophila melanogaster* larvae, a characteristic conferred by the *Erwinia virulence factor* (*evf*) (Acosta Muniz et al., 2007a; Basset et al., 2003). *Drosophila* employ multiple strategies to combat oral infection, including the secretion of antimicrobial peptides under the control of the Imd pathway,

the production of reactive oxygen species by NADPH oxidases such as Nox and Duox as well as behavioral adaptations (Bae et al., 2010; Buchon et al., 2009b). For instance, in response to infection, hosts can increase the speed of food bolus passage through the gut (Du et al., 2016) or decrease the ingestion of contaminated food (Soldano et al., 2016; Stensmyr et al., 2012). *Drosophila* larvae can detect the presence of *Ecc15* via olfaction and respond by decreasing food uptake (Keita et al., 2017). In addition, *Ecc15* ingestion impedes larval growth by inhibiting commensal bacteria-enhanced protein digestion (Erkosar et al., 2015). *Ecc15* is also pathogenic to adult *Drosophila,* in which it induces a massive loss of ECs when ingested and subsequently triggers an increase in stem cell-mediated tissue turnover (Bonfini et al., 2016; Buchon et al., 2009b; Buchon et al., 2009a). Tissue repair is essential to survive enteric infection and depends on the coordination of multiple signaling pathways including the JAK/STAT, EGFR, Wnt and TGF-β/Dpp pathways (Bonfini et al., 2016; Houtz et al., 2017). This posits the question: how does the larval gut reliably endure pathogenic injury without the support of ISC-mediated renewal?

In this study, we found that *Ecc15* damages the *Drosophila* larval midgut and, unlike in adults, is partially lethal to larvae. In addition, larvae that survive *Ecc15* infection display a developmental delay, which is not due to complete food uptake blockage. Larvae fed with *Ecc15* experienced epithelial damage, causing the gut to shrink in length. However, limited tissue repair allowed some larvae to survive infection. This tissue repair is achieved by the recruitment of AMPs and PCs that are directed to differentiate into new ECs. Surprisingly, AMPs were transiently depleted as there was no increase in proliferation in response to infection. The developmental delay induced by infection allowed the pool of AMPs to be reconstituted, an essential component to resume development and undergo metamorphosis. We also established that the Notch pathway, which is

required for the differentiation of AMPs into PCs, is not sufficient to drive differentiation into ECs. Furthermore, a combination of transcriptomics and functional genetics allowed us to demonstrate that AMP differentiation depends on JAK/STAT signaling, which is initiated by the release of cytokines from stressed ECs. Altogether, our results demonstrate how infection transiently diverts adult precursors from their developmental task to execute the renewal needed to allow host survival of infectious damage.

Results

Ecc15 infection induces partial lethality and a developmental delay in *Drosophila* larvae

To explore differences in the outcome of pathogenic infection on adult and developing hosts, we orally infected either *Drosophila* adult females or 2nd instar (L2) larvae with the insect pathogen *Ecc15*. As previously reported (Buchon et al., 2009b), adult flies survived this infection without any detectable impact on their lifespan (Figure 1A), a phenomenon attributable to the ability of the adult midgut to regenerate lost cells upon infection, thanks to the activity of its ISCs (Buchon et al., 2009b; 2009a; 2010). This homeostatic ability can be bypassed by strains of *Ecc15* that overexpress the virulence factor *evf (pOM evf)*. Ingestion of this strain becomes lethal in 20% of the flies, which suggests a competition between bacterial virulence and tissue repair mechanisms (Figure 1A). By contrast, in larvae even wildtype *Ecc15* induced mortality, at doses as low as OD_{600}=16 (70% lethality). *evf* overexpression intensified the lethality of these infections, bringing lethality up to ~95% (Figure 1B). These results demonstrate that larvae are more susceptible than adults to oral infection with *Ecc15*.

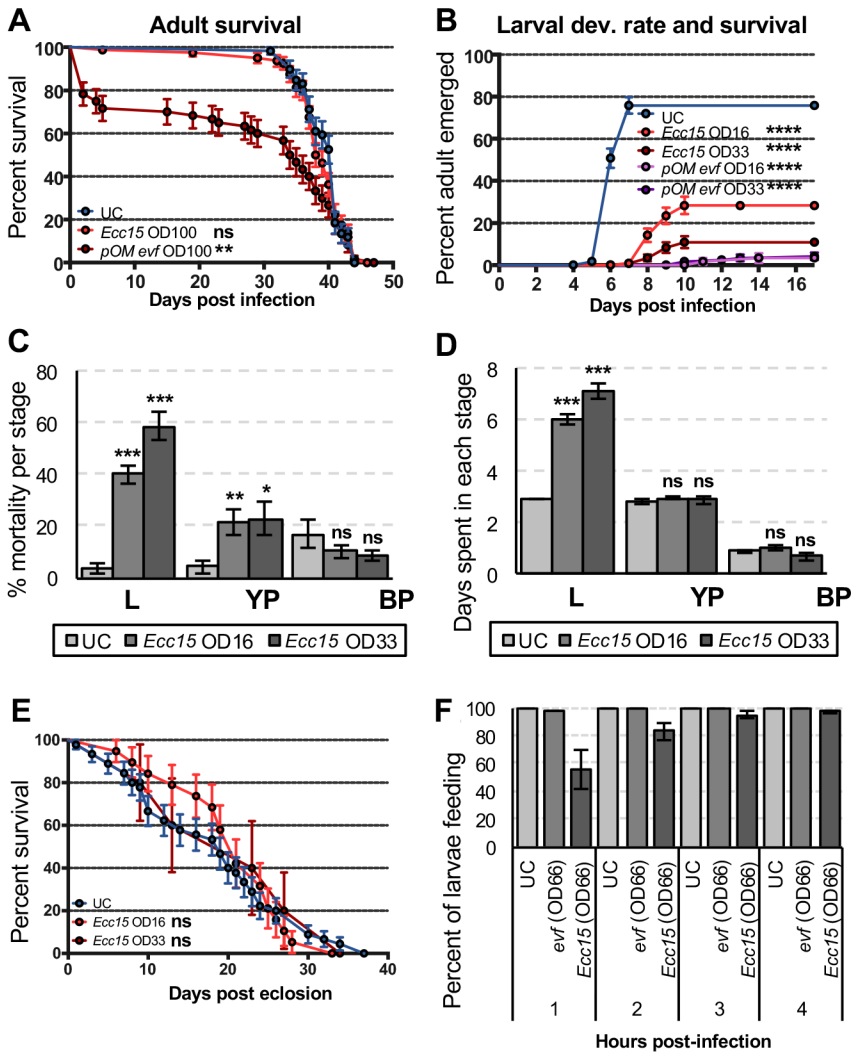

Figure 1. Oral *Ecc15* infection of larval *Drosophila* induces mortality and a developmental delay. (A) *pOM-evf Ecc15*, but not wildtype *Ecc15*, decreases adult *Drosophila* survival upon oral infection. (B) *Drosophila* larvae are susceptible to both wildtype and *pOM-evf Ecc15* and display delayed development to adulthood. (C) Percentage of deaths occurring during the larval (L), yellow pupal (YP) and black pupal (BP) stages following infection shows that most lethality occurs in larvae, and a fraction (~20%) during YP to BP transition. (D) The average transition time from L2 larvae to YP, YP to BP, and BP to adult for larvae infected with two different doses of *Ecc15* shows that the developmental delay occurs in larval stages. (E) Survival curves of adult flies that survived *Ecc15* infection as larvae show that larval infection during does not affect the lifespan of in surviving adults. (F) Percentage of larvae having ingested blue fly food medium following oral *Ecc15* infection shows that feeding cessation lasts only for few hours. Statistical significance: mean values of at least 3 repeats are represented ± SEM. *p<0.0332, **p<0.0021, ***p<0.0002, ****p<0.0001 (compared to UC, Log-rank test for survival curves). *p<0.05, **p<0.01, ***p<0.001 (compared to UC controls, student's t-test for measurements transition period and mortality measurements).

To characterize enteric *Ecc15* infections in larvae, we first assessed the stage at which lethality occurs. We monitored the percentage of *Drosophila* larvae that died within each stage of development and found that most infected larvae (up to 60%) died prior to pupation (between L2 and yellow pupa (YP); L, Figure 1C). We also observed that surviving larvae took 2-4 days longer (depending on the *Ecc15* dose) than unchallenged (UC) larvae to reach adult eclosion following treatment (Figure 1B). To determine if this developmental delay affects a particular stage, we measured the number of days spent in each developmental stage, and found that only the transition time from L2 larvae to pupation is lengthened, while the duration of the YP and black pupal (BP) stages remained unchanged between infected and UC groups (Figure 1D). In addition, the weight of YP of larvae infected with *Ecc15* or unchallenged was not different, suggesting they reach their target mass before engaging in pupation (Figure S1). Finally, the adult lifespan of flies that survived through metamorphosis following larval infection was not altered from that of UC flies (Figure 1E). Altogether, these results suggest that the larval stage is more susceptible to *Ecc15* infection, and that survivors of infection are able to resume normal pupal development and adult life after a developmental delay at the larval stage.

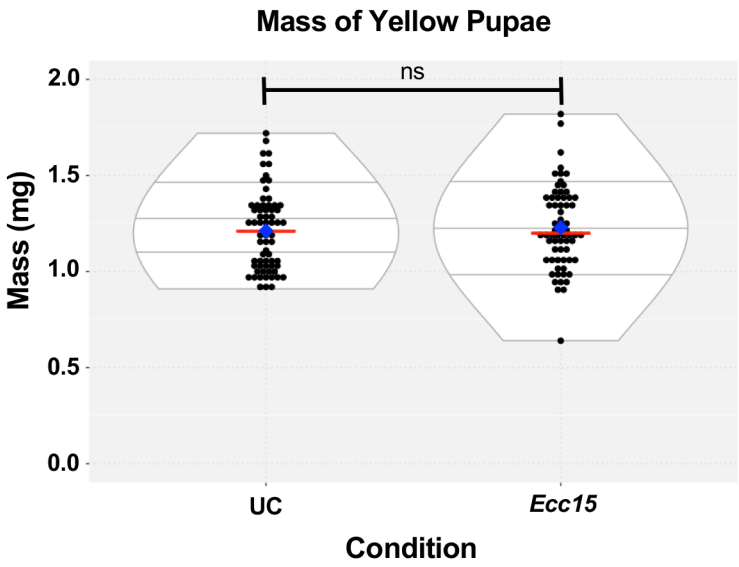

Figure S1. The weight of pupae is unchanged by larval infection.
The measured weight of yellow pupae (YP) that were infected with *Ecc15* at the L2 larval stage is not significantly different from that of UC YP, as compared by a t-test.

It was previously shown that oral infection by *Ecc15* triggers food uptake blockage in larvae (Acosta Muniz et al., 2007a; Keita et al., 2017). The resulting nutrient deprivation could explain both the strong susceptibility of larvae to infection as well as the observed developmental delay in surviving individuals. To test this hypothesis, we assayed food intake in larvae exposed to *Ecc15* and, in agreement with previous work, we observed a feeding cessation dependent on the virulence factor *evf* (Figure 1F). However, *Ecc15*-infected larvae resumed normal feeding within just 4 hours post-infection (Figure 1F). We surmise that this period of feeding interruption is too brief to account for the 2-4-day delay in development that we observed due to infection, and thus the delay must have a different cause. Altogether, these data suggest that *Drosophila* larvae that ingest *Ecc15* either die or experience a developmental delay prior to pupation and independent of food uptake blockage.

Damage to the larval midgut is repaired by differentiation of adult midgut progenitors

In adult *Drosophila*, ingestion of *Ecc15* induces midgut epithelial cell loss, which subsequently triggers ISC proliferation and differentiation, producing new cells required for gut regeneration, which is critical to survive infection (Liu et al., 2017). The larval midgut grows just by increasing the size and ploidy of ECs while adult midgut progenitors (AMPs) proliferate and accumulate in midgut imaginal islets during larval development. AMPs are only released at pupation and form the basis of the pupal and adult midgut epithelia (Mathur et al., 2010; Micchelli et al., 2011). This raises the possibility that larvae, which lack dedicated tissue-resident stem cells, may more easily succumb to enteric infection because of an inability to repair tissue through a proliferative stem cell response. To test this hypothesis, we investigated the effects of *Ecc15* infection on the midguts of *Drosophila* larvae. In UC conditions, the larval midgut is a long tube of approximately 12mm at the L2 and early 3rd instar (eL3) stages. Just before pupation, in the wandering L3 (wL3) stage, the gut shrinks (Figure 2A) by a process involving activation of autophagy to resorb larval tissue (Denton et al., 2009). Upon infection, we found that the midgut shrinks to the size of an UC wL3 larval gut (Figure 2A), suggesting that, as in adults, ingestion of *Ecc15* damages the larval midgut epithelium. However, the larval midgut does not recover its size as it does in adults, and instead remains shortened throughout larval maturation (Figure 2A). This lack of regeneration could either indicate that the larval midgut is not able to repair infectious damage at all, or that repair is limited to maintaining the gut at a wL3 length.

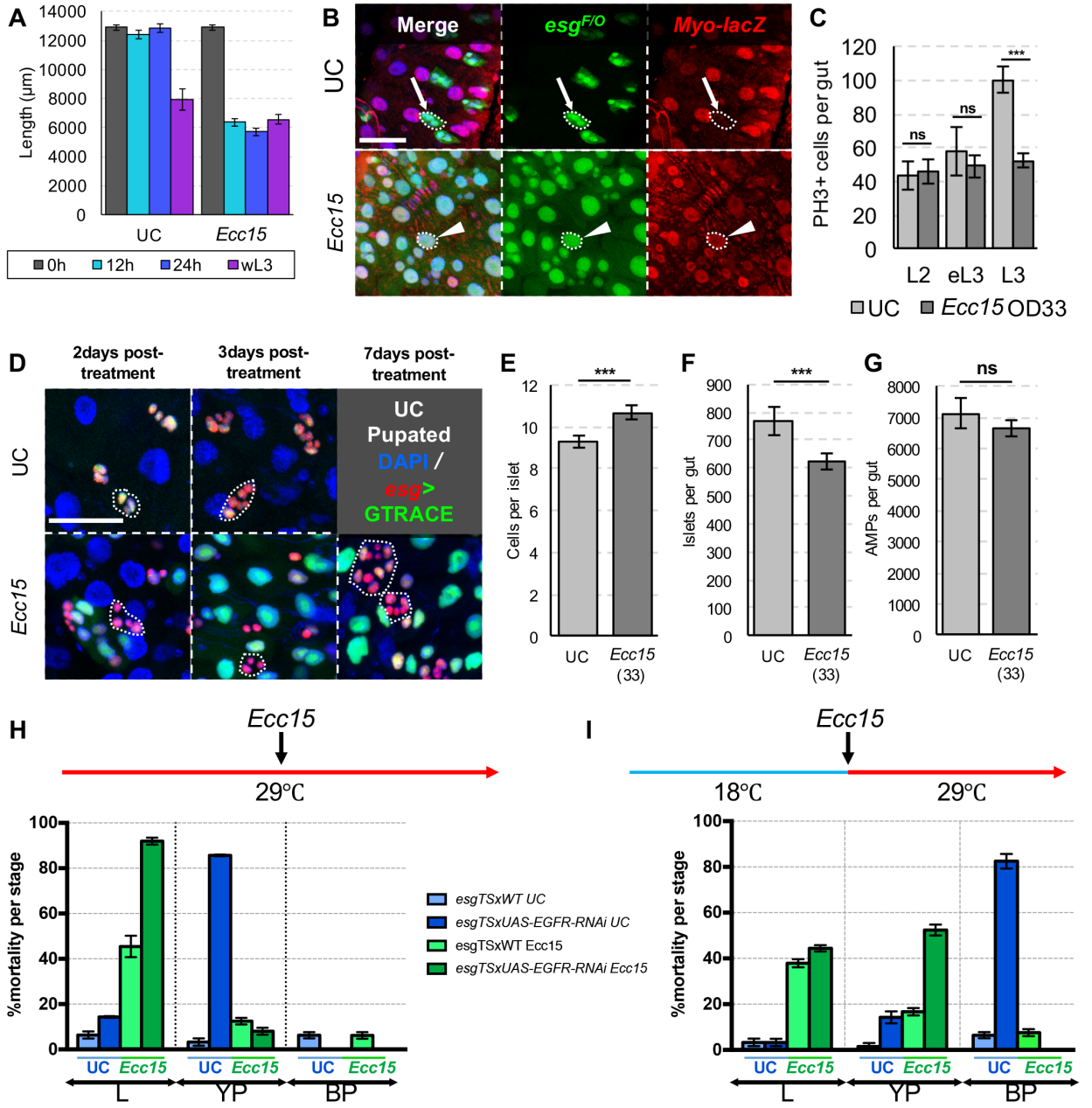

Figure 2. Infection of the larval midgut triggers a regenerative response via differentiation of AMP islets.

(A) Total midgut length measured 12, 24, and 96h post-treatment in L3 larvae (UC flies pupate before 96h) shows that *Ecc15* infection induces gut shrinkage. Additional measurements were taken of wL3 stage midguts for both conditions. UC wL3s were dissected 72h post-treatment, and infected wL3s were dissected at 96, 120, and 144h and the results averaged. The larval midgut length remains at this shortened length through the wL3 stage. (B) Lineage tracing of esg^{+} AMP islets with the $esg^{F/O}$ system (green) reveals that the AMPs undergo differentiation into ECs, which are marked by *Myo-lacz* (red), following oral *Ecc15* infection. Highlighted region shows that only upon *Ecc15* infection *Myo-lacZ* is found in newly differentiated ECs ($esg^{F/O+}$) tissues. (C) Total number of mitotically active AMPs ($PH3^{+}$) does not increase for early stage larvae following infection (L2 and earlyL3), and decreases for L3 stage larvae that have been orally infected with *Ecc15*. (D) G-TRACE lineage tracing shows that islet size is decreased compared to UC controls 2-3days post-infection, and returns to normal or greater size by 7days post-infection. AMPs

are marked in red and green, and their progeny is marked in green. (E-G) The number of cells within each islet (E), and the total number of islets per midgut (F), was recorded for wL3 stage larvae 3days post-treatment for UC and 4-6days post-treatment for the developmentally delayed infected group. These counts highlight a loss in the total islet number in response to infection, but an increase in islet size for larvae that were developmentally delayed for more than a day ($p<0.001$). The combination of these two events leads to a similar final number of total AMPS (G, non-significant difference). (H-I) Percentage of deaths occurring during the larval (L), yellow pupal (YP) and black pupal (BP) stages following infection (green) or UC treatment (blue) of Cs control and esg^{TS}-driven *EGFR-RNAi* larvae, in which expression of the RNAi construct was induced either from an early stage onwards (H) or at the time of treatment onwards (I) reveals that the development of AMPs prior to infection is critical for survival to pupation. Additionally, prevention of AMP reconstitution following infection-induced repair results in death during the YP stage. Nuclei are stained with DAPI (blue) throughout the figure. Scale bars are 50µm. Statistical significance: mean values of at least 3 repeats are represented ± SEM. *$p<0.05$, **$p<0.01$, ***$p<0.001$ (student's t-test). See also Figure S2.

To distinguish between these two possibilities, we monitored the larval midgut in detail for evidence of tissue renewal. We hypothesized that the AMPs, being a pool of undifferentiated progenitor cells, might act temporarily as tissue-resident stem cells to promote repair upon oral infection by *Ecc15*. To test this hypothesis, we surveyed the lineage of AMPs and PCs (esg^+ cells) using the $esg^{F/O}$ system, which labels all esg^+ cells and their entire progeny with a GFP reporter (Jiang et al., 2009). This analysis revealed that, upon infection, some midgut imaginal islets disappeared and gave rise to GFP positive polyploid cells, which were not detected under UC conditions. These new GFP-labelled polyploid cells were additionally found to express the EC-specific marker *Myo-lacZ,* suggesting that new ECs are generated in response to infection (Figure 2B). Of note, these new ECs have smaller nuclei compared to pre-infection larval ECs, suggesting that they do not reach the same ploidy level (Figure 2B). In the adult midgut and other systems, stem cell mediated tissue repair often involves both differentiation of progenitor cells into new epithelial cells and increased proliferation of stem cells in order to sustain regeneration (Bonfini et al., 2016; Buchon et al., 2009b; Jiang et al., 2009). To determine whether tissue repair in the larval midgut is accompanied by increased AMP proliferation, we next measured the number of mitotic cells ($PH3^+$ cells) per larval midgut. Surprisingly, we found that the number of mitotically

active AMPs (all $PH3^+$ cells were also esg^+) following infection had not increased (Figure 2C), and was in fact significantly lower in infected L3 larvae compared to UC L3 larvae. Altogether, our results demonstrate that, upon infection with *Ecc15*, differentiation of midgut imaginal islet cells in the absence of increased proliferation allows for a limited tissue repair response.

Since AMPs differentiate into new larval ECs following infection without a compensatory increase in proliferation, we hypothesized that the pool of AMPs might be depleted upon infection. Lineage tracing of islet cells with the *G-TRACE* system (Evans et al., 2009) allowed us to monitor simultaneously both the newly generated ECs (GFP^+ cells with polyploid nuclei) and the pool of undifferentiated AMPs (small RFP and GFP double-positive cells). We observed that, after the first 3 days post-infection, the number of AMPs within islets had decreased when compared to those of UC larvae, and accordingly the quantity of new ECs had increased within this time (Figure 2D). By seven days post-infection, however, the number of AMPs per islet appears to increase. Curiously, quantification of the number of AMPs per islet in wL3 larvae revealed that infected larvae had more AMPs per islet than UC larvae just prior to pupation (Figure 2E). Furthermore, the total number of islets in the guts of previously infected wL3 larvae had decreased due to infection, indicating that roughly 150 islets on average were completely lost during regeneration (Figure 2F). As a result, the average number of total AMPs per midgut was ultimately unchanged at the time of pupation between UC and infected larvae (Figure 2G). Altogether, our data indicate that infection with *Ecc15* triggers a transient induction of differentiation in AMPs to regenerate the larval midgut. This depletes the pool of available progenitors, which is later replenished over the course of the infection-induced developmental delay.

To assess this model functionally, we manipulated the number of AMPs by modulating the EGFR/Ras/MAPK pathway, which is required for developmentally regulated islet proliferation (Jiang et al., 2011). We first induced the AMP proliferation by overexpressing in islet cells a constitutively active form of Ras ($esg^{TS}>UAS\text{-}Ras^{V12}$), an activator of the EGFR pathway. AMPs in these guts over-proliferated and formed tumor-like clusters of cells, but did not become new ECs (i.e. polyploid cells) (Figure S2A), reinforcing the notion that tissue repair is mediated mostly by differentiation rather than proliferation. Blocking EGFR signaling in esg^{+} cells ($esg^{TS}>UAS\text{-}EGFR\text{-}IR$) resulted in the loss of esg^{+} and $PH3^{+}$ cells (Figure S2B-C), confirming a key role of this pathway in regulating AMP proliferation. These $esg^{TS}>EGFR\text{-}IR$ larvae reached pupation at a normal rate despite the lower number of AMPs, but they subsequently died at the YP stage (Figure 2H and S2D). This demonstrated that the total number of AMPs per midgut does not act as a checkpoint to initiate pupation, but is nevertheless a critical factor for pupal midgut formation. However, inhibiting AMP proliferation drastically reduced the number of *Ecc15*-infected larvae that survived to pupation compared to UC controls (Figure 2H). This suggests that larval midgut repair, despite being limited, is crucial to endure infectious damage and is dependent on AMPs. Finally, we monitored the survival of larvae that were reared to the L3 stage normally, but then had AMP proliferation blocked upon treatment and through the AMP recovery phase (switch to 29˚C to activate EGFR-IR concomitant with infection, Figure 2I and S2E-F). Interestingly, while UC larvae survived this treatment until the black pupa stage and developed at a normal rate, larvae infected with *Ecc15* died at the YP stage, suggesting that proliferation after the time of infection, and thus AMP recovery during developmental delay, is also critical for survival. Altogether these data imply that the pool of AMPs available to form the adult midgut epithelium is actively depleted by differentiation following enteric infection, and the developmental delay allows this pool to be

replenished over time. This constrained tissue repair is nonetheless required to survive infection and successfully undergo metamorphosis, as is the recovery of AMPs during the developmental delay. However, while the delay allows for AMP recovery, the number of AMPs itself does not regulate time to pupation.

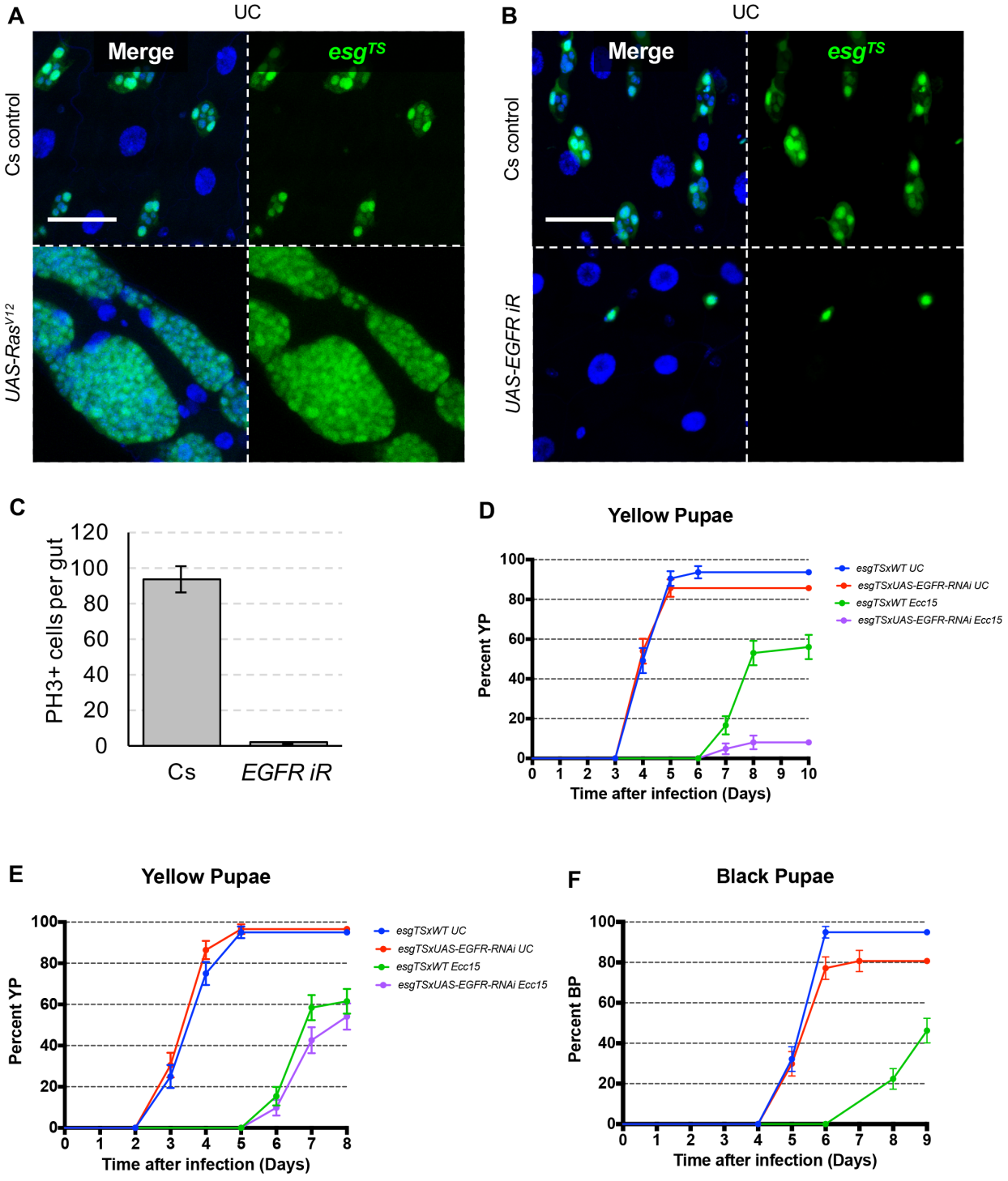

Figure S2. EGFR is necessary for AMP proliferation but lacking adequate AMPs does not induce a developmental delay. Refers to Figure 2.

(A) Ectopic induction of the EGFR pathway via overexpression of constitutively active Ras in AMPs (esg^{TS}, green) causes their overproliferation, but does not promote differentiation. (B-C) RNAi-mediated knockdown of *EGFR* in AMPs starting in early larval stages (esg^{TS}, green) prevents the formation of adult midgut precursor islets (B), by inhibiting AMP proliferation (C). (D) Development rate to the Yellow Pupal (YP) stage for WT and esg^{TS} driven, EGFR-RNAi larvae (induced in early larval stages) in UC and *Ecc15*-

infected conditions reveals that inhibition of islet development does not affect the rate of YP development n UC conditions, but greatly reduces the survival rate through the larval stages. (E-F) Development rate curves to the YP and BP stages for WT and *esg*^{TS} driven, EGFR-RNAi larvae (induced only at the time of treatment) in UC and *Ecc15*-infected conditions reveals that larvae that contain developed AMP islets, but lack the ability to renew them following infection, survive to pupation at the same rate as WT larvae in both conditions. However, infected larvae that cannot renew their islets do not survive to the BP stage. Scale bars are 50μm.

Infection triggers differentiation of PCs in a Notch-independent manner

As the midgut imaginal islets are composed of two cell types, the undifferentiated AMPs and the surrounding differentiated PCs, we next asked which of these cell types contributes to tissue repair upon infection. The differentiation of AMPs into PCs has been shown to be dependent on Notch signaling, and the Notch ligand, Delta, is a marker of AMPs while the Notch target gene *Su(H)* is a marker of PCs (Figure 3A) (Mathur et al., 2010). We observed that, during *Ecc15* infection, the typical enveloping shape of PCs appeared to be disrupted, and newly emerged ECs were *Su(H)-lacZ*$^{+}$, suggesting that new ECs may be the result of further PC differentiation (Figure 3A). To test this hypothesis, we performed a pulse-chase lineage tracing of PCs using the *Su(H)*$^{F/O}$ system (*Su(H)-Gal4; UAS-GFP,tub-Gal80*^{TS} *> UAS-FLP, act>CD2>Gal4*), in which we labeled PCs with a heritable GFP prior to infection and only for a limited window of time. After infection, GFP positive ECs were detected, demonstrating that infection triggers differentiation of PCs into ECs (Figure 3B).

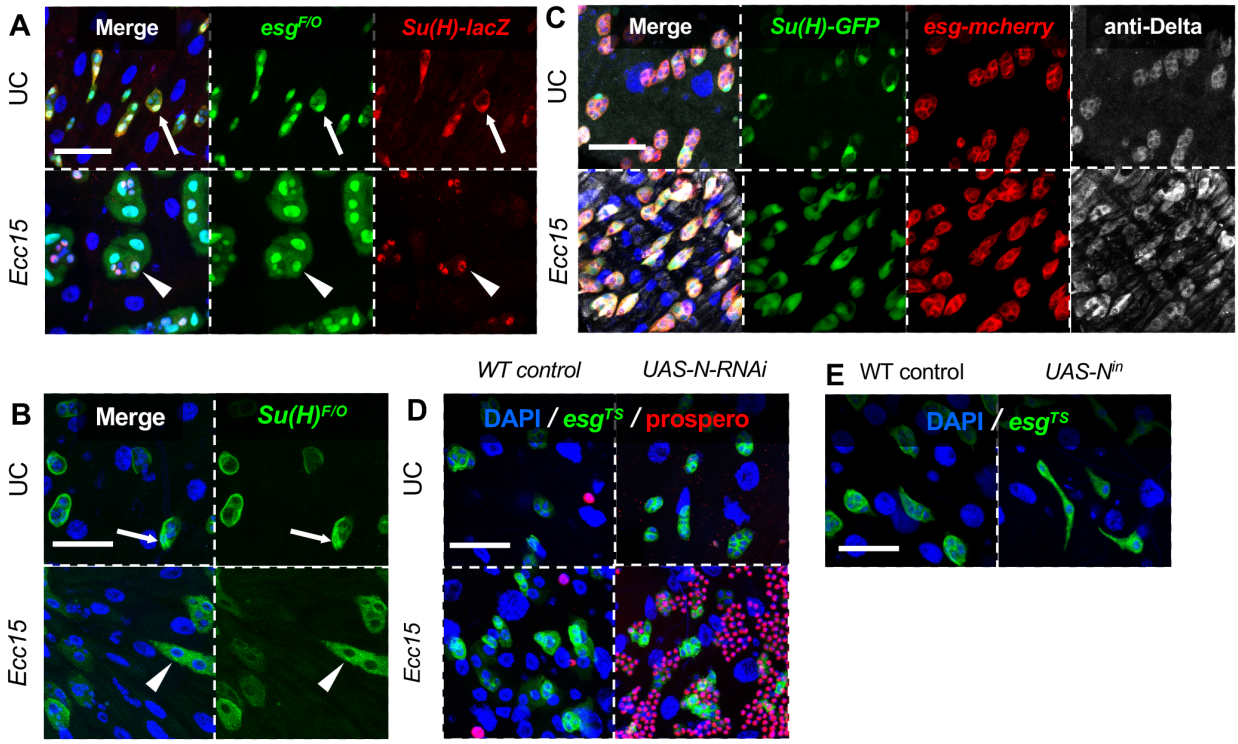

Figure 3. Activation of Notch signaling induces adult midgut progenitor cells to undergo partial differentiation to become peripheral cells.
(A) The Notch pathway is normally activated in islet PCs, marked with *Su(H)-lacZ* (red), and is switched on also in the AMPs during regenerative differentiation. The $esg^{F/0}$ construct labels both AMPs, PCs and their progeny (green). (B) Transient induction of the $Su(H)^{F/O}$ system (green) in PCs demonstrates that they contribute to midgut repair by differentiation into larval ECs. (C) Delta (white) localizes within AMP islets in both UC and *Ecc15*-infected guts and is increased by infection. Islets are marked with esg^{TS}>*UAS-RFP* (red), PCs are marked with *Su(H)-GFP* (green). (D) RNAi knockdown of *Notch* causes AMP islets (esg^{+}, green) to lose their enveloping PCs in UC conditions, and results in the formation of $prospero^{+}$ (staining in red) tumors upon oral *Ecc15* infection. (E) Overexpression of the Notch intracellular domain (N^{in}) in AMPs (esg^{+}, green) causes differentiation into elongated, PC-like cells. Confocal microscopy images were taken at 20x magnification. Nuclei are marked with DAPI (blue) throughout the figure. Scale bars are 50µm.

As the Notch pathway is a key regulator of ISC differentiation in the adult *Drosophila* midgut (Ohlstein and Spradling, 2007a) and is detected in newly differentiating larval ECs (Figure 3A), we hypothesized that levels of Notch pathway activity may control differentiation of AMPs and PCs into ECs. Accordingly, immunostaining against Delta combined with *esg* (esg^{TS}>*UAS-mCherry*) and *Su(H)-GFP* demonstrated that the Notch pathway is upregulated in islets 12h post-infection (Figure 3C). Specifically, we observed that Delta levels increased in islets and that the Notch pathway (*Su(H)-GFP*) was induced in AMPs in addition to PCs (Figure 3C). Accordingly,

blocking the Notch pathway in AMPs throughout early larval stages (*esg^{TS}>UAS-Notch-IR*) resulted in islets that lack ensheathing PCs in UC conditions, and infection caused these Notch deficient islets to form *prospero*+ tumors instead of ECs (Figure 3D). This confirms that the Notch pathway is required for proper differentiation of AMPs into PCs and is a prerequisite for generating new ECs in response to *Ecc15* infection. Finally, activation of the Notch pathway in the AMPs of L2 larvae, via overexpression of the intracellular domain of Notch (*esg^{TS}>UAS-Notch-intra*), caused the differentiation of all AMPs into elongated, PC-like cells, but was not sufficient to induce further differentiation into polyploid ECs (Figure 3E). Altogether, our results suggest that, while Notch pathway activity is required for AMPs to differentiate into PCs and is triggered in response to *Ecc15* infection, it is not enough to promote differentiation of PCs into ECs.

Upregulation of the DPP and JAK/STAT pathways in larval and adult midguts upon *Ecc15* infection

Our results indicated that additional regulators are required to regulate islet differentiation upon *Ecc15* infection. To identify candidate genes for the promotion of islet differentiation, we compared adult and larval midgut transcriptomes in UC and *Ecc15*-infected conditions 6h post-treatment. We first determined the overall transcriptomic differences between adult and larval guts in response to infection. Principal component analysis (PCA) showed that all three biological replicates clustered together, indicating good reproducibility of the response for each type of tissue sample, and demonstrated that, while the larval and adult midguts displayed differences in gene expression (separated by PC1, 11% of total variance), most of the variance originated in a common response to infection (separated by PC2, 82% variance) (Figure 4A). Specifically, 267 genes were upregulated in both adult and larval midguts following infection. Gene Ontology (GO) enrichment

analysis revealed that these included genes involved in immune (Imd and JAK/STAT pathways) and stress (*p38c* and *p53*) responses, as well as tissue regeneration (*Mmp1* and *NijA*) (Figure 4B and S3). 527 genes were upregulated only in the adult midgut and included genes involved in cell cycle and DNA replication (*mus209* (*PCNA*) and *hd*), reinforcing that ISC proliferation is increased upon infection in adult but not larval midguts. Finally, 308 genes were found to be uniquely upregulated in the larval midgut by *Ecc15* infection and displayed an enrichment for functions in cell growth and differentiation (*Thor* and *Akt1*), in agreement with the induction of differentiation-mediated tissue repair. Upon infection, both the larval and adult guts experienced downregulation of genes involved in metabolism and digestion (*mag* and *Ser8*), suggesting a decrease in digestive capabilities.

Figure 4. Transcriptional changes in response to infection of the larval and adult *Drosophila* midgut. (A) Principal component analysis (PCA) shows samples subjected to same treatment cluster together, indicating good repeatability. Most of the variance (PC1, 82%) is due to infection, while adult vs larval midgut contributes to 11% of the variance (PC2). (B-C) Venn Diagrams representing the number of genes found to be up or downregulated in response to infection in either the larval or adult guts, or in both.
(D) Summary table of several upregulated genes in response to larval gut infection, and the pathways to which they belong. White shading indicates low induction, Red shading indicates high induction. See also Figure S3 for GO tables.

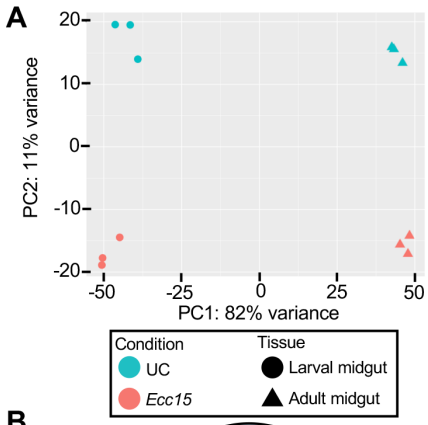

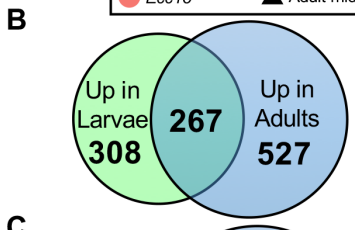

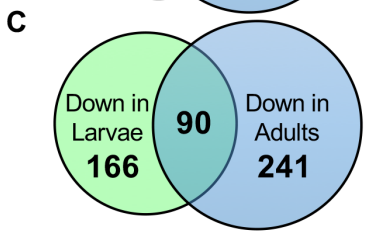

D

Genes upregulated by *Ecc15* in Larval Guts		
Gene	**Pathway**	**Fold induction**
dpp	Dpp	10.17
AttA	Imd	28.03
AttB	Imd	40.51
AttC	Imd	6.76
AttD	Imd	118.40
CecA1	Imd	10.05
CecA2	Imd	18.27
CecC	Imd	13.17
DptA	Imd	9.01
DptB	Imd	11.56
Dro	Imd	19.87
PGRP-LA	Imd	3.97
PGRP-LB	Imd	3.30
PGRP-LF	Imd	17.90
PGRP-SB1	Imd	5.03
Rel	Imd	6.77
dome	JAK/STAT	5.69
Drsl3	JAK/STAT	6.00
Socs36E	JAK/STAT	14.56
Stat92E	JAK/STAT	3.18
upd2	JAK/STAT	16.13
upd3	JAK/STAT	105.51
Nedd4	Notch	2.92
Su(H)	Notch	2.91
Dl	Notch	1.99
N	Notch	3.10

High

Low

A

GO term	Description	P-value
UPREGULATED IN BOTH		
GO:0006955	immune response	7.99E-12
GO:0006950	response to stress	8.51E-11
GO:0042060	wound healing	7.92E-07
GO:0010631	epithelial cell migration	2.76E-06
GO:0042246	tissue regeneration	2.07E-05
GO:0097696	STAT cascade	1.15E-04
GO:0007259	JAK-STAT cascade	1.15E-04
GO:0000165	MAPK cascade	1.36E-04
GO:0048729	tissue morphogenesis	7.20E-04
DOWNREGULATED IN BOTH		
GO:0008152	metabolic process	2.80E-07
GO:0006629	lipid metabolic process	5.27E-06
GO:0042178	xenobiotic catabolic process	6.07E-06
GO:0009407	toxin catabolic process	6.07E-06
GO:0006508	proteolysis	1.37E-04
GO:0098754	detoxification	3.23E-04
GO:0051180	vitamin transport	9.49E-04

B

GO term	Description	P-value
UPREGULATED ONLY IN LARVAE		
GO:0040008	regulation of growth	6.86E-08
GO:0045595	regulation of cell differentiation	8.51E-09
GO:0031667	response to nutrient levels	2.34E-05
GO:0002064	epithelial cell development	1.20E-07
GO:0001558	regulation of cell growth	3.31E-05
DOWNREGULATED ONLY IN LARVAE		
GO:0005975	carbohydrate metabolic process	1.11E-09
GO:0016052	carbohydrate catabolic process	6.53E-05
GO:0042593	glucose homeostasis	7.12E-04

C

GO term	Description	P-value
UPREGULATED ONLY IN ADULTS		
GO:0015031	protein transport	1.85E-05
GO:0022402	cell cycle process	1.31E-04
GO:0006260	DNA replication	2.10E-04
GO:0051169	nuclear transport	3.50E-04
GO:0006486	protein glycosylation	3.53E-04
DOWNREGULATED ONLY IN ADULTS		
GO:0000003	reproduction	2.05E-07
GO:0018991	oviposition	6.00E-04

Figure S3. GO Term analysis of genes regulated in the larval and adult midgut by Ecc15 infection. Refers to Figure 4.
(A) GO Term analysis of genes that were up or downregulated by *Ecc15* infection reveals that immunity, tissue repair, and stress responsive pathways, particularly JAK/STAT and the MAPK cascade, are induced by enteric infections in both larvae and adults. Genes that were downregulated by infection in adults and larvae were found to be enriched for metabolic and detoxification processes. (B) Genes that were upregulated in larval midguts by infection, but not in adults, are broadly involved in cell growth and differentiation (in accordance with the observation of AMP differentiation in response to infection), while those that are downregulated uniquely in larval midguts by infection are involved in carbohydrate metabolism. (C) Genes upregulated only in the adult gut by infection were found to be components of DNA replication and cell cycle regulation (consistent with the observation that progenitor proliferation is induced in the adult midgut by infection, but not the larval midgut). Those that are downregulated only in the adult midgut were specific to reproduction.

We next focused on the pathways that are the most upregulated in the larval gut upon infection, as these may potentially control the differentiation of AMPs and PCs into ECs (Figure 4D). As expected, one of the most upregulated pathways was the Imd pathway, a major branch of *Drosophila* immunity (Buchon et al., 2014). In agreement with our previous results (Figure 3C),

we detected a strong induction of the Notch pathway. Finally, we noted strong upregulation upon infection of two pathways that have been linked to stem cell differentiation in the adult midgut: the Dpp pathway (through upregulation of *dpp* itself) and the JAK/STAT pathway (identified via upregulation of the ligands *upd2* and 3, as well as the target gene *Socs36E*) (Beebe et al., 2010; Buchon et al., 2009a; H. Li et al., 2013; Z. Li et al., 2013; Zhai et al., 2017). Our results therefore suggested that Dpp and/or JAK/STAT may potentially influence infection-induced AMP differentiation.

The Dpp pathway is sufficient, but not necessary to induce AMP differentiation into ECs

The transcriptional upregulation of *dpp* by infection in the larval *Drosophila* midgut was somewhat surprising, as previous research has suggested that Dpp is secreted by the PCs to maintain Dpp pathway activation in AMPs where it acts to prevent their differentiation (Mathur et al., 2010). We therefore hypothesized that the Dpp pathway may counteract AMP differentiation in order to prevent complete AMP loss during repair. To test this, we first activated the Dpp pathway ectopically in islets, by Dpp overexpression ($esg^{TS}>UAS\text{-}dpp$) and by overexpression of a constitutively active form of the Dpp receptor, Thickveins ($esg^{TS}>UAS\text{-}tkv^{CA}$). Both constructs surprisingly caused AMPs to undergo differentiation into ECs (Figure 5A-B), suggesting that the Dpp pathway in AMPs, as in adult ISCs, promotes EC fate (Zhai et al., 2017). We then tested whether the Dpp pathway could be required for tissue renewal upon infection. However, blocking the pathway in AMPs by RNAi knockdown of *tkv* ($esg^{TS}>UAS\text{-}tkv\text{-}IR$) was insufficient to inhibit differentiation upon infection (Figure 5C). These results suggest that the Dpp pathway is neither involved in maintaining AMPs in an undifferentiated state, nor required to trigger infection-induced differentiation.

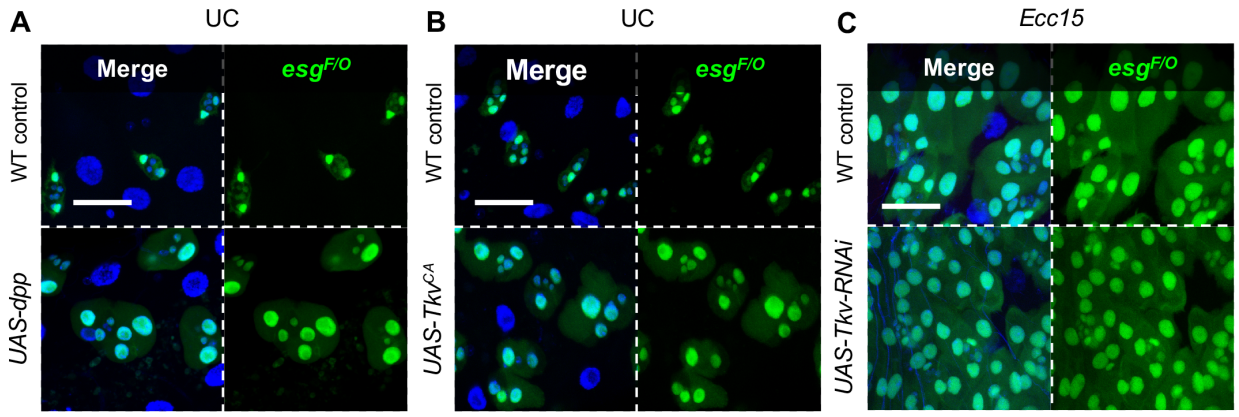

Figure 5. Dpp pathway activation is sufficient to promote AMP differentiation but not necessary in response to enteric infection.
(A-B) Ectopic activation of the Dpp pathway in AMPs ($esg^{F/O}$, green) by overexpression of the Dpp ligand (A) or a constitutively active form of the receptor, Tkv (B) induces differentiation of AMPs into new ECs. (C) Blocking the Dpp pathway via AMP-specific ($esg^{F/O}$, green) RNAi knockdown of *tkv*, however, does not prevent AMP differentiation following *Ecc15* infection. Scale bars are 50µm.

The JAK/STAT pathway is required and sufficient to trigger infection-induced differentiation of AMPs into new ECs.

To confirm the induction of the JAK/STAT pathway in the larval midgut upon infection, we monitored expression of a *10xSTAT-GFP* reporter transgene (Figure 6A). Interestingly, no signal was detected in UC larval midguts up to the late L3 larval stage, at which point the JAK/STAT pathway was found to be active in islet cells (both AMPs and PCs, Figure 6A). Upon infection with *Ecc15*, a *10xSTAT-GFP* signal was detected strongly in both the visceral muscles and in the differentiating AMPs of L3 larvae, suggesting that JAK/STAT signaling becomes intensified and active in more midgut tissues following infectious damage. Furthermore, a β-galactosidase reporter for *upd3* (*upd3-lacZ*), a key ligand responsible for inducing the JAK/STAT pathway in response to infection (Houtz et al., 2017), distinctly showed that *upd3* is transcriptionally induced in the ECs surrounding differentiating AMP islets (Figure 6B). It was previously shown that two different enhancer regions of *upd3* (called *upd3* enhancers C and R) mediated the *upd3* transcriptional response to *Ecc15* infection of the adult gut (Houtz et al., 2017). We next tested

whether these same enhancers were activated by *Ecc15* infection in larvae. The *upd3-C-GFP* reporter was not detected in the larval midgut under basal conditions but, following *Ecc15* infection, was induced in old larval ECs, in agreement with the results of the *upd3-lacZ* reporter, with which it shares overlapping enhancer sequences (Houtz et al., 2017). The *upd3-R-GFP* reporter was also switched on upon infection but appeared exclusively in AMP islets undergoing differentiation (Figure S4A-B). These results mirrored the adult gut, in which *upd3-C-GFP* reported infection-induced expression specifically in ECs while *upd3-R-GFP* was found to be activated in differentiating ISCs and EBs upon infectious damage. Altogether, this demonstrates that infection triggers an early induction of the JAK/STAT pathway in AMP islets via transcriptional activation of *upd3*.

Figure 6. The JAK/STAT pathway is activated upon bacterial infection of the larval midgut and is both necessary and sufficient to promote tissue repair via differentiation of AMPs into ECs.
(A) Stat92E (10x*Stat-GFP*, green) is active in 3rd instar larval midgut islet cells, and is switched on in the visceral muscles during infection. *Su(H)-lacZ* marks PCs (red). (B) *Upd3-lacZ* (red) is induced upon *Ecc15* infection in the larval ECs surrounding differentiating AMPs islets ($esg^{F/O}$, green). (C) Blocking the JAK/STAT pathway in AMPs through $esg^{F/O}$-driven (green) expression of *UAS-lat; UAS-DomeDN* has no effect in UC conditions, but prevents AMPs from fully differentiating into polyploid ECs upon infection. (D) Overexpression of the Upd3 ligand in AMPs induces differentiation into new ECs. (E) Model of AMP proliferation and differentiation in basal and bacterially challenged conditions: upon infection with *Ecc15*, Notch triggers differentiation of AMPs into PCs. In addition, the JAK/STAT pathway controls the differentiation of PCs and AMPs into new larval ECs. Because AMP proliferation is not upregulated, the pool of adult precursors is transiently depleted. Developmental delay allows for replenishment of AMPs before pupation. Nuclei are marked with DAPI (blue) throughout the figure. Scale bars are 50μm. See also Figure S4.

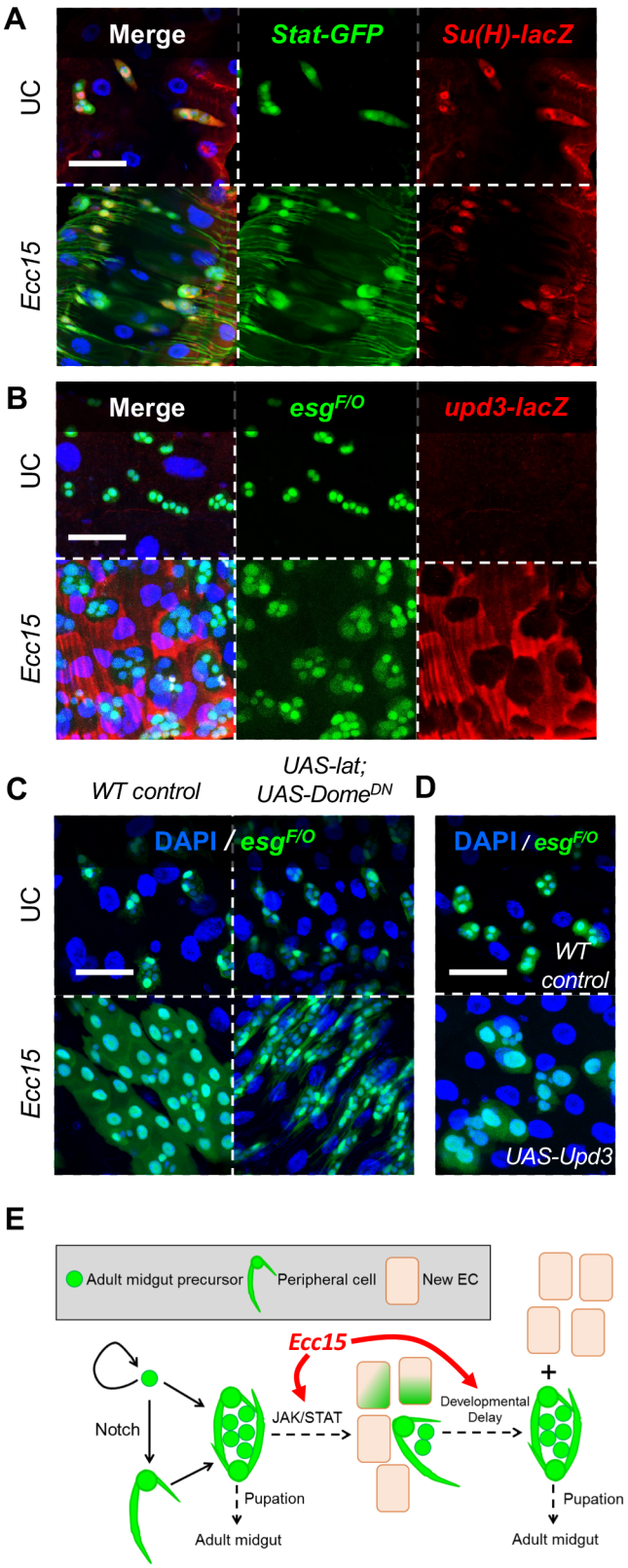
A
Merge
Stat-GFP
Su(H)-lacZ
UC
Ecc15
B
Merge
esgF/O
upd3-lacZ
UC
Ecc15
C
WT control
UAS-lat;
UAS-DomeDN
D
DAPI / esgF/O
UC
Ecc15
DAPI / esgF/O
WT
control
UAS-Upd3
E
Adult midgut precursor
Peripheral cell
New EC
Ecc15
Notch
JAK/STAT
Developmental
Delay
Pupation
Adult midgut
Pupation
Adult midgut

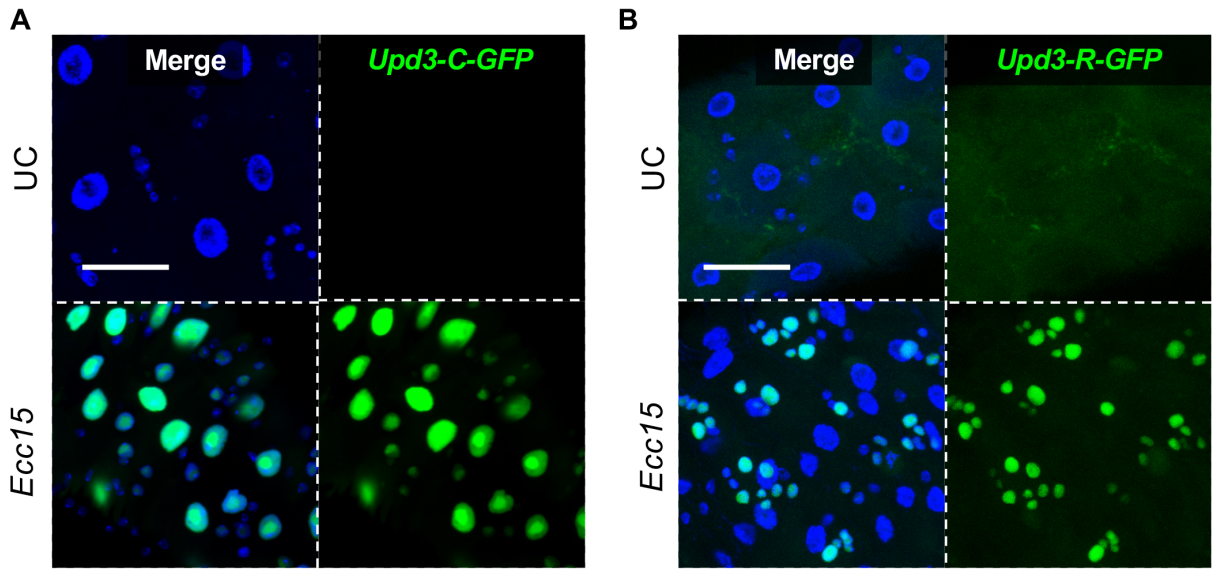

Figure S4. Upd3 transcription in the larval midgut in response to enteric infection is regulated by the same two enhancer sequences as the adult midgut. Refers to Figure 6.
(A) The enhancer sequence of *upd3-C-GFP* is activated in the ECs of the larval midgut upon *Ecc15* infection. (B) The *upd3-R-GFP* enhancer sequence is activated only in differentiating AMPs following *Ecc15* infection. Scale bars are 50µm.

We next sought to determine if the JAK/STAT pathway regulates AMP differentiation during oral *Ecc15* larval infection. Blocking the JAK/STAT pathway by overexpressing a combination of both an inhibitor of the JAK/STAT pathway, Latran, and a dominant negative form of the JAK/STAT receptor Domeless ($esg^{F/O}$ > *UAS-lat; UAS-Dome*^{DN}), showed no effect on islets in UC conditions, but prevented AMPs from differentiating into ECs upon infection (Figure 6C). Conversely, activation of JAK/STAT by overexpression of Upd3 in AMP islets ($esg^{F/O}$ > *UAS-upd3*) triggered differentiation of islet cells into ECs (Figure 6D). In total, these results demonstrate that the JAK/STAT pathway is activated in the larval midgut following *Ecc15* infection through transcriptional upregulation of *upd3*, and that this activation is both required and sufficient to cause islet cells to differentiate into new ECs.

Discussion

Unlike most epithelial tissues, such as the adult *Drosophila* midgut (Buchon et al., 2010; Duronio, 1999), the transient epithelium of the larval *Drosophila* midgut lacks progenitor cells to mediate constant turnover (Mathur et al., 2010), possibly due to the transient nature of larval tissues. Nevertheless, the larval midgut is exposed to environmental challenges such as ingested pathogenic microbes. In this manuscript, we asked how infection alters the developmental program of the *Drosophila* midgut, and how infectious damage is dealt with by tissue lacking resident stem cells. We found that, in response to infection with *Ecc15*, the larval midgut mounts limited tissue repair by transiently recruiting progenitors from imaginal structures (Figure 6E). Specifically, ingestion of *Ecc15* triggers the expression of the cytokine *upd3* and activation of the JAK/STAT pathway in imaginal islet cells, resulting in the differentiation of progenitors into new ECs. This process transiently depletes the pool of AMPs, which is subsequently reconstituted, during a developmental delay following infection. Our study gives insight into an alternative method of epithelial repair, in which imaginal adult midgut tissue is recruited for regeneration of the larval gut epithelium, controlled by the Notch, Dpp and JAK/STAT pathways.

Limited tissue repair could make developing organisms more susceptible to infection

While adult flies do not succumb to a wild type *Ecc15* infection, the high mortality caused by the same bacterium in developing larvae highlights the constraints of an organism during its developmental stages. Indeed, infection with *Ecc15* killed ≥ 60% of larvae, while *Ecc15* exposure did not affect adult survival. We speculate that one of the mechanisms underlying such differences is the ability to repair damaged tissue. While in adults the midgut is able to fully regain its size 48hrs post-infection by *Ecc15* (Buchon et al., 2010), the larval midgut never recovers to its original

size. Instead, limited tissue repair occurs and maintains the gut in a shortened state until the time of pupation. This incomplete regeneration could indicate two different scenarios. First, it is possible that the amount of tissue repair in larvae is constrained in order to maintain a sufficient number of AMPs for development of the adult midgut epithelium. Alternatively, it is possible that the number of AMPs present at the time of infection is a limiting factor, and that it is not enough to buffer damage in dying larvae. Considering that most larvae (up to 60%) die from infection, and that limiting the number of AMPs using RNAi against EGFR resulted in an increase in susceptibility, we feel that the second model is more probable. Accordingly, it is possible that the fraction of the population that dies during YP to BP transition had enough AMPs to survive infection as a larva, but not enough to progress normally through pupal development. Moreover, increasing the dose of *Ecc15* leads to increased lethality, suggesting that larvae are constrained to tolerate only a fixed amount of damage. This result is counterintuitive, as developing organisms generally have higher reparative capability compared to adults (Tang et al., 2014; Yannas 2005). This could be a particularity of insects that restrict cell proliferation to imaginal structures and achieve larval growth by polyploidization. Such a "weakness" in the tolerance to pathogens could also explain why most successful biocontrol strategies against insects target the larval stage (Vallet-Gely et al., 2008).

Developmental delay allows recovery of the pool of AMPs after infection

One consequence of using the pool of imaginal cells to repair the larval midgut without increasing AMP proliferation is a transient depletion of AMPs. Strikingly, when we measured the total number of AMPs in the guts of larvae that survived *Ecc15* ingestion and reached the wandering stage, we found that the number was approximately equal to that of UC wandering stage larvae.

Guts from infected larvae had fewer islets, demonstrating that some imaginal structures are lost during tissue repair. However, the remaining islets contained more precursor cells than in typical UC guts, which thus preserved the total AMP number at the wandering larval stage between infected and UC guts. AMP reconstitution without an increase in the proliferation rate relies on a developmental delay for completion. In addition, we demonstrated that AMP renewal over the course of the delay is key for *Drosophila* survival, since blocking this recovery led to pupal lethality. Developmental delays have been extensively demonstrated as being central to coordinating repair of damaged imaginal structures with organismal development (Halme et al., 2010; Hariharan and Serras, 2017; Smith-Bolton, 2016; Smith-Bolton et al., 2009). Our data present a new example of such a delay that occurs as a consequence of larval epithelial damage that is repaired by imaginal precursor cells, rather than damage to an imaginal structure. It is possible that other larval tissues may transiently use imaginal cells to repair themselves, but to our knowledge this has yet to be reported. Alternatively, the larval midgut could be the only structure that is repaired in such a way, reflecting its important barrier and digestive functions.

The fact that developmental delay allows for lost AMPs to be replenished to their normal number before pupation suggests that the quantity of AMPs is tightly controlled and crucial for metamorphosis success. However, although the delay is required for survival and recovery of AMP islets, it is not induced by the actual depletion of AMPs. Specifically, we found that the loss of EGFR in islet cells after infection, which blocks AMP recovery, did not slow or block the transition to the pupal stage, though it did lead to complete pupal lethality. It was proposed that the delay could result from food uptake blockage induced by infection (Keita et al., 2017); however, we found that feeding is resumed only a few hours after infection, which suggests that it is not

responsible for slowing development. It is still possible that nutrient absorption in *Ecc15*-infected guts is affected, as the organ is severely shortened and new ECs are smaller and display lower ploidy than ECs in UC guts. Accordingly, it was previously found that infection is associated with decreased expression of genes involved in protein digestion (Erkosar et al., 2015), and our transcriptome analysis confirms that digestive and metabolic functions are reduced. Alternatively, signals similar to the ones secreted in response to imaginal disc damage could play a role in this delay. For instance, our transcriptome analysis suggests that some key genes previously identified as regulating the insulin pathway, a key pathway to promote larval growth and development, are also regulated in the gut by infection, including *IMPL2* (Grewal, 2008; Kwon et al., 2015).

The response to infection in adults and larvae: one network but different cell responses

In this study we identified a novel regenerative modality for systems devoid of dedicated stem cells. This response shows striking similarities and differences when compared with the adult midgut response. Parallel to the larval midgut, the adult *Drosophila* midgut is comprised of differentiated absorptive ECs and EEs. These differentiated cells are maintained through a population of ISCs (Micchelli and Perrimon, 2006; Ohlstein and Spradling, 2007b). ISCs give rise to either EEs through a pre-EE stage, or to ECs by first partially differentiating into enteroblasts (EBs) (Beehler-Evans and Micchelli, 2015; Zeng and Hou, 2015). EBs are "poised" for differentiation and become ECs when required (Antonello et al., 2015). This process has strong parallels with the larval midgut, and similar markers and pathways define epithelial cell lineages in both stages. Indeed, we could consider AMPs as ISC equivalents in the larval gut. PCs, which act both as differentiated progenitor cells and a niche for AMPs, could be considered to be cellular paralogs to EBs. Indeed, both EBs and PCs engage differentiation in response to damage (Buchon

et al., 2009a), and AMPs and PCs express the ISC and EB marker, *esg*. However, despite these parallels major differences exist between the two systems, including the fact that no turnover occurs basally in larvae, and no proliferation is induced by infection. These simple differences render the larval digestive tract not truly "homeostatic," which has important consequences for larval survival following GI tract damage.

Parallels in the genetic network controlling tissue repair can also be found. In both systems, Notch signaling and the JAK/STAT pathway are essential for differentiation (Beebe et al., 2010; Ohlstein and Spradling, 2007a; Perdigoto et al., 2011). While these pathways work in parallel for EC differentiation in the adult gut (Zhai et al., 2017), their action seems uncoupled in the larval midgut, which allows for the existence of a differentiated intermediate, the PC. Accordingly, in UC larvae we detect JAK/STAT activation only starting in the late 3rd instar larvae stage, suggesting that infection triggers the premature transition of PCs into ECs that normally occurs during pupation. This raises the possibility that the repaired larval midgut is "patched" by pupal or adult-like ECs rather than by new larval ECs. The lower ploidy of the ECs generated upon infection of the larval midgut agrees with this hypothesis. This is again in striking contrast with the response of the adult midgut to infection, which triggers the generation of ECs with higher ploidy than their UC counterparts (Xiang et al., 2017). Transcriptomic analyses globally revealed that the Imd, Notch, TGF-β/Dpp and JAK/STAT pathways are all induced in the larval midgut by *Ecc15* infection. We further determined that activation of the TGF-β/Dpp pathway in AMPs induces differentiation into ECs, but was not required for the process. In the adult midgut, the TGF-β/Dpp pathway regulates multiple aspects of epithelial maintenance, including ISC self-renewal and quiescence, EC differentiation and the regulation of *upd3* expression in ECs (Guo et al., 2013; Houtz et al., 2017;

H. Li et al., 2013; Z. Li et al., 2013; Zhou et al., 2014). In contrast, previous studies have shown that Dpp signaling can prevent the differentiation of AMPs in larvae, suggesting a contrast in roles between adults and larvae (Mathur et al., 2010). Surprisingly, we found that ectopic activation of Dpp signaling in AMPs via overexpression of the Dpp ligand or a constitutively active form of its receptor, Tkv, induced their differentiation. It is possible that the differentiation that we observe is a result of a neomorphic effect due to protein overexpression. However, our *Tkv* knockdown experiment in AMPs did not lead to premature differentiation of AMPs, suggesting that Dpp could, like in adults, contribute to progenitor differentiation rather than block it. In comparison, we found that the JAK/STAT pathway, rather than the Dpp pathway, is responsible for infection-induced differentiation. The induction of the JAK/STAT pathway upon infection was controlled in both adult and larval midguts by the transcriptional activation of the Upd3 cytokine in ECs (Houtz et al., 2017; Osman et al., 2012). Strikingly, we found that similar enhancers are used to induce *upd3* expression in both adults and larvae suggesting also a common sensing mechanism.

Conclusion

Altogether, our results demonstrate that, while the cellular bases and molecular mechanisms underlying tissue repair in adults and larvae are largely similar, specific differences result in a dramatically dissimilar outcome to infection. This implies that precise developmental cues, possibly hormonal regulation, alters tissue repair mechanisms with important consequences for health. In addition, our results also illustrate how the constraints of development can sensitize hosts to stresses such as infection. The apparent tradeoff between the constraints of development and the impact of environmental stresses such as infection could be conserved, and suggest that adult and immature intestinal homeostasis could differ in mammals as well. Finally, our data suggest that

limited homeostatic abilities at the larval stage could explain why larvae are more susceptible to biocontrol strategies.

Materials and Methods

Fly stocks and Husbandry

Drosophila stocks were maintained at room temperature (~23°C) on standard fly medium (sucrose, cornmeal, yeast, and agar). Control lines: as controls during Gal4/UAS experiments, we used the F1 progeny of the driver line crossed to wild-type stocks such as Canton-S (Cs) (RRID: BDSC_64349). Gal4 Drivers: *Myo1A-Gal4, UAS-GFP, tub-Gal80^{TS}; upd3-lacZ* (*Myo^{TS},* EC-specific), *Su(H)GBE-Gal4; UAS-GFP, tub-Gal80^{TS}* (*Su(H)^{TS},* EB-specific), *esg-Gal4; UAS-GFP, tub-Gal80^{TS}* (*esg^{TS}*, adult midgut progenitor-specific) as well as *esg-Gal4, UAS-mcherry, tub-Gal80^{TS}*. Conditional *Gal4^{TS}* flies were obtained by crossing virgin females of the driver strain with males of the *UAS-transgene* line. For RNAi and overexpression experiments, F1 larvae (*driver > UAS-transgene*) were raised to 1st instars at 18°C, to allow for normal development up to this stage. Larvae were then switched to 29°C for 2-3days to allow for maximum transgene expression and RNAi-mediated gene knockdown. By this time, larvae were in 2nd and 3rd instar stages. UAS-transgene stocks: Transgenic fly lines were obtained from Bloomington (TRiP lines), VDRC (Vienna) or NIG (Japan). Reporter lines: *upd3.1-lacZ*, *esg-lacZ, Myo-lacZ*. A list of the fly lines used in this report can be found in the key resources table.

Bacterial Oral Infection

Erwinia carotovora ssp. carotovora 15 (*Ecc15*) is a Gram-negative plant and insect pathogen, which is semi-lethal when ingested by *Drosophila* larvae, and nonlethal to adult flies. The

pathogenicity of *Ecc15* in insects is mediated by the *Erwinia* virulence factor (Evf). Strains of *Ecc15* mutant for the *evf* gene (*Ecc15 evf*) or overexpressing it (*Ecc15 pOM evf*) were also used. All bacteria were maintained on standard LB agar plates. Bacteria were cultured in LB broth at 29°C for 16 hours. Oral infection of larvae was performed as previously described (Acosta Muniz et al., 2007b): larvae were collected from standard fly medium in 1X PBS and selected by stage (determined by observation of mouth hook and spiracle development), then moved to 1.5ml tubes containing 400µl of crushed, organic banana and 200µl of either 1X PBS solution (control) or a bacterial pellet solution, at OD_{600} = 100 concentration (for a final OD600 of 33) unless otherwise noted. Orally treated larvae were incubated at 29°C for 30 minutes before being transferred to fresh vials of standard fly medium, along with the contents of the 1.5ml incubation tubes. Infected larvae were then incubated at 29°C until dissection or for the duration of survival experiments. Oral infection of adult flies was performed as previously described (Houtz and Buchon, 2014): flies were starved for 2 hours in empty vials at 29°C, and subsequently moved to fly medium vials, in which the food was covered by a filter paper disc containing 150µl of either 2.5% sucrose solution (UC control), or 5% sucrose solution mixed with an equal volume of a OD_{600} = 200 bacterial pellet. Orally treated flies were incubated at 29°C until dissection or for the duration of survival experiments.

Survival and development rate experiments

Larvae were grown at 29°C for two days after egg deposition (AED) and 2nd instar larvae were collected for treatment. For temperature inducible experiments, flies were allowed to hatch and develop to first instars at 18°C before shifting to 29°C. Following treatment, flies were monitored at 29°C each day and the number of flies that had reached the yellow pupa (YP), black pupa (BP),

or adult stages was recorded. Emerged adults were collected from these experiments, when appropriate, and maintained at 29°C to monitor their survival. For adult survival following infection, 20 female flies aged 3 days post-eclosion were collected for each treatment group and shifted to 29°C upon infection. Their survival was monitored daily, with the date of infection marked as day zero.

Feeding cessation experimentation

Second instar larvae were treated as usual with either 1X PBS, or a bacterial pellet of wildtype or *evf* mutant *Ecc15* at a final concentration of OD_{600} = 66. Following treatment, larvae were transferred to vials of fly medium supplemented with 2% FD&C Blue #1 dye (Spectrum Chemical). Larvae were collected in 1X PBS each hour for 4 hours and checked under a microscope for the presence of blue food in the gut.

Immunohistochemistry and fluorescence imaging

Dissected *Drosophila* midguts were fixed in 4% paraformaldehyde in 1X PBS for 45 to 90 minutes and successively washed 3 times with 0.1% TritonX in PBS. Guts were then incubated for an hour in blocking solution (1% bovine serum albumin, 1% normal donkey serum, and 0.1% Triton X-100 in PBS). Overnight primary antibody staining was performed at room temperature (RT). Guts were washed 3 times with 0.1% TritonX in PBS and secondary antibody staining was performed for two or more hours in PBS. The exception to this procedure was staining against the Delta isotope, in which case an alternate blocking solution was used (3% bovine serum albumin and 0.1% Triton X-100 in PBS) for 3 hours, and antibody staining was performed in 1% BSA and 0.1% Triton X-100 in PBS at 18˚C. Primary antibodies used: rabbit anti-pH3 (1:000, Millipore

Cat# 06-570, RRID:AB_310177), rabbit anti-β-Galactosidase (1:1000, MP Biomedicals Cat# 0855976, RRID:AB_2334934), goat anti-β-Galactosidase (1:1000, MP Biomedicals), mouse anti-Prospero (1:100, DSHB Cat# Prospero (MR1A), RRID:AB_528440), and mouse anti-Delta (1:100, DSHB Cat# c594.9b, RRID:AB_528194). Secondary antibodies used: donkey anti-rabbit-555 (1:2000, Thermo Fisher Scientific Cat# A-31572, RRID:AB_162543), donkey anti-goat-555 (1:2000, Thermo Fisher Scientific Cat# A-21432, RRID:AB_2535853), donkey anti-mouse-488 (1:2000, Thermo Fisher Scientific Cat# A-21202, RRID:AB_141607), and donkey anti-mouse-647 (1:1000, Thermo Fisher Scientific Cat# A-31571, RRID:AB_162542). DNA was stained in 1:50,000 DAPI (Sigma-Aldrich) in PBS for 30min, and samples received a final three washes in 1X PBS before mounting in antifade medium (Citifluor AF1). Imaging was performed on a Zeiss LSM 700 fluorescent/confocal inverted microscope.

Transcriptome analysis

Oral infection of larvae was performed as previously described. 50 larval guts per condition were dissected 6h post-treatment and immediately transferred into TRIzol (Life Technologies) kept on ice and subsequently homogenized, for a total of 3 replicates. Total RNA was isolated using a hybrid modified TRIzol/RNeasy (Qiagen) extraction protocol. RNA underwent quantification and Quality check (QC) procedures via Fragment Analyzer (Advanced Analytical), before 3' end RNA-seq libraries preparation. Following RNA extraction and QC, we utilized QuantSeq 3' mRNA-Seq Library Prep Kit (Lexogen) to prepare 3' end RNA-seq libraries. Libraries were again QCed with Fragment Analyzer before pooling and sequencing. Illumina NextSeq 500 platform using standard protocol for 75 bp single-end read sequencing at the Cornell Life Sciences Sequencing core facility was utilized to sequence libraries. 5 to 6 million reads were made per

sample, which approximately equals a 20x coverage by conventional RNAseq. Quality control of raw reads was performed with fastqc and reads were trimmed by trimmomatic and then mapped to the Drosophila transcriptome using STAR. DEseq2 was used for differential expression analysis and PCAs were performed using custom R scripts (available upon request). Gene Ontology was performed using the online tool GOrilla.

Quantification and statistical analysis

All analyses were performed in Prism (GraphPad Prism V7.0a, GraphPad Software, La Jolla, CA, USA). For survival assays, the curves represent the average percent survival ±SE of three or more biological replicates (n=20 flies for each biological replicate). A Log-rank test was used to determine significance (*p<0.05 **p<0.01 ***p<0.001 ****p<0.0001). In bacterial load quantification assays, the horizontal lines represent median values for each time point. Three biological replicates were included. Following normalization, results were analyzed using a two-way ANOVA followed with Sidak's post-tests for specific comparisons (*p<0.05 **p<0.01 ***p<0.001 ****p<0.0001). For all other experiments, mean values of three or more biological repeats are presented ±SE. Significance was calculated by a Student's t-test following normalization (*p<0.05 **p<0.01 ***p<0.001 ****p<0.0001).

Acknowledgements

We would like to thank Jonathan Revah for his exploratory experiments that contributed to this project. In addition, we thank Jeff Hodgson, Peter Nagy and Bretta Hixson for comments on the manuscript. This work was supported by NSF IOS1656118 and NSF IOS1653021 to Nicolas Buchon.

References

1. Acosta Muniz, C., Jaillard, D., Lemaitre, B., Boccard, F., 2007a. Erwinia carotovora Evf antagonizes the elimination of bacteria in the gut of Drosophila larvae. Cell Microbiol 9, 106–119. doi:10.1111/j.1462-5822.2006.00771.x

2. Acosta Muniz, C., Jaillard, D., Lemaitre, B., Boccard, F., 2007b. Erwinia carotovora Evf antagonizes the elimination of bacteria in the gut of Drosophila larvae. Cell Microbiol 9, 106–119. doi:10.1111/cmi.2007.9.issue-1

3. Antonello, Z.A., Reiff, T., Ballesta-Illan, E., Dominguez, M., 2015. Robust intestinal homeostasis relies on cellular plasticity in enteroblasts mediated by miR-8-Escargot switch. EMBO J 34, 2025–2041. doi:10.15252/embj.201591517

4. Bae, Y.S., Choi, M.K., Lee, W.-J., 2010. Dual oxidase in mucosal immunity and host-microbe homeostasis. Trends Immunol 31, 278–287. doi:10.1016/j.it.2010.05.003

5. Basset, A., Tzou, P., Lemaitre, B., Boccard, F., 2003. A single gene that promotes interaction of a phytopathogenic bacterium with its insect vector, Drosophila melanogaster. EMBO Rep 4, 205–209. doi:10.1038/sj.embor.embor730

6. Beebe, K., Lee, W.-C., Micchelli, C.A., 2010. JAK/STAT signaling coordinates stem cell proliferation and multilineage differentiation in the Drosophila intestinal stem cell lineage. Dev Biol 338, 28–37. doi:10.1016/j.ydbio.2009.10.045

7. Beehler-Evans, R., Micchelli, C.A., 2015. Generation of enteroendocrine cell diversity in midgut stem cell lineages. 142, 654–664. doi:10.1242/dev.114959

8. Bonfini, A., Liu, X., Buchon, N., 2016. From pathogens to microbiota: How Drosophila intestinal stem cells react to gut microbes. Dev Comp Immunol 64, 22–38. doi:10.1016/j.dci.2016.02.008

9. Buchon, N., Broderick, N.A., Chakrabarti, S., Lemaitre, B., 2009a. Invasive and indigenous microbiota impact intestinal stem cell activity through multiple pathways in Drosophila. Genes Dev 23, 2333–2344. doi:10.1101/gad.1827009

10. Buchon, N., Broderick, N.A., Kuraishi, T., Lemaitre, B., 2010. Drosophila EGFR pathway coordinates stem cell proliferation and gut remodeling following infection. BMC Biol 8, 152. doi:10.1186/1741-7007-8-152

11. Buchon, N., Broderick, N.A., Lemaitre, B., 2013. Gut homeostasis in a microbial world: insights from Drosophila melanogaster. Nat Rev Micro 11, 615–626. doi:10.1038/nrmicro3074

12. Buchon, N., Broderick, N.A., Poidevin, M., Pradervand, S., Lemaitre, B., 2009b. Drosophila intestinal response to bacterial infection: activation of host defense and stem cell proliferation. Cell Host Microbe 5, 200–211. doi:10.1016/j.chom.2009.01.003

13. Buchon, N., Silverman, N., Cherry, S., 2014. Immunity in Drosophila melanogaster - from microbial recognition to whole-organism physiology. Nat Rev Immunol 14, 796–810. doi:10.1038/nri3763

14. Colombani, J., Andersen, D.S., Léopold, P., 2012. Secreted peptide Dilp8 coordinates Drosophila tissue growth with developmental timing. Science 336, 582–585. doi:10.1126/science.1216689

15. Denton, D., Simin, R., Baehrecke, E.H., Kumar, S., 2009. Autophagy, not apoptosis, is essential for midgut cell death in Drosophila. Curr Biol 19, 1741–1746. doi:10.1016/j.cub.2009.08.042

16. Du, E.J., Ahn, T.J., Kwon, I., Lee, J.H., Park, J.-H., Park, S.H., Kang, T.M., Cho, H., Kim, T.J., Kim, H.-W., Jun, Y., Lee, H.J., Lee, Y.S., Kwon, J.Y., Kang, K., 2016. TrpA1 Regulates Defecation of Food-Borne Pathogens under the Control of the Duox Pathway. PLoS Genet 12, e1005773. doi:10.1371/journal.pgen.1005773

17. Duronio, R.J., 1999. Establishing links between developmental signaling pathways and cell-cycle regulation in Drosophila. Curr Opin Genet Dev 9, 81–88.

18. Erkosar, B., Storelli, G., Mitchell, M., Bozonnet, L., Bozonnet, N., Leulier, F., 2015. Pathogen Virulence Impedes Mutualist-Mediated Enhancement of Host Juvenile Growth via Inhibition of Protein Digestion. Cell Host Microbe 18, 445–455. doi:10.1016/j.chom.2015.09.001

19. Evans, C.J., Olson, J.M., Ngo, K.T., Kim, E., Lee, N.E., Kuoy, E., Patananan, A.N., Sitz, D., Tran, P., Do, M.-T., Yackle, K., Cespedes, A., Hartenstein, V., Call, G.B., Banerjee, U., 2009. G-TRACE: rapid Gal4-based cell lineage analysis in Drosophila. Nat Meth 6, 603–605. doi:10.1038/nmeth.1356

20. Grewal, S.S., 2008. Insulin/TOR signaling in growth and homeostasis: A view from the fly world. The International Journal of Biochemistry & Cell Biology. doi:10.1016/j.biocel.2008.10.010

21. Guo, Z., Driver, I., Ohlstein, B., 2013. Injury-induced BMP signaling negatively regulates Drosophila midgut homeostasis. J Cell Biol 201, 945–961. doi:10.1083/jcb.201302049

22. Halme, A., Cheng, M., Hariharan, I.K., 2010. Retinoids regulate a developmental checkpoint for tissue regeneration in Drosophila. Curr Biol 20, 458–463. doi:10.1016/j.cub.2010.01.038

23. Hariharan, I.K., Serras, F., 2017. Imaginal disc regeneration takes flight. Curr Opin Cell Biol 48, 10–16. doi:10.1016/j.ceb.2017.03.005

24. Houtz, P., Bonfini, A., Liu, X., Revah, J., Guillou, A., Poidevin, M., Hens, K., Huang, H.-Y., Deplancke, B., Tsai, Y.-C., Buchon, N., 2017. Hippo, TGF-β, and Src-MAPK pathways regulate transcription of the upd3 cytokine in Drosophila enterocytes upon bacterial infection. PLoS Genet 13, e1007091. doi:10.1371/journal.pgen.1007091

25. Houtz, P.L., Buchon, N., 2014. Methods to assess intestinal stem cell activity in response to microbes in Drosophila melanogaster. Methods Mol Biol 1213, 171–182. doi:10.1007/978-1-4939-1453-1_14

26. Jaszczak, J.S., Wolpe, J.B., Bhandari, R., Jaszczak, R.G., Halme, A., 2016. Growth Coordination During Drosophila melanogaster Imaginal Disc Regeneration Is Mediated by Signaling Through the Relaxin Receptor Lgr3 in the Prothoracic Gland. Genetics 204, 703–709. doi:10.1534/genetics.116.193706

27. Jiang, H., Edgar, B.A., 2009. EGFR signaling regulates the proliferation of Drosophila adult midgut progenitors. 136, 483–493. doi:10.1242/dev.026955

28. Jiang, H., Grenley, M.O., Bravo, M.-J., Blumhagen, R.Z., Edgar, B.A., 2011. EGFR/Ras/MAPK signaling mediates adult midgut epithelial homeostasis and regeneration in Drosophila. Cell Stem Cell 8, 84–95. doi:10.1016/j.stem.2010.11.026

29. Jiang, H., Patel, P.H., Kohlmaier, A., Grenley, M.O., Mcewen, D.G., Edgar, B.A., 2009. Cytokine/Jak/Stat signaling mediates regeneration and homeostasis in the Drosophila midgut. Cell 137, 1343–1355. doi:10.1016/j.cell.2009.05.014

30. Karin, M., Clevers, H., 2016. Reparative inflammation takes charge of tissue regeneration. Nature 529, 307–315. doi:10.1038/nature17039

31. Keita, S., Masuzzo, A., Royet, J., Kurz, C.L., 2017. Drosophila larvae food intake cessation following exposure to Erwinia contaminated media requires odor perception, Trpa1 channel and evf virulence factor. J Insect Physiol 99, 25–32. doi:10.1016/j.jinsphys.2017.02.004

32. Kwon, Y., Song, W., Droujinine, I.A., Hu, Y., Asara, J.M., Perrimon, N., 2015. Systemic organ wasting induced by localized expression of the secreted insulin/IGF antagonist ImpL2. Dev Cell 33, 36–46. doi:10.1016/j.devcel.2015.02.012

33. Lemaitre, B., Hoffmann, J.A., 2007. The host defense of Drosophila melanogaster. Annu Rev Immunol 25, 697–743. doi:10.1146/annurev.immunol.25.022106.141615

34. Li, H., Qi, Y., Jasper, H., 2013. Dpp signaling determines regional stem cell identity in the regenerating adult Drosophila gastrointestinal tract. Cell Rep 4, 10–18. doi:10.1016/j.celrep.2013.05.040

35. Li, Z., Zhang, Y., Han, L., Shi, L., Lin, X., 2013. Trachea-derived dpp controls adult midgut homeostasis in Drosophila. Dev Cell 24, 133–143. doi:10.1016/j.devcel.2012.12.010

36. Liu, X., Hodgson, J.J., Buchon, N., 2017. Drosophila as a model for homeostatic, antibacterial, and antiviral mechanisms in the gut. PLoS Pathog 13, e1006277. doi:10.1371/journal.ppat.1006277

37. Mathur, D., Bost, A., Driver, I., Ohlstein, B., 2010. A transient niche regulates the specification of Drosophila intestinal stem cells. Science 327, 210–213. doi:10.1126/science.1181958

38. Micchelli, C.A., Perrimon, N., 2006. Evidence that stem cells reside in the adult Drosophila midgut epithelium. Nature 439, 475–479. doi:10.1038/nature04371

39. Micchelli, C.A., Sudmeier, L., Perrimon, N., Tang, S., Beehler-Evans, R., 2011. Identification of adult midgut precursors in Drosophila. Gene Expr Patterns 11, 12–21. doi:10.1016/j.gep.2010.08.005

40. Ohlstein, B., Spradling, A.C., 2007a. Multipotent Drosophila intestinal stem cells specify daughter cell fates by differential notch signaling. Science 315, 988–992. doi:10.1126/science.1136606

41. Ohlstein, B., Spradling, A.C., 2007b. Multipotent Drosophila intestinal stem cells specify daughter cell fates by differential notch signaling. Science 315, 988–992. doi:10.1126/science.1136606

42. Perdigoto, C.N., Schweisguth, F., Bardin, A.J., 2011. Distinct levels of Notch activity for commitment and terminal differentiation of stem cells in the adult fly intestine. Development 138, 4585–4595. doi:10.1242/dev.065292

43. Smith-Bolton, R., 2016. Drosophila Imaginal Discs as a Model of Epithelial Wound Repair and Regeneration. Adv Wound Care (New Rochelle) 5, 251–261. doi:10.1089/wound.2014.0547

44. Smith-Bolton, R.K., Worley, M.I., Kanda, H., Hariharan, I.K., 2009. Regenerative growth in Drosophila imaginal discs is regulated by Wingless and Myc. Dev Cell 16, 797–809. doi:10.1016/j.devcel.2009.04.015

45. Soldano, A., Alpizar, Y.A., Boonen, B., Franco, L., López-Requena, A., Liu, G., Mora, N., Yaksi, E., Voets, T., Vennekens, R., Hassan, B.A., Talavera, K., 2016. Gustatory-mediated avoidance of bacterial lipopolysaccharides via TRPA1 activation in Drosophila. elife 5. doi:10.7554/eLife.13133

46. Stensmyr, M.C., Dweck, H.K.M., Farhan, A., Ibba, I., Strutz, A., Mukunda, L., Linz, J., Grabe, V., Steck, K., Lavista-Llanos, S., Wicher, D., Sachse, S., Knaden, M., Becher, P.G., Seki, Y., Hansson, B.S., 2012. A conserved dedicated olfactory circuit for detecting harmful microbes in Drosophila. Cell 151, 1345–1357. doi:10.1016/j.cell.2012.09.046

47. Vallet-Gely, I., Lemaitre, B., Boccard, F., 2008. Bacterial strategies to overcome insect defences. Nat Rev Micro 6, 302–313. doi:10.1038/nrmicro1870

48. Xiang, J., Bandura, J., Zhang, P., Jin, Y., Reuter, H., Edgar, B.A., 2017. EGFR-dependent TOR-independent endocycles support Drosophila gut epithelial regeneration. Nat Commun 8, 15125. doi:10.1038/ncomms15125

49. Zeng, X., Hou, S.X., 2015. Enteroendocrine cells are generated from stem cells through a distinct progenitor in the adult Drosophila posterior midgut. 142, 644–653. doi:10.1242/dev.113357

50. Zhai, Z., Boquete, J.-P., Lemaitre, B., 2017. A genetic framework controlling the differentiation of intestinal stem cells during regeneration in Drosophila. PLoS Genet 13, e1006854. doi:10.1371/journal.pgen.1006854

51. Zhou, J., Florescu, S., Boettcher, A.-L., Luo, L., Dutta, D., Kerr, G., Cai, Y., Edgar, B.A., Boutros, M., 2014. Dpp/Gbb signaling is required for normal intestinal regeneration during infection. Dev Biol. doi:10.1016/j.ydbio.2014.12.017

CHAPTER V

DISCUSSION

Epithelial tissue renewal is often mediated by the activity of somatic stem cells, which divide and differentiate in order to self-replenish while replacing old or dying cells that are extruded from the epithelial layer. Gastrointestinal (GI) tract epithelia exhibits particularly rapid, homeostatic turnover compared to other tissue types (Andersson-Rolf et al., 2017), which accompanies its high degree of exposure to biotic and abiotic stresses introduced to the lumen along with the ingestion of nutrients. Indeed, intestinal tissue is unique in its constraints, having to balance digestive/absorptive functions with its necessary role as a steady barrier against damage and microbial infection (Peterson and Artis, 2014). These challenges necessitate continual and efficient tissue turnover in order to maintain a homeostatic epithelial layer while preserving gut functions. Therefore the process of epithelial renewal must be carefully maintained in the GI tract, a feat that is accomplished by the regulation of cytokine signaling to orchestrate epithelial turnover and repair (Andersson-Rolf et al., 2017). However, despite the grave importance of maintaining epithelial turnover in the GI tract, the genetic pathways that coordinate ISC-mediated tissue regeneration following infectious damage remain poorly characterized. In particular, the precise signaling that links the detection of pathogens or pathogen-associated damage in the gut to subsequent renewal have yet to be elucidated. The theme of my PhD has been the characterization of the networks that regulate intestinal repair by bridging the gap between detection of tissue damage or disturbance and activation of epithelial repair responses. My first major project explored the transcriptional control of the primary pro-regenerative cytokine in the adult *Drosophila* midgut, while the second investigates the regulation of a limited larval midgut repair response, in which imaginal adult midgut progenitors are recruited to differentiate for lost tissue replacement.

Over the course of my research I have successfully identified key regulatory pathways that are activated in *Drosophila* midgut epithelial cells in response to pathogen-induced tissue loss, and converge on the regulation of the TFs that direct transcription of the key JAK/STAT cytokine, Upd3. This cytokine, which is in the IL-6 family of JAK/STAT cytokines in *Drosophila* (Osman et al., 2012), is vital for the initiation of ISC-mediated midgut repair. Interestingly, the same pathways that induce *upd3* transcription in ECs are subsequently activated in the ISCs to coordinate their increased proliferation and differentiation. In addition, my more recent research suggests that the JAK/STAT, Notch and TGF-β/Dpp pathways also regulate midgut damage repair following enteric infection in *Drosophila* larvae, though by an alternative process.

Lacking dedicated ISCs, the transient larval midgut instead utilizes the developing adult midgut imaginal islets to replace lost tissue. To my knowledge, this is the first report of imaginal adult tissue being recruited for the repair of larval structures. The differentiation of these precursors into new ECs to be integrated into the larval gut epithelium requires Notch and JAK/STAT pathway activation, and may also be promoted via activation of Dpp. Altogether, this demonstrates that a small set of genetic regulatory pathways are activated in the intestinal epithelium following tissue loss, and that these pathways are capable of converging on the initiation of GI tract repair via distinct mechanisms. Thus, the regulatory network directing intestinal repair is conserved in the pathways that are switched on to signal epithelial cell loss or stress, but that these pathways can promote regeneration dynamically, depending on the set of constraints of a given situation. This reuse of the same pathways upstream of repair might result from a conserved role in detecting stress, wounding or pathogens, and thus allow for the direction of parallel responses to these events. Indeed, we might view the recruitment of AMPs and PCs in the larval gut as analogous to the stimulation of ISCs and EBs for tissue repair in the adult gut.

Utilizing developmental tissue for repair of transient organs in an immature stage organism represents an adaptation to otherwise lethal damage to the immature organs, thus allowing infected larvae to survive and continue their development, though at a delayed pace in order to rebuild the lost imaginal tissue. Interestingly, my data suggests that the delay observed in infected larvae is not directly linked to the development of the AMP islets, and thus is likely to be triggered as an additional response to the *Ecc15* infection or the subsequent tissue loss in the midgut. Given the conserved nature of the pathways that direct tissue repair in these two scenarios, it is possible that the developmental delay is controlled by a network that also serves a role in response to enteric infection in adult flies.

Altogether, my research demonstrates that intestinal tissue repair in response to pathogen-induced damage is adaptive to the particular constraints present, but nevertheless utilizes a conserved set of genetic pathways to link the detection of infectious injury to an appropriate repair response.

Future Directions

The exact cause of developmental delay in larvae following *Ecc15* infection remains unidentified and thus poses a potential avenue for future study. Indeed, I have begun to investigate what pathways might constitute the genetic network that initiates the developmental delay, but have not accrued enough data to confidently identify the pathway linking oral infection to the extended time to pupation. My initial results are in the appendix of this dissertation. As discussed in the appendix, I hypothesized that the retinoid synthesis pathway or dilp8 (both of which have been shown to play a role in delaying the onset of pupation in the event of damage or improper growth of the imaginal wing disc tissue in larvae) might regulate the developmental delay observed

after enteric *Ecc15* infection. However, my initial results have been somewhat inconclusive. I found that the retinoid synthesis genes *Fdh* and *Aldh* are required to survive infection by *Ecc15* pre-pupation, but that they are both downregulated in the midgut by infection. Additionally, I noted that the carotenoid scavenger receptor, *santa-maria*, is transcriptionally upregulated in infected larval midguts. Thus, the role of the retinoid synthesis pathway in promoting larval survival to enteric infection may be the result of its activity in tissue other than the midgut. I therefore would propose the use of tissue specific driver lines to determine in what tissue the retinoid synthesis pathway is required for larval survival following oral *Ecc15* infection. An additional, important test to perform is to check that the sensitivity to infection that we observe results from the loss of the classic retinoid synthesis pathway function: absorbing and processing carotenoids for the storage and mobilization of retinal (Vitamin A). To accomplish this, I suggest determining whether a dietary source of retinol is required to survive enteric *Ecc15* infection. The diet of *Drosophila* is readily malleable, and recipes exist for chemically defined fly food. By raising *Drosophila* larvae on chemically defined media with and without the addition of retinol, and under axenic conditions to further limit potential sources of vitamins, we can deduce if a dietary source of retinoids is required for larval survival of enteric bacterial infection. Even if retinoids are not involved in inducing the developmental delay upon infection, an immune function of dietary retinoids is nonetheless novel and fascinating, and worthy of further research.

In addition, I believe that it will be important to clarify if limited tissue repair by AMP differentiation, and delayed onset of pupation, are triggered by the detection of pathogenic microbes or by the sensing of damage to the midgut epithelium.

Finally, my study into the transcription factors and upstream pathways that activate *upd3* transcription in adult ECs to promote tissue regeneration could also be followed up by additional

studies. For instance, we found that the transcriptionally inhibitor, Snail, was required for proper *upd3* induction following *Ecc15* infections, but we have yet to confirm the mechanism by which this TF may be necessary for *upd3* induction. We hypothesized that Snail, which acts as a positive regulator of epithelial to mesenchymal transitions during *Drosophila* development, might play a similar role in the *Drosophila* midgut by promoting the extrusion of enterocytes upon enteric infection. If this is the case, then we should be able to inhibit a subset of ECs from undergoing delamination upon infection by RNAi-mediated knockdown of *snail* (*sna*). We possess a genetic construct that induces Gal4 and UAS-GFP expression in random, individual ECs throughout the midgut at room temperature that we might use to test this, by combining it with the *UAS-sna-RNAi* construct that we used during the TF RNAi screen. We would then observe for retention of the GFP-tagged ECs following infection (as well as following a week of basal turnover) compared to controls in which the random EC marking line is crossed to a wild type control such as Canton S (Cs).

I hope that the future directions that I have discussed here may lead to further discoveries in the areas that I have invested myself in as a PhD student, and thus deepen our understanding of the genetic mechanisms that govern intestinal epithelial repair following bacterially-induced damage.

References:

1. TOR-independent endocycles support Drosophila gut epithelial regeneration. *Nat Commun* 8, 15125.

2. Yannas, I. V. (2005). Similarities and differences between induced organ regeneration in adults and early foetal regeneration. *Journal of the Royal Society Interface*, 2(5), 403–417.

3. Zeng, X. and Hou, S. X. (2015). Enteroendocrine cells are generated from stem cells through a distinct progenitor in the adult Drosophila posterior midgut. 142, 644–653.

4. Zhai, Z., Boquete, J.-P. and Lemaitre, B. (2017). A genetic framework controlling the differentiation of intestinal stem cells during regeneration in Drosophila. *PLoS Genet* 13, e1006854.

5. Zhou, J., Florescu, S., Boettcher, A.-L., Luo, L., Dutta, D., Kerr, G., Cai, Y., Edgar, B. A. and Boutros, M. (2014). Dpp/Gbb signaling is required for normal intestinal regeneration during infection. *Dev Biol*.

APPENDIX

The retinoid synthesis pathway is required in larvae to survive oral *Ecc15* infection.

Upon discovering that larval *Drosophila* experience a developmental delay following *Ecc15* infection, I became interested in what might regulate this pause. Initially, I hypothesized that the delay might be related to similar postponements of pupation that have been observed in larval *Drosophila* following damage to imaginal wing discs. Studies of this induced delay discovered that it requires retinoid synthesis pathway activity in the damaged wing discs, which subsequently signals, either by retinoic acid or a downstream metabolite, the brain to inhibit prothoracic hormone (PTTH) expression and subsequently block ecdysone production in the ring gland (Halme et al., 2010). Additional studies of developmental delays in *Drosophila* larvae, caused by imaginal tissue growth problems, have found that the expression of *dilp8* in imaginal wing discs can coordinate a pause in whole organism growth (Colombani et al., 2012). I therefore decided to check whether mutants for two retinoid synthesis pathway genes (*Fdh* and *Aldh*), or a mutant for *dilp8*, experience the same developmental delay upon oral Ecc15 infection that control larvae exhibit.

Interestingly, my initial results show that *Fdh* and *Aldh* mutants have ordinary developmental and survival rates in unchallenged conditions, but are unable to survive oral *Ecc15* infection (Fig. A.1). The few *Fdh* mutant larvae that survived to pupation seemed to show a greater developmental delay than usual, and none of them survived to adult eclosion. Interestingly, our RNAseq data shows that *Fdh* and *Aldh* expression is strongly reduced following oral *Ecc15* infection (Table A.1). This decrease in expression could be indicative of retinoid synthesis down regulation, or be due to the massive loss of enterocytes in the infected midgut. However, the expression of the carotenoid scavenger receptor, *santa-maria*, is increased by infection in the larval midgut. Based on these early results, I suggest that the retinoid synthesis pathway plays a vital role

in the survival of larval *Drosophila* following oral infection by *Ecc15*. Specifically, I posit that loss of the retinoid synthesis pathway may block the infection-induced developmental delay and thus cause the death of larvae when they attempt to pupate despite the ongoing intestinal damage and reduced pool of available AMPs. More data is required to confirm if this is the actual case, especially since the downregulation of *Fdh* and *Aldh* upon infection is counter-intuitive to this hypothesis. It is possible that the retinoid synthesis pathway is required outside of the midgut to regulate the developmental delay, if it is indeed involved in this process.

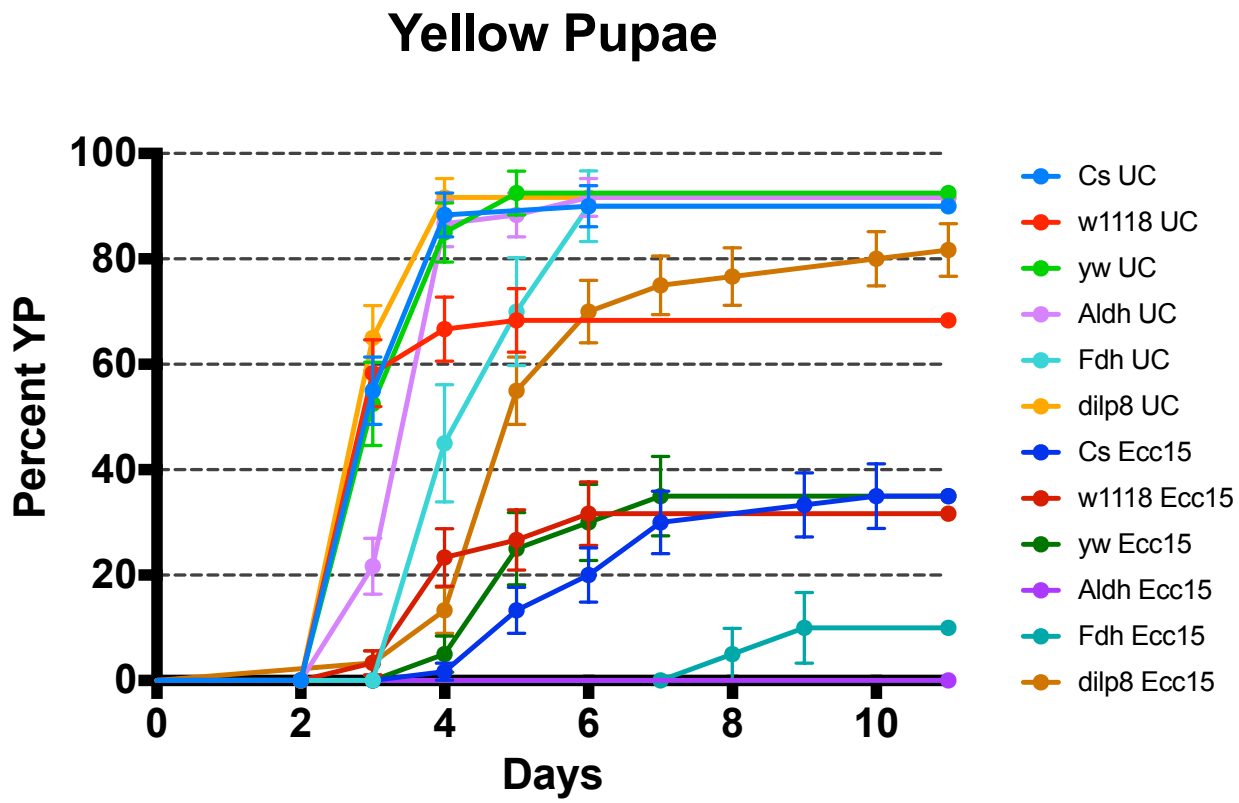

Figure A.1. Survival and development rates for retinoid synthesis and dilp8 mutants. Mutants of retinoid synthesis pathway genes (*Aldh* and *Fdh*) do not display decreased survival in unchallenged conditions, compared to controls (*Cs*, *w1118* and *yw*). However, they are much more susceptible to oral *Ecc15* infection than controls. Dilp8 mutants, on the other hand, have higher than ordinary survival to oral *Ecc15* infections.

Table A.1. Expression of retinoid synthesis genes and *dilp8* in unchallenged and Ecc15-infected conditions from RNAseq data.

Gene	Larval midgut UC	Larval midgut Ecc15
Fdh	252.2	177.3
Aldh	672.3	273.6
santa-maria	13.3	23.3
Ilp8	0.0	0.0

Additionally, although the expression values for *dilp8* recorded in the RNAseq are too low to suggest that it might be regulated in the larval midgut following infection, *dilp8* mutants surprisingly display increased survival following *Ecc15* infection compared to controls (Fig. A.1 and Table A.1). The mutants nevertheless seem to experience a developmental delay following infection, suggesting that dilp8 plays a role outside of the midgut in improving survival to infection, and that the improved survival is not linked to the timing of the developmental delay.

References

1. Colombani, J., Andersen, D. S. and Léopold, P. (2012). Secreted peptide Dilp8 coordinates Drosophila tissue growth with developmental timing. *Science* 336, 582–585.

2. Halme, A., Cheng, M. and Hariharan, I. K. (2010). Retinoids regulate a developmental checkpoint for tissue regeneration in Drosophila. *Curr Biol* 20, 458–463.